To the Graduate Council:

I am submitting herewith a dissertation written by Trairat Neimsuwan entitled "The Influence of Selected Wood Characteristics and Composites Production Parameters on the Sorption Behavior of Wood Materials." I have examined the final electronic copy of this dissertation for form and content and recommend that it be accepted in partial fulfillment of the requirements for the degree of Doctor of Philosophy, with a major in Natural Resources.

Siqun Wang
Major Professor

We have read this dissertation
and recommend its acceptance:

Adam M. Taylor

Brian K. Via

Ian D. Hartley

Timothy G. Rials

Xiaofei P. Ye

Accepted for the Council:

Carolyn R. Hodges

Vice Provost and Dean
of the Graduate School

(Original signatures are on file with official student records.)

THE INFLUENCE OF SELECTED WOOD CHARACTERISTICS AND COMPOSITES PRODUCTION PARAMETERS ON THE SORPTION BEHAVIOR OF WOOD MATERIALS

A Dissertation
Presented for the
Doctor of Philosophy Degree
The University of Tennessee, Knoxville

Trairat Neimsuwan
December 2007

Copyright 2007 © by Trairat Neimsuwan

All Rights Reserved

DEDICATION

This dissertation is dedicated to my father, Mr. Trairong Neimsuwan, who encourages and fully supports me to do every thing in my life.

Also, I dedicated my dissertation to my mother, Mrs. Lek Neimsuwan, for her unconditional love and believe in me.

Finally, this dissertation is dedicated to all those who believe in value of knowledge.

"We may use wood with intelligence only if we understand wood"

Frank Lloyd Wright

ACKNOWLEDGMENTS

The author would like to express his appreciation to his professor, Dr. Siqun Wang, for his advices and directions he provided to this research. His insight and guidance in this project were invaluable, particularly technical guideline and during the writing process. The author also thanks his committee members, Dr. Timothy G. Rials, Dr. Adam M. Taylor, Dr. Ian D. Hartley, Dr. Brian K. Via and Dr. Xiaofei P. Ye, for their advices and the time they spent reviewing this dissertation.

The author acknowledges financial support from the USDA McIntire-Stennis Cooperative Forestry Program, CSREES Wood Utilization Research Program and the Tennessee Agricultural Experiment Station (Project TEN000MS-96). These funding made the project possible. A special thank is extended to Tennessee Forest Products Center for the assistance providing all instruments used in this study. The author also thanks Dr. Steve Kelley for providing wood samples and their related properties, and Dr. Les Groom for providing fiber samples.

Finally, the author expresses sincere thanks to a group of people: the staff of Tennessee Forest Product Center (Prof. Timothy Young, Mr. Bill Moschler, and Dr. David Harper, and Mr. Chris Helton). The office staffs were very helpful in resolving administrative problems, allowing the author to focus on his classes and research.

ABSTRACT

The goal of this research was to investigate the influence of selected wood characteristics and composites production parameters on the sorption behavior of wood materials. A better understanding of the sorption behavior of different wood structures and types could be useful in protecting wood against wood deterioration. The differences among tree ring locations within the stem cross-section have not been explained in terms of sorption behavior. The purpose of the first task was to investigate the effect of differences among earlywood, latewood, and tree ring location within the stem cross-section on the water vapor sorption. A loblolly pine (*Pinus taeda*) tree was cut into earlywood and latewood from the 2nd to 50th tree rings. A sorption kinetics test was conducted from 11% to 89% RH. Results showed that earlywood had higher sorption rates and diffusion coefficients than latewood, while outer tree rings had higher sorption rates and diffusion coefficients than inner tree rings.

An understanding of sorption behavior of individual fibers with varying refiner pressure is necessary to better engineer wood fiber-based composites. The second task was to investigate water vapor sorption of refined fiber as affected by steam pressure using small-scale measurements. Juvenile and mature loblolly pine wood was refined at 2 to 18 bar of steam pressure. Fiber properties were determined by Scanning Electron Microscope (SEM), Dynamic Contact Angle (DCA), X-ray Diffraction (XRD), and a water activity meter. A sorption kinetics test was conducted from 11% to 89% RH. Higher rates of sorption were found in juvenile fiber refined under low steam pressure.

Higher water activity and lower cystallinity was found at low-steam-pressure-refined fibers.

The volume of oriented strandboard (OSB) produced has significantly increased over the last few decades. Wood, resin, and wax play a key role in manufacture and in-service properties. How resin and wax affect the water vapor sorption behavior of resinated and waxed strands remain unclear. The third task was to investigate the effect of processing parameters on the sorption behavior of wood strands under varying environmental conditions. Loblolly pine strands were created with 2 to 4% and 0.5 to 1.5% for resin and wax loading. The resinated strand was pressed with different platen temperatures (120, 160, and 200°C) and compression rates (1.05 and 1.65). A sorption kinetics test was conducted from 11% to 89% RH. Higher resin and wax loading levels resulted in reduced water vapor sorption in early sorption periods. Higher press platen temperatures and compression rates also decreased the sorption properties of resinated loblolly pine strands. Wax loading had more influence on sorption properties than resin loading. Press platen temperatures had more influence on sorption behavior than compression rate.

TABLE OF CONTENTS

CHAPTER PAGE

1. Introduction 1

1.1 Project description 1

1.2 Rationale and significance 3

1.3 Project goal and technical objectives 4

2. Literature review 5

2.1 Introduction 5

2.2 Wood structure 5

2.3 Wood chemistry 17

2.4 Physical nature and mechanics of wood 22

2.4.1 Physical properties of wood 22

2.4.2 Mechanical properties 23

2.5 Water characteristics 24

2.6 Sorption behavior 27

2.6.1 Static of sorption 28

2.6.2 Kinetics of sorption 32

2.6.3 Energetics of sorption 34

2.7 Sorption mechanisms 36

2.8 Parameters affecting sorption 38

2.8.1 Surface modification 38

2.8.2 Heat treatment 39

2.8.3 Wettability 40

2.8.4 Crystallinity 41

2.8.5 Refining process 41

2.9 Wood-based composite application 42

2.10 Summary 44

3. Water vapor sorption of small loblolly pine samples 45

3.1 Introduction 45

3.2 Materials and methods 46
3.2.1 Wood specimen and basic properties 46
3.2.2 Sorption isotherm 48
3.2.3 Sorption kinetics 49
3.2.4 Evaluation of sorption isotherms 50
3.2.5 Evaluation of diffusion coefficients 52
3.2.6 Evaluation of surface resistance 53
3.2.7 Evaluation of sorption rate 54
3.3 Results and discussions 55
3.3.1 Sorption isotherms 55
3.3.2 Sorption rate 57
3.3.3 Sorption diffusion 63
3.3.4 Chemical analysis 69
3.4 Summary 71
4. Effects of refining steam pressure on the water vapor sorption of loblolly pine fibers 72
4.1 Introduction 72
4.2 Materials and methods 75
4.2.1 Specimens 75
4.2.2 Sorption isotherm 75
4.2.3 Kinetics of sorption 76
4.2.4 Scanning electron microscopy 76
4.2.5 X-ray powder diffraction 77
4.2.6 Water activity 78
4.2.7 Contact angle 78
4.3 Results and discussion 79
4.3.1 Surface morphology 79
4.3.2 Sorption isotherm 81
4.3.3 Wettability 85
4.3.4 Water activity 86

4.3.5 Sorption rate 89
4.3.6 Crystallinity 94
4.4 Summary 97
5. Effect of processing parameters on water vapor sorption of wood strands 98
5.1 Introduction 98
5.2 Experimental design 100
5.3 Materials and methods 101
5.3.1 Materials 101
5.3.2 Sample preparation 101
5.3.3 Sorption kinetics 103
5.3.4 Evaluation of sorption kinetics 103
5.4 Results and discussion 103
5.4.1 Resin loading results 103
5.4.2 Wax loading results 112
5.4.3 Pressing parameters 119
5.5 Summary 131
6. Conclusions and recommendations 132
6.1 Conclusions 132
6.2 Recommendations for future work 133
6.3 List of publications 134
References 136
Vita 153

LIST OF FIGURES

FIGURE **PAGE**

Figure 2-1. The cell alignment of softwood (Siau 1984). 6
Figure 2-2. The cell alignment of hardwood (Siau 1984). 7
Figure 2-3. Schematic drawing of a 17-year-old coniferous tree showing the manner in which the trunk increases in thickness and in height through the addition of growth (annual increment) (Panshin and deZeeuw 1980). 9
Figure 2-4. The properties of juvenile wood diagram (Haygreen and Bowyer 1996). 10
Figure 2-5. The earlywood and latewood transition (Haygreen and Bowyer 1996). 12
Figure 2-6. The image of bordered pit structure: a) is side-view, and b) is cross-section view (Haygreen and Bowyer 1996, Kollmann and Côte 1968). 13
Figure 2-7. The transition of sapwood and heartwood (Haygreen and Bowyer 1996). 14
Figure 2-8. The model cell wall arrangement (Fengel and Wegener 1984). 15
Figure 2-9. The schematic structure of a portion of cellulose microfibril with crystallines and amorphous (Siau 1995). 16
Figure 2-10. The chemical composition in cell wall layer (Panshin and deZeeuw 1980). 17
Figure 2-11. Schematic representation of structure of cellulose (Li et al. 2006). 19
Figure 2-12. Schematic representation of structure of hemicelluloses (Adler 1977). 19
Figure 2-13. Schematic representation of structure of lignin (Adler 1977). 20
Figure 2-14. The phase diagram of water (not to scale) (Skaar 1988). 25
Figure 2-15. The five types of sorption isotherms (Time 1998). 29
Figure 2-16. Sorption mechanism: region I is chemi-sorption, region II is physi-sorption, region III is capi-sorption (adapted from Hartley et al. 1992). 37

Figure 3-1. Diagram showing sliver preparation from loblolly pine growth increment. 48
Figure 3-2. Climate control instrument used during the measurement. 51
Figure 3-3. The graphical analysis of initial diffusion coefficient. 54
Figure 3-4. Moisture sorption of ealywood and latewood. 58

Figure 3-5. The moisture sorption of various tree rings of wood (Number in the bracket is specific gravity). 59
Figure 3-6. The comparison of initial sorption rate of earlywood and latewood at different tree rings (The same letters are not significantly different at α = 5%). 62
Figure 3-7. The comparison of second slope of earlywood and latewood at different tree rings (The same letters are not significantly different at α = 5%). 64
Figure 3-8. Comparison of diffusion coefficient of earlywood and latewood at different tree rings (The same letters are not significantly different at α = 5%). 65
Figure 3-9. Comparison of surface emission coefficient of earlywood and latewood at different tree rings (The same letters are not significantly different at α = 5%). 67
Figure 3-10. Comparison of surface resistance coefficient of earlywood and latewood at different tree rings (The same letters are not significantly different at α = 5%). 68

Figure 4-1. Climate control instrument used during the measurement. 77
Figure 4-2. The image of wood fiber refined at (a) juvenile wood at 2 bar, b) mature wood at 2 bar, c) juvenile wood at 18 bar, d) mature wood at 18 bar. 80
Figure 4-3. The SEM image of wood fiber refined at a) juvenile wood at 2 bar, b) mature wood at 2 bar, c) juvenile wood at 18 bar, d) mature wood at 18 bar. 82
Figure 4-4. Sorption isotherm of lignocellulosic fiber refined under varying pressures. . 83
Figure 4-5. Water activity of refined fiber at 65% RH (The same letters are not significantly different at α = 5%). 88
Figure 4-6. Comparison of sorption rate of various refined fibers. 91
Figure 4-7. Comparison of initial sorption rate of various refined fiber (The same letters are not significantly different at α = 5%). 92

Figure 4-8. Comparison of second slope of various refined fibers (The same letters are not significantly different at α = 5%)..... 93
Figure 4-9. Crystallinity of refined fiber from varying refining pressure..... 96

Figure 5-1. The cutting diagram (4 loading level and 4 replications for each study)..... 102
Figure 5-2. Water vapor uptake behavior of strands loaded with different resin levels. 105
Figure 5-3. The moisture sorption of resinated strand loaded with different resin levels. 107
Figure 5-4. Initial sorption rate and second slope of resnated strands (The same letters are not significant at α = 5%)..... 109
Figure 5-5. Diffusion coefficient, surface emission coefficient, and surface resistance coefficient of resinated strand with various resin loading (The same letters are not significantly different at α = 5%)..... 111
Figure 5-6. Water vapor uptake behavior of wood strands loaded with different wax levels. 113
Figure 5-7. Moisture sorption of wood strands loaded with different wax levels. 115
Figure 5-8. Initial sorption rate and second slope of waxed strands (The same letters are not significantly different at α = 5%)..... 117
Figure 5-9. Diffusion coefficient, surface emission coefficient, and surface resistance coefficient of waxed strands with various wax loading (The same letters are not significantly different at α= 5%)..... 118
Figure 5-10. Water vapor uptake behavior of resinated strands pressing with different compression rates..... 120
Figure 5-11. Water vapor uptake behavior of resinated strands pressing with different platen temperatures. 121
Figure 5-12. The moisture sorption of resinated strand pressed with different compression rates..... 124
Figure 5-13. The moisture sorption of resinated strand pressed with different platen temperatures. 125

Figure 5-14. Initial sorption rate and second slope of pressed strands (The same letters are not significantly different at α = 5%)..... 128
Figure 5-15. Diffusion coefficient, surface emission coefficient, and surface resistance coefficient of pressed strands (The same letters are not significantly different at α = 5%)..... 129

LIST OF TABLES

TABLE **PAGE**

Table 2-1. A comparison of the chemical composition of softwood and heartwood (Kollmann and Côte 1968). 21

Table 3-1. Saturated salt solution and resultant relative humidity at 23±2ºC (Lide 1994). 49

Table 3-2. Fitted and physical constants calculated for the Hailwood-Horrobin equation isotherms. 56

Table 3-3. Initial sorption rate (K_1), second slope (K_2), diffusion coefficient (D), surface emission coefficient (σ), and surface resistance coefficient (S) of wood. 60

Table 3- 4. MANOVA results and dependent variable ANOVA for intial sorption rate. 62

Table 3- 5. MANOVA results and dependent variable ANOVA for second slope. 64

Table 3- 6. MANOVA results and dependent variable ANOVA for diffusion coefficient. 65

Table 3- 7. MANOVA results and dependent variable ANOVA for surface emission coefficient. 67

Table 3- 8. MANOVA results and dependent variable ANOVA for surface resistance coefficient. 68

Table 3- 9. The physical properties, mechanical properties, and chemical composition of the loblolly pine (all values are weight percent). 70

Table 4-1. Fitted and physical constants calculated for the Hailwood-Horrobin equation..... 84

Table 4-2. Contact angle of refined fiber at various refining steam pressure. 86

Table 4-3. Water activity of refined fiber with various refining steam pressure. 87

Table 4-4. Sorption rate of refined fibers with various refining steam pressures. 90

Table 4-5. Crystallinity of refining fiber varying pressures. 95

Table 5-1. Experimental design for resin study. 102
Table 5-2. Water vapor uptake rate and EMC of strands loaded with different resin levels. 105
Table 5-3. Initial sorption rate (K_1), second slope (K_2), diffusion coefficient (D), surface emission coefficient (σ), and surface resistance coefficient (S) of resinated wood. 108
Table 5-4. Water vapor uptake rate and EMC of strands loaded with different wax levels. 113
Table 5-5. Initial sorption rate (K_1), second slope (K_2), diffusion coefficient (D), surface emission coefficient (σ), and surface resistance coefficient (S) of waxed strand. 116
Table 5-6. Initial uptake rate and EMC of strands pressing with different platen temperatures and compression rates. 122
Table 5-7. Initial sorption rate ($K_{1)}$, second slope (K_2), diffusion coefficient (D), surface emission coefficient (σ), and surface resistance coefficient (S) of resinated strand pressed with different compression rates and temperature. 127

1. INTRODUCTION

1.1 Project description

Wood-based composites usage has significantly increased in recent decades. In-service, such composites are always surrounded by some form of water, i.e. liquid water and water vapor. Interaction between wood and water is inevitable. Initial phases of this work involved investigations of the influence of wood characteristics such as tree ring and process parameters such as resin and wax loading on sorption ability.

Wood is a hygroscopic and hydrophilic material, which can absorb moisture from its surrounding environment. The interaction between wood and water has been investigated to inform a variety of view points. It was well known that wood has complicated structure and is a composite material on its own. Therefore, the significant internal structural differences between various wood characteristics react differently to moisture in the environment. In this research wood characteristics were investigated to understand influence of earlywood/latewood and tree ring location on sorption ability.

Wood fiber is commonly used in wood fiber-based composites, especially medium density fiberboard (MDF). The efficiency of MDF production is dependent on breaking down solid wood into wood fiber. The thermomechanical process is a convenient and inexpensive method to produce fiber. However, the major disadvantage of wood fiber-based composites is its hydrophilic properties. Many parameters influence

the efficiency and properties of fiber. Refining steam pressure could change fiber physical and mechanical properties. Therefore, the effect of stream pressure on sorption behavior was investigated. A better understanding of the influence of various refining conditions on the refined fiber is useful to engineer structural wood fiber-based composites.

Wood-based composites in service are always exposed to moisture in the environment; therefore, moisture absorption is unavoidable. The interaction of water and wood composites usually depends on many factors such as wood properties, additive properties, temperature, orientation of reinforcement, and reaction between water and matrix. Adhesive use is one important factor, which highly affects board properties. A better utilization of resin may lead to improved panel properties or reduced costs by lowering resin consumption while maintaining panel performance. Although most sorption research focuses on the sorption behavior of end-products in outdoor environments, understanding of the sorption behavior of individual components under processing condition is limited. The understanding of sorption and diffusion processes in different resin and wax systems will contribute to the knowledge of their performance.

Sorption issues for wood application are of concern because water is responsible for fungal attacks. Moisture sorption is dependent on various parameters such as the relative humidity of atmosphere, temperature, wood structure, and wood chemical composition. Moisture movement usually is divided into vapor diffusion through the void structure, and bound water diffusion through cell walls. Due to the complex mechanism for sorption, the investigation of sorption processes under ultra-scale could be helpful for wood utilization.

1.2 Rationale and significance

This research has the potential for far-reaching impact on the wood products industry, especially wood durability. Intrinsic moisture properties relate to mold susceptibility. A basic understanding of water properties, its behavior, and its mobility relating to mold growth is required for continued improvement of wood-based composites quality. This understanding provides tools for examining mold growth under various conditions and extends to applications in process control. This available information impacts environmental benefits of understanding the water uptake behavior of wood-based composites and its relationship to mold susceptibility.

Hot-pressing is the most important step for wood-based composites production. The hot-press consolidation process affects wood furnish, resin, wax and other additives. During pressing, it takes only a few minutes for consolidating a wood composite mat into a panel. Water vapor and wood interact during this short pressing period. The influence of resin/wax systems, steam movement, and mat densification makes sorption more complicated. Polymeric methylene isocyanate (MDI) resin requires water to cure and bond wood strands together. The high moisture sorption capacity of wood as hydrophilic material affects adhesion with hydrophobic materials and may cause material degradation and loss of strength. Therefore, sorption kinetics of wood is useful information to understand wood behavior and bonding mechanism during hot pressing, and dimensional stability and mold susceptibility during service. To better understand intrinsic moisture properties during hot pressing and in-service, the study of various parameters of wood-based composites production interacting with water is needed. The development of analytical determination methods for intrinsic moisture properties in oriented strandboard

(OSB) and MDF as function of the process variation could also be helpful. A deep understanding of sorption mechanisms and theory could also be helpful.

The significance of this research is to improve the understanding the behavious of wood strands experiencing severe environments. The behavior of various wood strands and modified wood which experience severe environment can provide benefit for wood materials application during the manufacture of wood-based composites. This knowledge has the potential to provide insight into the development of new processes and products.

1.3 Project goal and technical objectives

The overall goal of this research effort was to understand the moisture sorption of wood material. The specific objectives of this research were to:

1. Investigate the effect of differences among earlywood, latewood, and tree ring location with the stem cross section of Loblolly pine (*Pinus teada*) on water vapor sorption kinetics under ambient conditions.

2. Investigate water vapor sorption behavior of lignocellulosic fibers as affected by steam pressure of thermomechanical refining using small-scale measurements.

3. Investigate the effect of processing parameters on the sorption behavior of wood strands under varying environmental conditions.

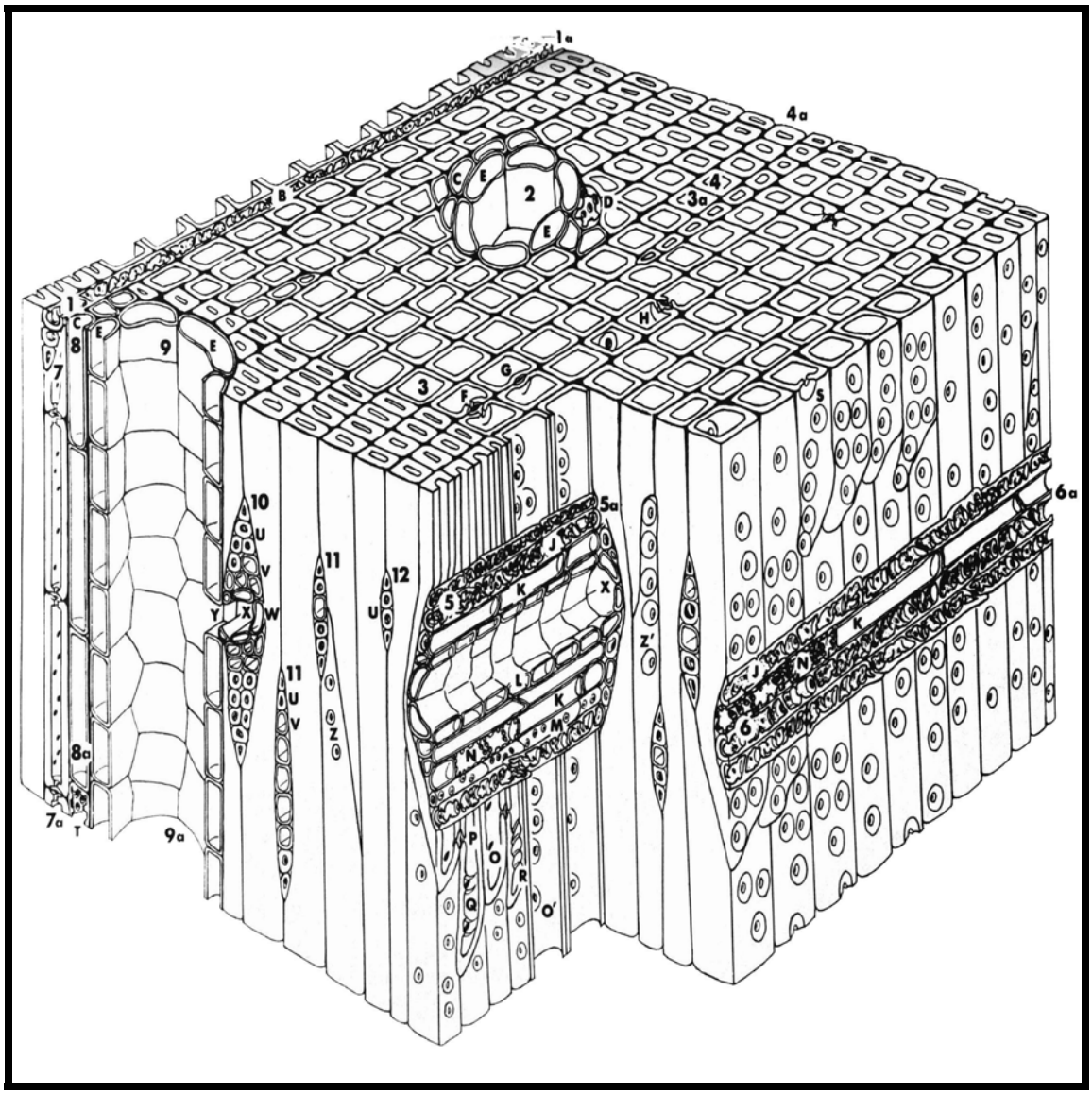
2. LITERATURE REVIEW

2.1 Introduction

This literature review section can be divided into wood characteristics, water characteristics, sorption behavior, sorption mechanism, parameters affecting sorption, and wood-based composites application involving with moisture. First, a brief description of wood structure and wood properties is presented. Second, water structure and properties are described. Third, the sorption behavior such as statics, kinetics, and energetic properties are discussed. Fourth, sorption mechanisms such as chemi-sorption and physi-sorption are described. Finally, wood applications involving with moisture and moisture influencing wood properties/composites during service are briefly explained.

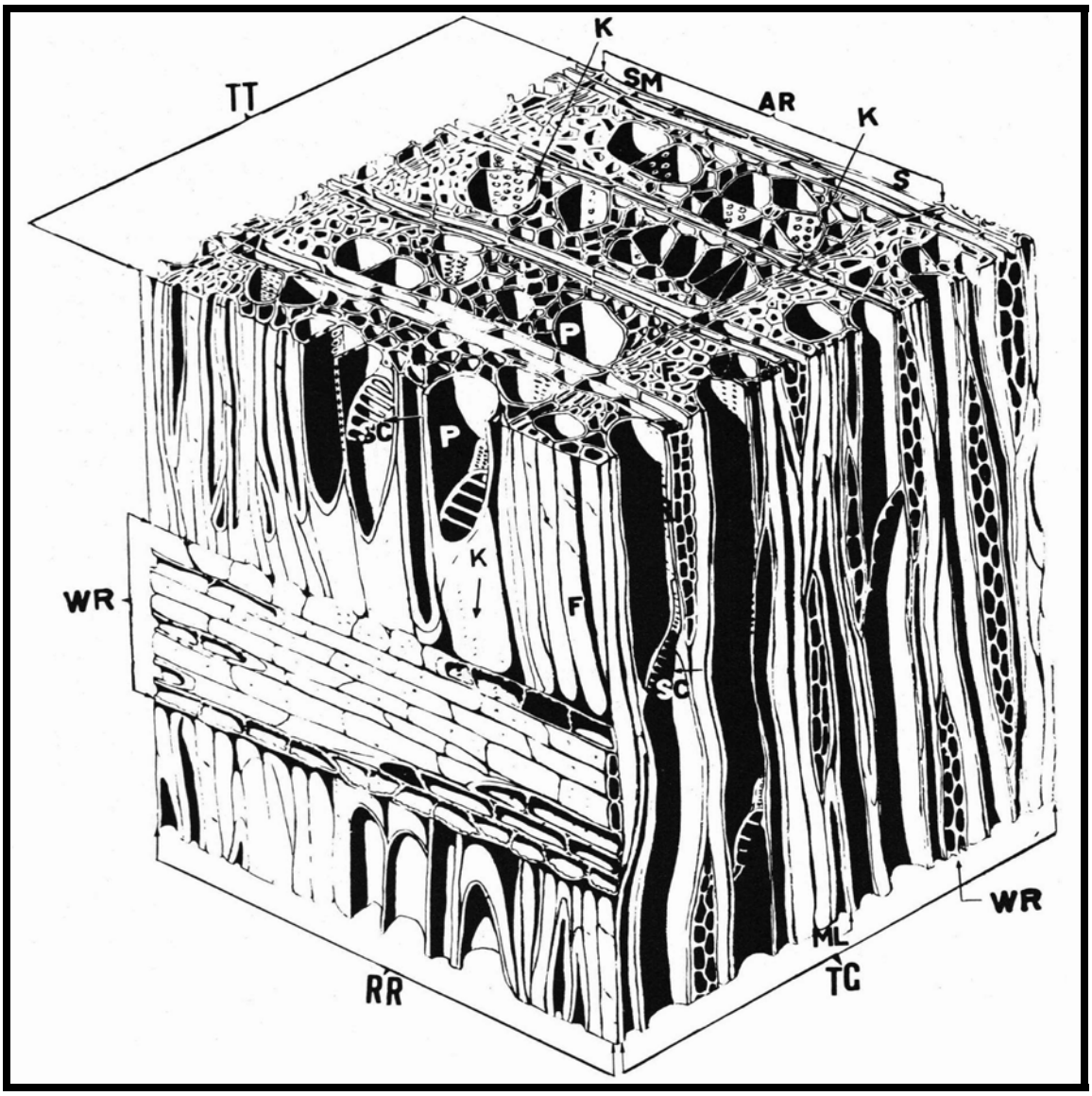
2.2 Wood structure

Woods can be traditionally divided into two categories: softwoods and hardwoods. The cell structures of softwoods and hardwoods are quite different in term of their anatomy. The alignment of cells in softwoods and hardwoods is shown in Figures 2-1 and 2-2. The softwoods normally contain 90-95% of long, slender cells which flattened and tapered closed edges. These cells are called longitudinal trachieds, which are arranged parallel to the stem axes. The storage and transport functions occur within



1-1a a ray; B dentate ray tracheid; 2 resin canal; C thin-walled longitudinal parenchyma; E epithelial cells; 3-3a early tracheids; F radial bordered pit pair cut trough torus and pit apertures; G pit pair cut below pit apertures; H tangential pit pair; 4-a latewood; 5-5a sectioned uniform ray; J dentate ray tracheid; K thin walled parenchyma; L epithelial cells; M unsectioned ray tracheid; N thicked-walled parenchyma; O latewood radial pit (inner aperature); O' early radial pit (inner aperture); P tangential bordered pit; Q Callitroid-like thickenings; R spiral thickening; S radial bordered pits; 6-6a a sectioned uniseriate heterogeneous ray; 7-7a strand tracheids; 8-8a longitudinal parenchyma (thin-walled); T thick-walled parenchyma; 9-9a longitudinal resin canel; 10 fusiform ray; U ray tracheids; V ray parenchyma; W horizontal epithelial cells; X horizontal resin canel; Y opening between horizontal and vertical resin canals; 11 uniseriate heterogeneous rays; 12 uniseriate homogenous ray; Z small tangential pits in latewood; Z' larger tangential pits in earlywood.

Figure 2-1. The cell alignment of softwood (Siau 1984).



TT cross section plane; RR radial surface plane; TG tangential surface plane. V vessels or pores; SC scalariform preformation plates; F fibers; P pits; WR wood rays; AR annual ring; S earlywood (springwood); SM latewood (summerwood); ML middle lamella.

Figure 2-2. The cell alignment of hardwood (Siau 1984).

the parenchyma cells. The hardwoods mostly contain libriform fibers and trachieds as strengthening cells, and vessel elements as longitudinal conducting cells (Fengel and Wegener 1984, Haygreen and Bowyer 1996).

The formation of the tree growth increment is generated from the vascular cambium, which results in the accumulation of xylem in any given year. The vascular cambium is a living cell layer between the wood and the bark. Figure 2-3 shows the growth increment of a 17-year-old coniferous tree. The main stem of a tree increases over a period of year. This increase appears as concentric rings when cut transversely. It appears as a cone-shaped zone of tissue, when cut longitudinally (Panshin and deZeeuw 1980). Juvenile wood is the portion of xylem surrounding the pith, in which the cells have different properties from the 'mature' wood that surrounds it. The juvenile wood cells generally have uniform diameters along the length. The juvenile wood portion generally has shorter tracheids, thinner cell walls, and larger lumen diameters. It also has lower specific gravity, larger fiber angle, lower strength, lower percentage of latewood, higher moisture content (MC), less cellulose but a higher lignin content than mature wood. The cellulose content in cell wall generally increases from pith to bark (Haygreen and Bowyer 1996). A comparison of major properties of juvenile and mature wood is shown in Figure 2-4. Growth increment shows a succession of rings around the pith called annual rings. These annual or growth rings can be identified as the abrupt changes of wood structure during the growth period. At the beginning, the developing of large lumina and cell diameter occurs whereas the small lumina and radial diameter take place at the end of growth period. This difference can be also identified as the transition of cells

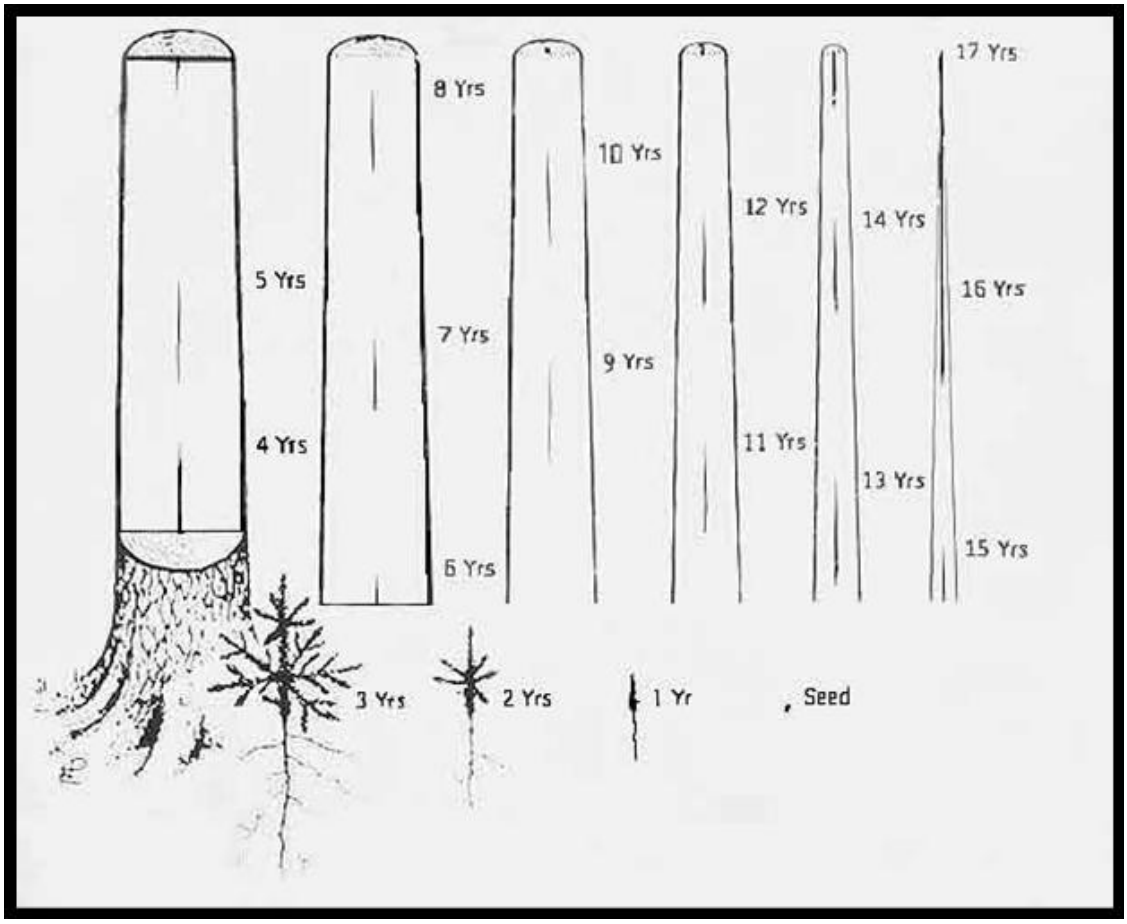


Figure 2-3. Schematic drawing of a 17-year-old coniferous tree showing the manner in which the trunk increases in thickness and in height through the addition of growth (annual increment) (Panshin and deZeeuw 1980).

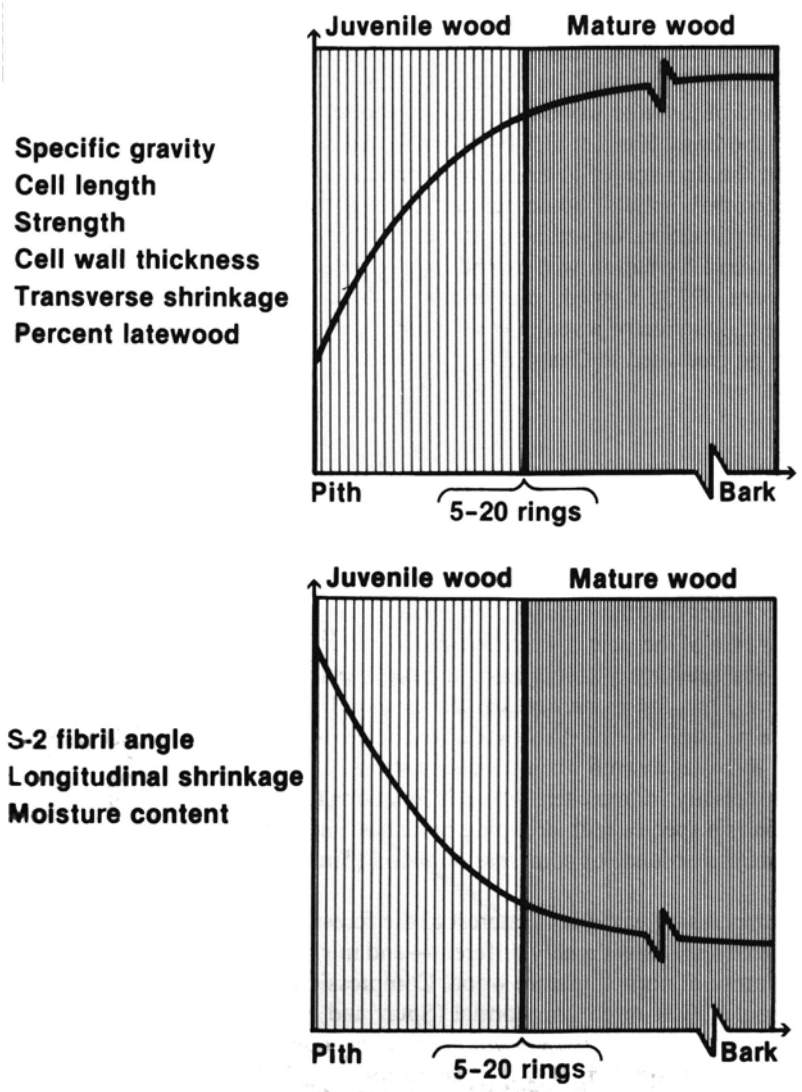


Figure 2-4. The properties of juvenile wood diagram (Haygreen and Bowyer 1996).

from earlywood to latewood. The earlywood-latewood transition is shown in Figure 2-5 and the pith structure is shown in Figure 2-6. In this transition, the cell diameters are smaller, the cell cavities are relatively large, and the cell walls are thicker for earlywood. The shape of lumen cross-sections is hexagonal for earlywood whereas it is approximately rectangular slit-shaped for latewood. The water transportation from cell to cell is through bordered pit pairs, which have circular openings. Pits contribute more than 70% of flow resistance (Banks and Levy 1980). There are between 100 and 300 pit pairs per tracheid in earlywood whereas only 10 to 15 pit pairs per tracheid were found in latewood (Time 1998). Normally the pits in latewood are smaller than in earlywood. The aspiration of pit openings of earlywood is more significant than latewood pit openings (Banks and Levy 1980).

Sapwood contains living cells whereas heartwood is completely dead. Sapwood has a lighter color whereas sometimes heartwood is darker in color. The transition of sapwood and heartwood is shown in Figure 2-7. Sapwood sometimes has significantly lower durability, lower insect-resistance, higher average MC, and higher permeability than heartwood. Liquid water is difficult to penetrate to heartwood and heartwood can be difficult to dry (Haygreen and Bowyer 1996). Sapwood surfaces of Norway spruce (*Picea abies*) are much wetter and have higher affinity to water than heartwood surfaces (Bergstrom and Blom 2006a, Bergstrom and Blom 2006b, Bertaud and Holmbom 2004, Ekman 1979,). The rate of moisture uptake was greater for sapwood samples than for heartwood samples of Scots pine (*Pinus sylvestris*) and Norway spruce (*Picea abies*) (Kortelainen et al. 2006, Lenth and Haslett 2003).

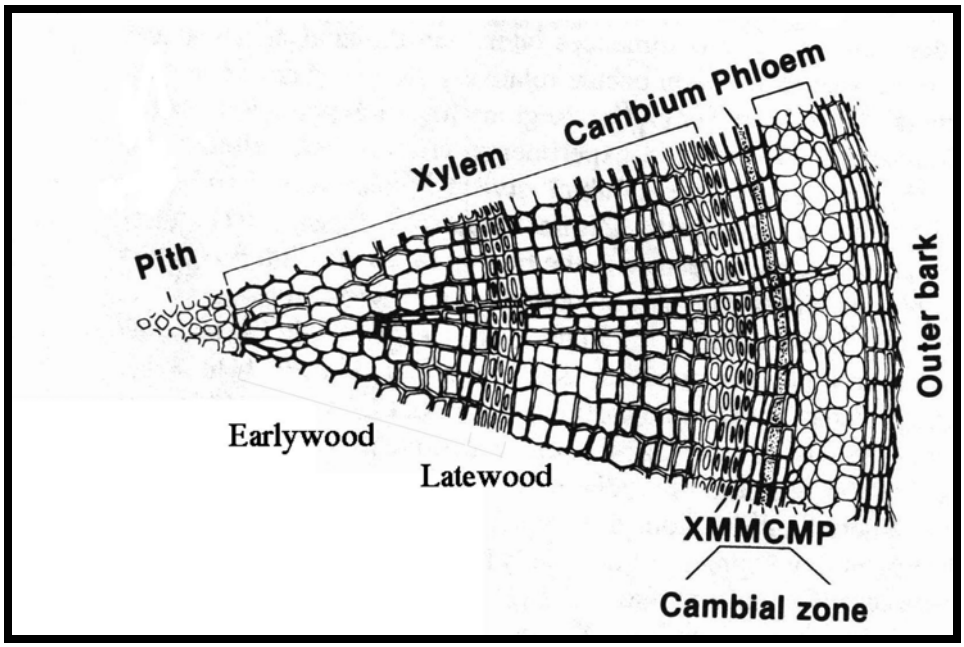


Figure 2-5. The earlywood and latewood transition (Haygreen and Bowyer 1996).

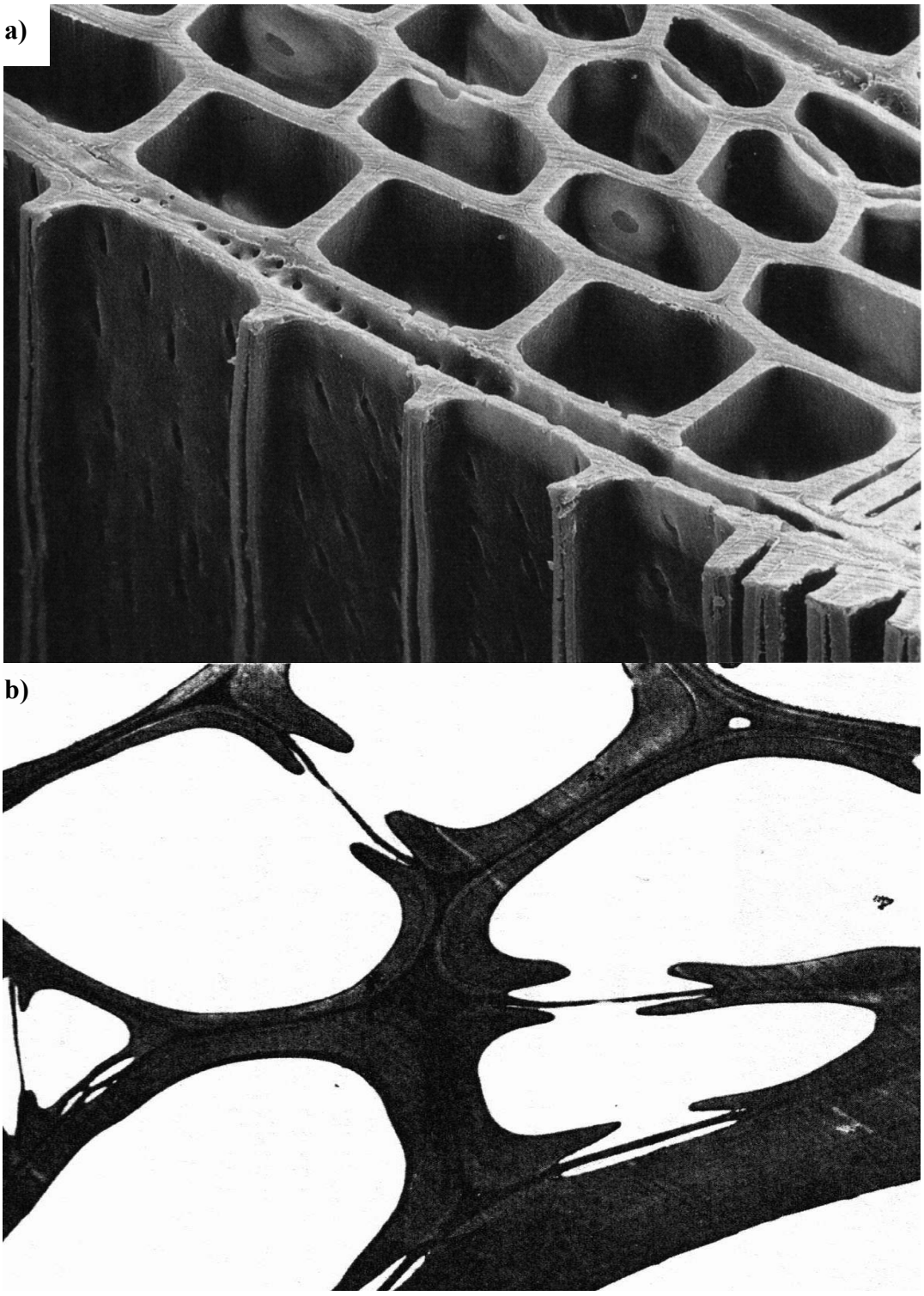


Figure 2-6. The image of bordered pit structure: a) is side-view, and b) is cross-section view (Haygreen and Bowyer 1996, Kollmann and Côte 1968).

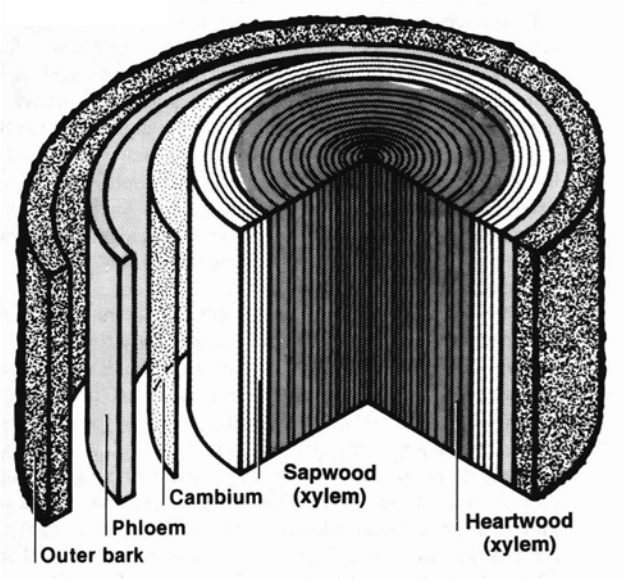
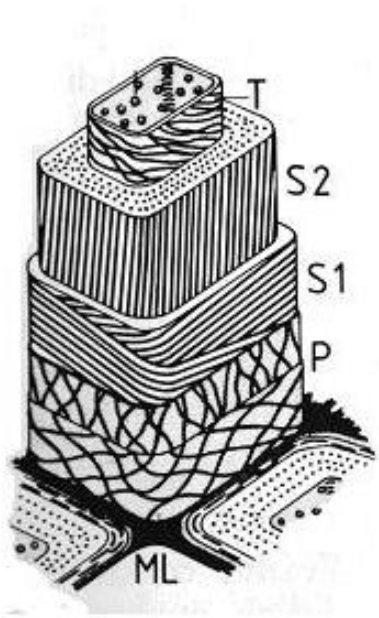


Figure 2-7. The transition of sapwood and heartwood (Haygreen and Bowyer 1996).

Cell walls play a major role in determining wood properties because of different chemical composition and orientation of the structural elements for each layer. The cell wall arrangement is shown in Figure 2-8. Cell walls are composed of primary walls (P), middle lamella (M), secondary walls (S). The primary wall is first developed in the cell wall and formed at the cambium. The secondary wall is second developed and formed inside the primary wall. The middle lamella refers to inter cellulose substance, which glues the cell together. The middle lamella and adjacent primary wall are not vividly identified. The term compound middle lamella is use for the combination of middle lamella and adjacent primary wall (Fengel and Wegener 1984). The secondary wall consists of three layers: a relatively narrow outer layer, a narrow or thin inner layer and a



ML middle lamella; P primary wall; S1 secondary wall1; S2 secondary wall2; T or S3 tertiary wall or secondary wall3.

Figure 2-8. The model cell wall arrangement (Fengel and Wegener 1984).

middle layer of variable thickness. The thickest middle layer (S2) has fibril oriented approximately parallel to the long axis, which is oriented from 10 to 30 degree from the cell axis. The inner layer (S3) has fibril oriented from 60 to 90 degree from the cell axis and outer layer (S1) has helical slope from 50 to 70 degree to the longitudinal axis. The tertiary wall (T) is inner layer of secondary wall (S3) at the luminal layer (Haygreen and Bowyer 1996).

The wood cell is composed of three groups of structural substances: framework, matrix and encrusting materials. The schematic structure of a portion of cellulose microfibril with crystalline and amorphous regions is shown in Figure 2-9. The cellulose

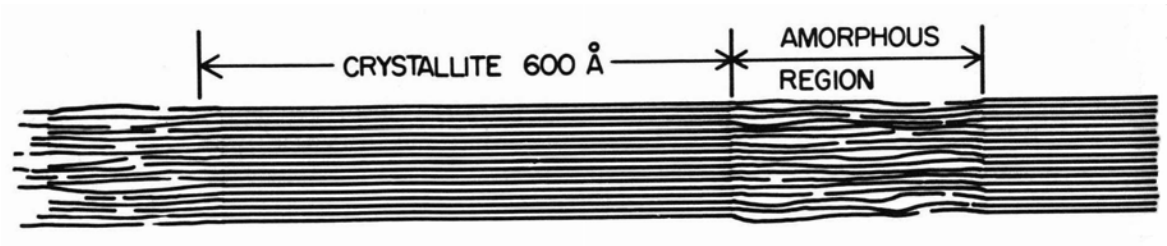


Figure 2-9. The schematic structure of a portion of cellulose microfibril with crystallines and amorphous (Siau 1995).

normally acts as a framework substance occurring in the form of microfibril. The closely packed portion of microfibril is the crystalline region and this microfibril is joined together by less dense and less orderly amorphous regions. The microvoids in microfibril frameworks are filled with the amorphous substrances as matrix and encrusting substances. Hemicelluloses and other carbohydrate materials (excluding cellulose) are associated with the cell wall as the matrix substances. Lignin is a three-dimensional polymer with apparently no ordered arrangement and provides clear evidence of microvoid system in the cell wall. Lignin in wood is concentrated on the middle lamella and primary wall (Bodig and Jayne 1982, Siau 1995).

The chemical composition of cell walls is shown in Figure 2-10. The S2 layer has higher cellulose than S3 and S1 whereas S1 layer has more lignin than S2 and S3 layer. The S3 layer has more hemicelluloses than S2 and S1 layer. The S1 and S3 has thinner layer than S2 and the S3 layer appears to be more heavily lignified than S2 (Haygreen and Bowyer 1996, Panshin and deZeeuw 1980).

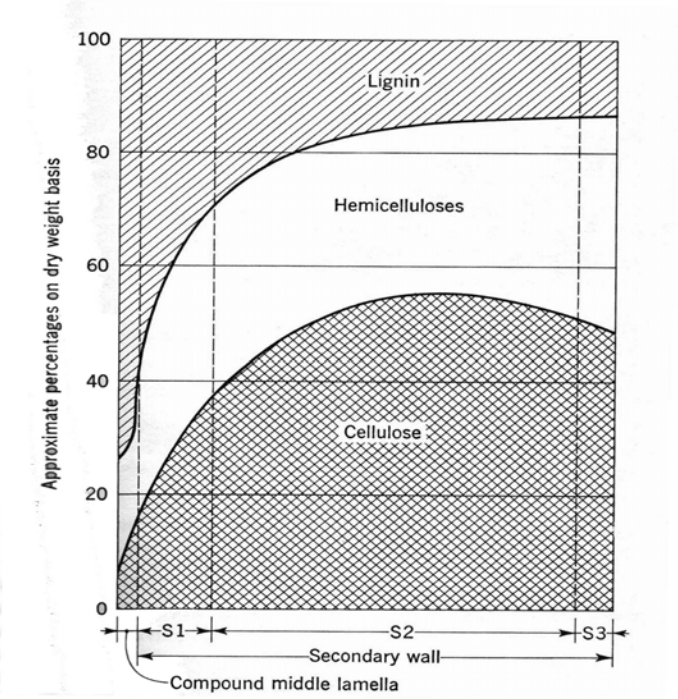


Figure 2-10. The chemical composition in cell wall layer (Panshin and deZeeuw 1980).

2.3 Wood chemistry

Cellulose is a major and the simplest wood component of the cell wall components. This cellulose is a linear high-molecular-weight polymer, which is built from β-D-glucose. The number of glucose units in cellulose (degree of polymerization) varies from a few to 15,000 units depending on the location in cell wall. Cellulose consists of (1-4)-link β-D-glucoglycan unit, which is joined to form a linear-molecular chain. These glucose units are presented as a C1-chair conformation with the three *OH*-groups all equatorial (Bodig and Jayne 1982, Fengel and Wegener 1984). Forty to 50% of wood mass is composed of cellulose, which is largely responsible for the water

adsorption characteristics of the materials because of its numerous *OH*-groups (Siau 1984). Figure 2-11 shows the structure of cellulose.

Hemicelluloses closely associate with cellulose in the cell wall. Most hemicelluloses comprise two carbohydrate polymers; a xylose- and a mannose-containing polysaccharide. The molecular chains of these hemicelluloses are much shorter than cellulose. Hemicelluloses have a side-group and a branch-group. Hemicelluloses are more associated to lignin than cellulose because of its amorphous state. Hemicelluloses are relatively low-molecular-weight polysaccharides. Xylan is the predominant type of hemicelluloses in hardwoods. Xylan is a polyose with a homopolymer backbone of xylose units. It is linked by β-(1-4)-glycosidic bonds (Bodig and Jayne 1982, Fengel and Wegener 1984, Kollmann and Côte 1968). Figure 2-12 shows the structure of hemicelluloses. Twenty-five to 30% of total wood mass is hemicelluloses, which contribute to wood's hydrophilic properties (Ma and Rudolph 2006). The loss of hemicelluloses by any process can reduce hygroscopic properties and increase resistance to attack by micro-organisms (Rowell et al. 2002).

Lignin is a three-dimensional polymer with apparently no ordered arrangements. The molecules of lignin comprise an aromatic system of phenylpropane units, which are linked together by C-O-C and C-C linkage (Bodig and Jayne 1982, Fengel and Wegener 1984, Kollmann and Côte 1968). Lignin is an amorphous substance located in the compound middle lamella as well as in the secondary walls. Lignin can be softened at temperatures of 165-175ºC. Twenty to 30% of total wood mass is lignin, which has much less attraction to water than the holocelluloses (Ma and Rudolph 2006). Figure 2-13 shows the structure of lignin.

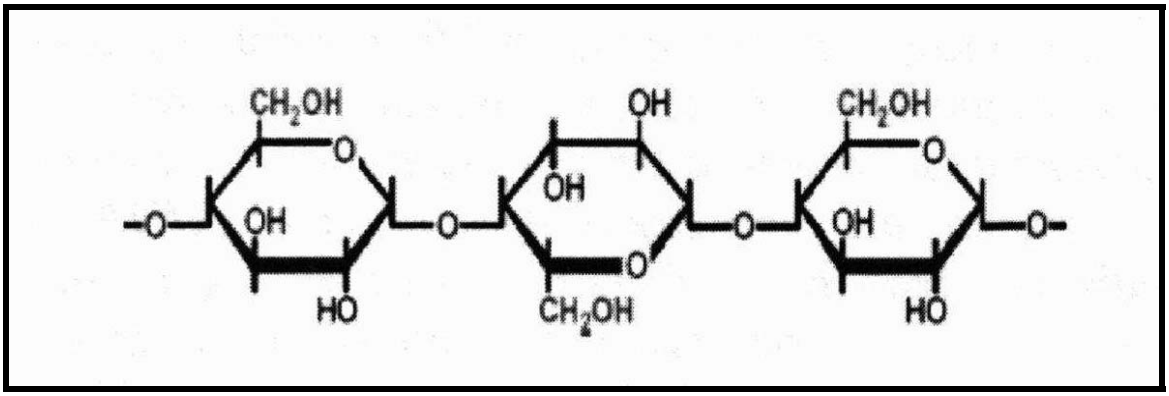


Figure 2-11. Schematic representation of structure of cellulose (Li et al. 2006).

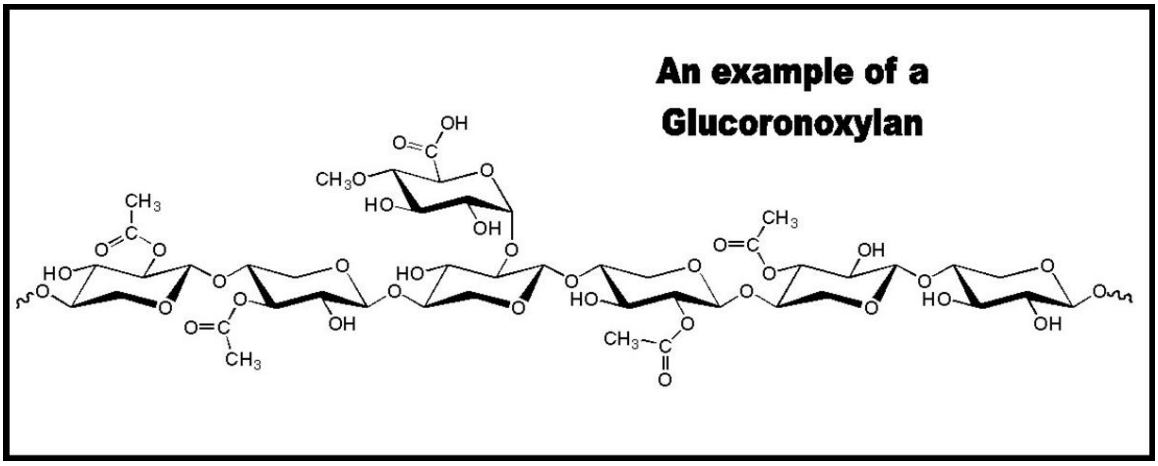


Figure 2-12. Schematic representation of structure of hemicelluloses (Adler 1977).

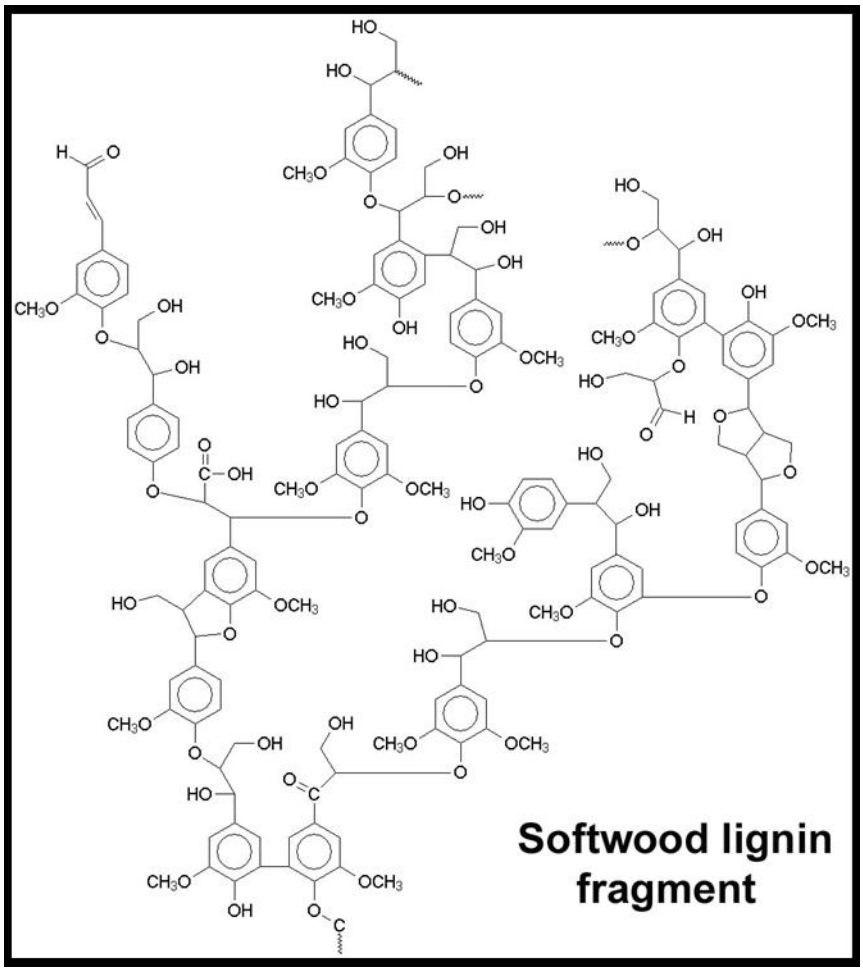


Figure 2-13. Schematic representation of structure of lignin (Adler 1977).

Minor substances are found in small amount of extractives such as starch, pectic substances, terpenes, aromatic compound, aliphalic compound, alcohols, inorganic substances, etc. Aromatic (phenolic) compounds include tannin. Aliphatic acid is saturated and unsaturated higher fatty acids. It is found mostly in the form of their esters with glycerol (fat and oils) or higher alcohols (waxes). Alcohol is mostly aliphatic alcohol occurring as ester compound whereas the aromatic sterols are mainly found as glycosides. Inorganic substances include potassium, calcium and magnesium (Fengel and Wegener 1984).

A comparison of major elemental constitutes of wood is shown in Table 2-1. A higher percentage of hemicelluloses and lignin is found in softwoods whereas the percentage of cellulose is barely different between hardwoods and softwoods. In case of sorption properties, it has been stated that the sorptive capacity of the hemicelluloses is greater than that of cellulose, whereas the sorptive capacity of lignin is less (Christensen and Kelsey 1958).

Table 2-1. A comparison of the chemical composition of softwood and heartwood (Kollmann and Côte 1968).

Type	**Cellulose**	**Hemicellulose**	**Lignin**
	(% dry weight)		
Hardwood	40-44	15-35	18-25
Softwood	40-44	20-32	25-35

2.4 Physical nature and mechanics of wood

The brief description of anatomical and chemical properties of wood has already been explained. However other two important properties should be explained: physical properties and mechanical properties.

2.4.1 Physical properties of wood

The physical properties basically involve the inherent structural organization of wood. These properties can be explained in five ways: (1) the amount of cell wall substances in proportion to the wood volume, (2) the amount of water in the cell wall, (3) the proportion and quantity of the primary components of the cell wall including the extractive substances, (4) the type, size, proportion, and alignment of various cells making the woody tissue, and (5) the wall orientation of cells in different types of cell.

The first point mainly involves the specific gravity, which is closely related to physical properties. The second point relates to MC, which affects dimension change, plasticity, and energy transfer in wood. The third point involves the variability between different kinds of wood. The last two points involved the wood grain direction (Panshin and deZeeuw 1980).

Water existing in wood has two different forms: mobile and immobile water. Mobile water generally is called unbound or free water, which is loosely absorbed on wood surface and inside of lumen. Immobile water is hydrated in the crystalline structure with hydrogen bonding. Sometimes this water is trapped with amorphous structure (Zografi 1988). The bound water can be divided into freezing bound water and non-freezing bound water (Hatakeyama et al. 2000). The first phase transition (melting or

crystallization) of water was called freezing water whereas no transition down to 130°K (≈ -143°C) was called non-freezing water (Berthold et al. 1994). The sum of nonfreezing and freezing bound water is equivalent to the fiber saturation point. The movement of water molecules in the outer layer of nonfreezing water and bulk water is quite equivalent. The nonfreezing water is dependent on the number and type of adsorption sites (Maloney at al. 1998). The MC at which the cell wall is completely filled with water is called the fiber saturation point (FSP). The MC at equilibrium with relative humidity (RH) of the ambient air is called the equilibrium moisture content (EMC) (Siau 1995).

2.4.2 Mechanical properties

Mechanical properties involve wood behavior under applied forces. This behavior can be expressed in many ways, depending on force types and wood organization. The force per unit area or volume is called stress. This stress can be divided into compressive, tension, shear, and bending stress. The change in shape and size after applied stress is called strain, which is presented as deformation per unit area or volume. If the deformation is completely and instantaneously recoverable, it is called elastic deformation. If this deformation is only partly recovery, it is called plastic deformation (Bodig and Jayne 1982). Plastic deformation starts with the first application of load and increases with time. Plastic deformation can described in two ways: (1) under a constant magnitude of load wood deforms plastically in direct relation to the duration of the load application known as creep, (2) under constant deformation and a decreasing magnitude of stress resistance to the deformation with increasing time know as relaxation. The

elastic and plastic behavior in wood is generally combined together (Panshin and deZeeuw 1980).

The strength properties and elastic characteristics are closely related to moisture content in wood, particularly below the fiber saturation point (around 25% MC). The strength increases with the moisture drop. It varies inversely with the moisture content of the wood below the fiber saturation point. The moisture drop can produce the differences in specific gravity which results in strength change. When the wood dries below the fiber saturation point, water is removed from the cell wall. The cellulose molecules move closer together and form the tightly bonded (Haygreen and Bowyer 1996, Panshin and deZeeuw 1980).

2.5 Water characteristics

Water can exist in three phases depending on the temperature and the pressure of its environment: (1) solid, (2) liquid, and (3) vapor. The phase diagram for water is shown in Figure 2-14. Some phases of water can coexist at some temperatures and pressures. At the critical temperature (374°C) and pressure (218 atm) (≈ 221 bars), the liquid and vapor phase is no longer distinguishable. In the liquid phase, most molecules have insufficient vibrational energy to attract the adjacent molecules. However due to the wide ranges of energy among molecules, the individual molecule has momentarily sufficient energy to escape from the force field and become a vapor molecules. The pressure against this escape is called vapor pressure. The higher temperature makes the higher amount of water vapor molecules and adding to the vapor pressure. In the liquid phase, the average distance between the centers of water molecules is calculated by using

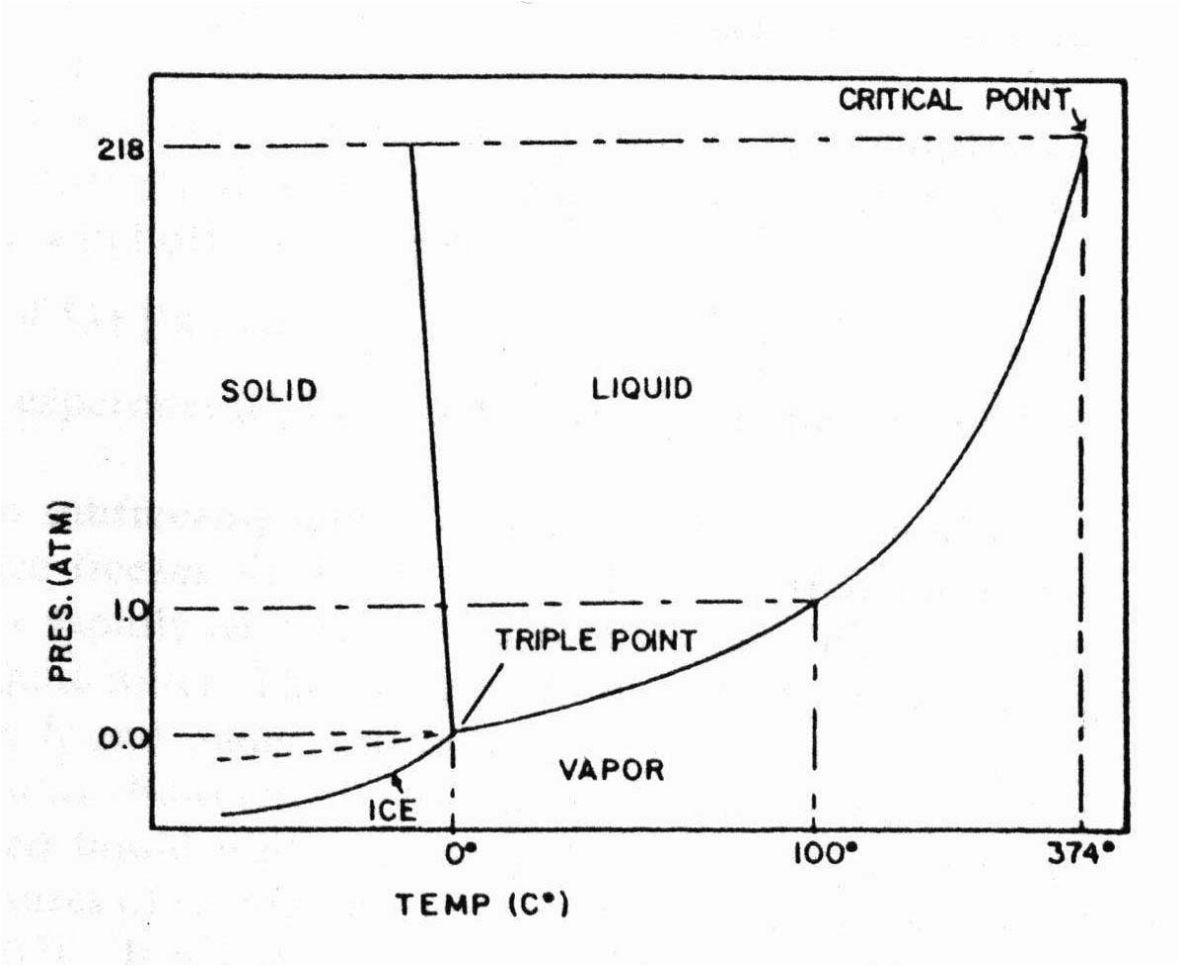


Figure 2-14. The phase diagram of water (not to scale) (Skaar 1988).

Avogadro's number (6.02 x 10^{23} molecules/g mol). The water molecule generally has the gram molecular weight of approximately 18 g/mol, and its molar volume is 18 cm^3 at room temperature. One water molecule occupies 18/(6.02 x10^{23}) = 30 x 10^{-24} cm^3 and the average distance between molecules is around 3 x 10^{-8} cm or 30 nm. A water vapor molecule has a space around it that is 8 to 60 times larger than that of liquid water molecules (Skarr 1988).

Water activity (a_w) or equilibrium relative humidity (ERH) is approximated by relative vapor pressure of water (P/P_0) and is a traditional indicator of water availability (Scott 1953). Both a_w and ERH are commonly used to describe the free water of a substance (Labuza 1984). The a_w is defined as the vapor pressure ratio of substance (P_{sub}) to pure water (P_{H_2O}) at the same temperature (Bessadok et al. 2007).

$$a_w = \frac{P_{sub}}{P_{H_2O}} \tag{2-1}$$

$$ERH = \frac{P_{sub}}{P_{H_2O}} \bullet 100 = a_w \bullet 100 \tag{2-2}$$

The a_w was used to monitor microbial safety and is dependent on food composition. However, mold germination is poorly correlated with a_w. Water mobility has better correlated with biological activity, which depends on glass transition temperature (T_g) than a_w. At a glassy state, water has high mobility (Pham et al. 1999). For composite use, OSB specimen has a_w ranging from 0.33 to 0.83 after 30 hours hours treatment under 100%RH. This level of a_w is high enough for spore germination. Comparing mold susceptibility of OSB made from southern pine and aspen, southern pine OSB has higher mold susceptibility than aspen OSB (Ye et al. 2006).

The nuclear magnetic resonance (NMR) relaxometry is a novel technique to monitor the molecular mobility and water availability of water by NMR water relaxation times. Water molecules can interact with another water molecule and/or with molecules of wood polymer. The mobile water molecules take a long time to reach the equilibrium point but it relaxs very slowly and take a very long time. Spin-lattice relaxation time (T1) is defined as the time constant characterizing the relaxation process that the excited protons releases energy back into the ground stage. This T1 relaxation is explained as the interaction between water molecules and other molecules surrounding them. Spin-spin relaxation time (T2) is defined as the time constant characterizing the exponential decay of the relaxation process from purely random spin-spin interactions in the transverse plane. The T2 relaxation was described as the interaction among water molecules (Ye et al. 2006).

2.6 Sorption behavior

Sorption commonly includes adsorption (and/or absorption) and desorption. Absorption and adsorption are completely different. Absorption is capillary action by pore or void in wood. This process generates little heat and swelling. On the other hand, adsorption is a formed-solution process. This process generates heat (heat of sorption) and swelling. For wood picking up moisture, this process is mainly an adsorption process. However, wood is porous materials. Both absorption and adsorption take place. Therefore, the term ‘uptake and/or sorption’ was used for porous materials (Chin et al. 1999). The diffusion (D), sorption (S), and permeation (P) coefficients were estimated in order to determine the transport behavior of water into wood (Kumar and Siddaramaiah

2007). Sorption generally is divided into three types: (1) statics of sorption such as sorption isotherm, which mostly is involved with vapor pressure, (2) kinetics of sorption such as velocitits of sorption, and (3) energetics of sorption such as heat of sorption (Sheppard and Newsome 1934).

2.6.1 Static of sorption

Sorption statics are described as sorption capacity at equilibrium point. Several moisture sorption theories have assumed that moisture is taken up by wood internal sorption sites attractive to water. Most natural cellulosic material follows the types 2 sigmoid isotherm (Stamm and Smith 1969). The five types of sorption isotherm are shown in Figure 2-15. Several theories are used to describe the moisture sorption isotherm of biological materials. Sorption isotherm theory is divided into three categories: (1) monolayer models, (2) multilayer models, (3) empirical models. Two approaches are used to develop theoretical sorption theory: firstly, sorption is considered as a surface phenomenon, and secondly sorption is considered as a solution phenomenon. The major sorption isotherm theory was described as follows:

The Brunauer-Emmett-Teller (BET) theory is described as the sorption of gases on surfaces. It assumed that one to many layers of water molecules may be sorbed on these sorption sites and the thermodynamic properties of the secondary layers of water are essentially the same as those of the liquid water (Brunaeur et al. 1938). It is a multilayer sorption model. This BET theory is modified from Langmuir, which assumed that only a single layer of vapor molecules could be condensed on these internal surface. The BET sorption equation is shown as follows:

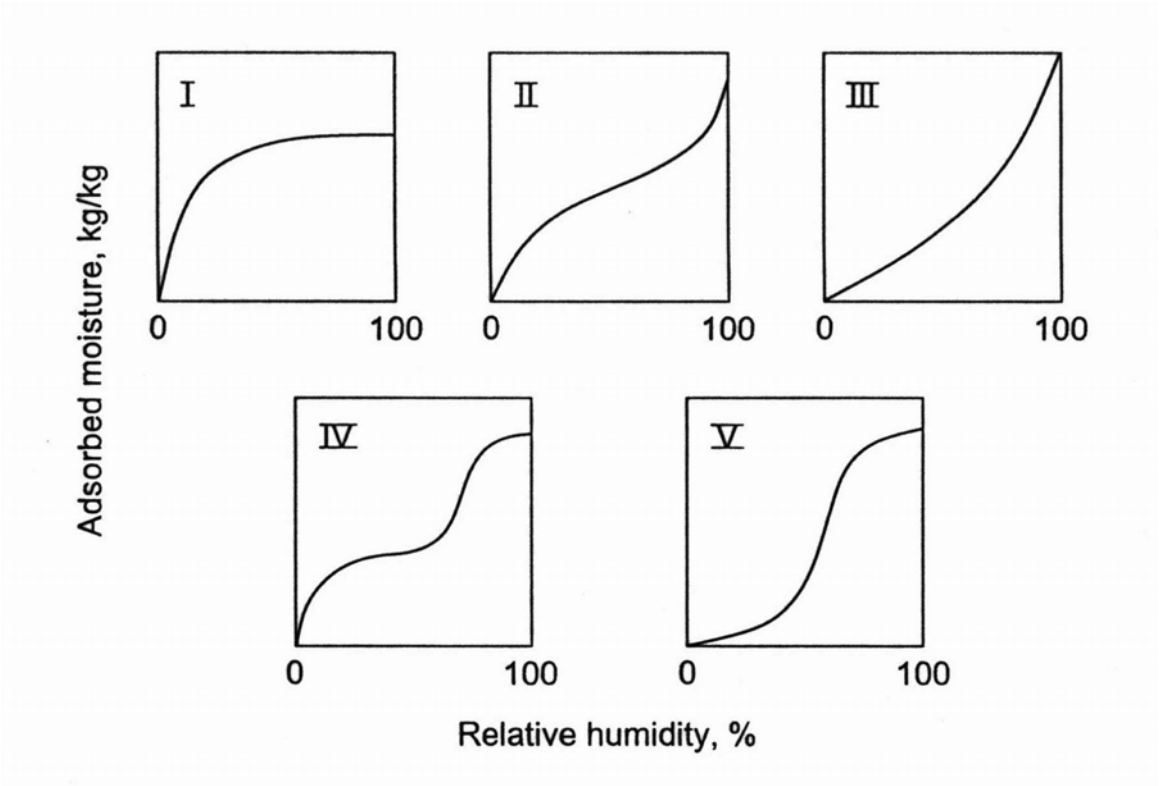


Figure 2-15. The five types of sorption isotherms (Time 1998).

$$m = \frac{m_0 Ch}{(1-h)}\left(\frac{1-(n+1)h^n + nh^{n+1}}{1+(C-1)h - Ch^{n+1}}\right) \tag{2-3}$$

where:

$m_0 =$ the moisture content fraction corresponding to complete monolayer coverage of all available sorption sites.

$m =$ the moisture content fraction of water absorbed.

$h =$ the relative humidity fraction.

$C =$ a parameter related to the binding energy of water vapor molecules to the surface.

$n =$ the number of sorbed layers.

The Dent theory is modified from BET theory, in which water is presumed to be sorbed in two forms. The primary molecules are sorbed on primary sorption sites within the cell wall and secondary molecules are sorbed on secondary sites. Primary sites have high binding energy from accessible *OH*-group whereas secondary sites have lower binding energy from the rest. Dent's theory assumes that the thermodynamic properties of secondary water are different from ordinary liquid water (Dent 1977). The Dent sorption equation is shown as follows:

$$m = \frac{m_0 b_1 h}{(1-b_2 h)(1-b_2 h + b_1 h)} \tag{2-4}$$

where:

$b_1 =$ the parameter that describes the primary molecules compared to the external condensed liquid in saturated vapor.

b_2 = the parameter that describes a relationship between the secondary adsorbed molecules to that of the external condensed liquid.

The Hailwood-Horrobin (H-H) sorption theory assumptions are identical to Dent model. The H-H model is an empirical model from sigmoid type 2 isotherms, whereas Dent's is theoretical (Skarr 1988). The Hailwood-Horrobin theory describes a part of the sorbed water as a hydrate with the wood and the balance is a solid solution in the cell wall. In the model derived here only a single hydrate is considered. The cell wall is presumed to consist of three chemical species: dry wood, hydrated wood, and dissolved water (Hailwood and Horrobin 1946). Based on these assumptions, the following model was developed.

$$m = \frac{m_0 Ch}{1+Ch}\left(\alpha \sum_{i=0}^{n-1} h^i + (1-\alpha) \sum_{i=0}^{p-1} h^i \right) \tag{2-5}$$

where:

m_0 = the moisture content fraction at the unimolecular layer formation.

m = the moisture content fraction of sorbed water.

h = the relative humidity fraction.

C = the constant related to the binding energy of the water molecules to the adsorption site. The fraction of the adsorptions sites that contain up to p>n layers.

i = the number of sorbed layers.

The above equation can be reduced to the following equation.

$$m = \frac{m_0 Ch}{1+Ch}\left(\frac{1-\alpha h^n - (1-\alpha)h^P}{1-h} \right) \tag{2-6}$$

The BET and Dent theory is based on multilayer concept whereas the H-H theory is based on an ideal solution concept (Hartley and Avramidis 1994).

2.6.2 Kinetics of sorption

Sorption kinetics is mainly defined as the rate of sorption in materials. During the last century, two techniques of diffusion measurement were developed. The first one is the traditional cup method based on Fick's first law in a steady state experiment. This method is not quite valid for bound water diffusion because its boundary condition is not satisfied. The second one is the sorption method based on Fick's second law in an unsteady state experiment. This method overcomes the disadvantage of the cup method. However, this method requires the assumption of a constant diffusion value, which results in significant errors due to the mass transport problems (Olek et al. 2005). This rate of sorption can be divided into the steady state and the unsteady state. In the unsteady state, dynamic diffusion coefficient of a liquid or vapor into medium under continuously change its boundary condition or both flux and gradient are variable in space and time. In steady state, static diffusion coefficients are calculated under a uniform rate of transfer through a fixed distance, with a specified concentration gradient or constant (Lehmann 1972).

For steady state, diffusion is defined as molecular mass flow or a gradient of concentration of diffusion substances (Siau 1995). Fick's first law is applied and derived from Darcy's and Fourier'law for wood and it is expressed as:

$$D = \frac{w/tA}{\Delta C / L'} \tag{2-7}$$

where:

D = the water vapor diffusion coefficient (m^2/s).

w/t = the rate of water vapor transport (kg/s).

A = the cross-section area of specimen normal to the direction of flow (m^2).

L = the length in the flow direction (m).

ΔC = the concentration of difference (kg/m^3).

Bound water diffusion coefficient is described as the unsteady state. The plot of moisture content fraction (E) vs. square root of time is used to calculate diffusion coefficients. The linear part should be up to two thirds of the equilibrium value and the linear plots intersected should cross the origins (Siau 1995). The diffusion coefficient calculated is expressed as follows:

$$D = \frac{\pi L^2 E^2}{16t} \tag{2-8}$$

where:

D = the diffusion coefficient of the cell wall in the longitudinal direction (m^2/s).

E = the fraction of moisture content at time t to that at equilibrium.

In the plot of E vs. square root of time, the linear portion of the plot does not intersect the origin due to surface resistance. The initial sorption technique is used for diffusion coefficient calculation. However, it is able to separate the surface resistance from the internal resistance by expressing both the surface emission coefficient and the bound water diffusion coefficient in wood (Choong and Skaar 1969, 1975). The moisture sorption rate by wood generally is controlled by the external surface resistance due to the boundary layer and the internal surface resistance due to the wood characteristics itself. The boundary layer depends on the difference between MC and the wood surface (Skaar

1984). The sum of the two resistances is called total surface resistance. However, cell wall relaxation is a major parameter in surface resistance during sorption (Siau 1995). The true diffusion coefficient is due to the internal resistance alone, whereas the surface emission coefficient includes external resistance. The surface emission coefficient typically is the inverse of the surface resistance. The measured or apparent diffusion coefficient includes both external and internal surface resistance. However, the moisture diffusion is a combination of two mechanisms: the vapor diffusion through the void structure, and the bound water diffusion through the cell walls (Avramidis and Siau 1987, Droin et al. 1988).

2.6.3 Energetics of sorption

Sorption energetics mostly involves heat of sorption. Enthalpy increases during transition of water from solid to vapor state. The solid state has lower enthalpy than the liquid phase. The enthalpy increases with increasing MC until the fiber saturation point. At this point the enthalpy is identical to liquid phase. The differential heat of sorption is well known as the different binding energy between wood and water. The determination of different heat of sorption can be divided into two methods: the isosteric method, based on the Clausius-Clapeyron equation at different temperature, the calorimetric method, based on the direct heat of melting from calorimetry (Skarr 1988, Yasuda et al. 1995). The Clausius-Clapeyron equation is shown as follows:

$$\frac{d \ln a_w}{d[1/T]} = -\frac{Q_n^{st}}{R} \tag{2-9}$$

where:

Q_n^{st} = the net sorption isosteric heat (kJ/kg).

R = the gas constant (kJ/kg K).

a_w = the water activity (decimal fraction of equilibrium relative humidity).

T = the absolute temperature (K).

The integral heat of sorption is difficult to measure directly by calorimetry due to the extremely small amount of wood and need for constant MC. Heat of sorption is defined as the heat generated per gram of dry wood during sorption. Total heat of sorption is the heat generated during sorption from MC at zero percent. The difference between heat generated from zero moisture to any MC was called integral heat of sorption (Skarr 1988).

The differential heat of sorption is also known as the isosteric heat of sorption. It is an indicator of the state of water adsorbed by the solid medium. The net isosteric heat is the total heat of sorption in the medium minus the heat of vaporization of water at any temperature. The differential entropy of any material is the proportion of the number of available sorption sites at a specific energy level. The isosteric heat of sorption was found to increase with decreasing MC whereas the net equilibrium heat (net integral enthalpy) decreases with increasing MC (Muhtaseb et al. 2004).

The calorimetric approach obtains enthalpy change by measuring the heat generated in the process of completely wetting wood in water. The heat lost during measuring can decrease the precision of measurement. The isosteric approach calculates the differential thermodynamic properties of moisture sorption by wood based on the sorption isotherm. This approach assumes that the sorption process is reversible although

it is not perfectly reversible because of hysteresis and time-dependent phenomena (Cao and Kamdem 2004).

2.7 Sorption mechanisms

The important sorption sites of wood polymers by water are hydroxyl groups (-*OH*), carboxylic acid groups (-*COOH*) (mostly in the xylan of the pulp) and sulfonic acid (-$S(=O)_2$-*OH*) groups (mainly in lignin after sulfonation reaction) (Berthold et al. 1994). Moisture sorption by cellulose predominantly occurs in the disordered region. However the sorption mechanism can be divided into three regions based on the sorption isotherm. Region I corresponds to the RH range from 0% to 30% and represents chemi-sorption. Region II ranges from 30% to 55% as physi-sorption and region III is at the higher relative humilities as capi-sorption (capillary condensation) (Hartley et al. 1992). Hartley and Avramidis (1993, 1994) presented more details for these region based on the Zimm-Lundberg water cluster analysis. The transition points at 25°C are 47% RH (Region I to Region II) and 94% RH (region II to region III) (Figure 2-16). These critical points have an EMC of approximately 8% and 21%, respectively. The water inside the cell wall is divided into three fractions: the freezing water in the relatively small pores, non-freezing water in the relatively small pores, and bulk water in relatively large pores (Maloney and Poulapuro 1999).

Another aspect of sorption has three basic mechanisms: (1) the monolayer of water molecules is formed with the hydrogen bonds at polar sites on molecular surfaces of the crystalline region of the cell wall, (2) the multilayer is formed in solid solution, (3) the capillary condensation based on the Kevin equation is involved with the condensation

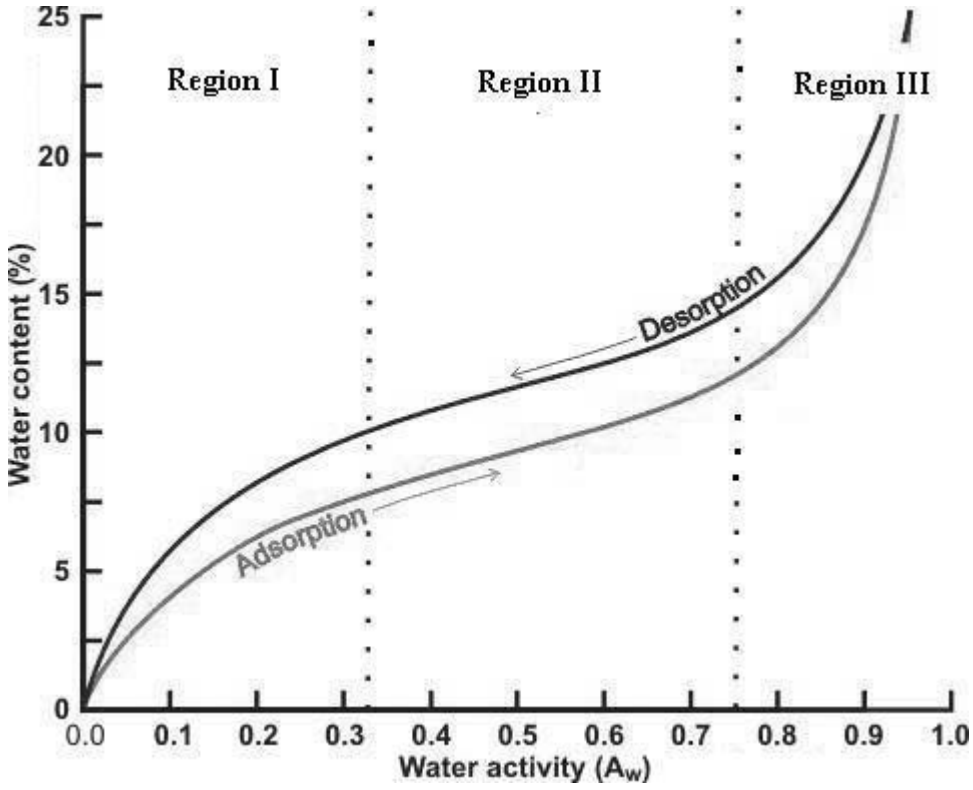


Figure 2-16. Sorption mechanism: region I is chemi-sorption, region II is physi-sorption, region III is capi-sorption (adapted from Hartley et al. 1992).

of water vapor relative to vapor pressure and capillary size (Wangaard and Granados 1967). The Kevin equation is shown as follows:

$$\ln(1/h) = 36\gamma/(rRT) \tag{2-10}$$

where:

γ = the surface tension of the air-water interface (N/m).

r = the capillary redius (m).

R = the gas constant (kJ/kg K).

h = the relative humidity (decimal fraction of relative humidity).

T = the absolute temperature (K).

2.8 Parameters affecting sorption

There are several factors affecting sorption behavior in wood. This section can be divided into surface modification, heat treatment, wettability, water activity, and crystallinity.

2.8.1 Surface modification

The early state of sorption involves the surface phenomenon. The surface modification of wood, particularly wood fibers may influence sorption properties. Various surface modifications can reduce water sorption. Mercerization is a technique to immerse fiber in a sodium hydroxide solution. Latex coating is the dipping of fiber into natural rubber latex. Gamma irradiation is a technique involving expose to gamma radiation. Silane treatment is the dipping of the fiber in an alcohol-waxes mixture containing a tri-ethoxy vinyl silane coupling agent. Isocyanate treatment is a technique

for treating fibers with toluene diisocyanate. Acetylation is a treatment of fibers with acetic anhydride. Peroxide treatment is a technique to treat fibers with benzoyl peroxide. All these treatment can reduce water sorption (Sreekala and Thomas 2003). Most chemical treatments result in the lower levels of EMC at a given RH. Some chemical treatment makes substitution of cell wall *OH*-groups with an acryl group (*–(O=)C-CH=CH$_2$*) in order to remove the potential sorption site. This acryl group occupies space within the cell wall, which is denied to any sorbed water molecules (Papadopoulos and Hill 2003).

2.8.2 Heat treatment

Heat treatment is a very old technique to improve the durability of wood. It also causes darken color, enhances dimensional stability, reduces EMC. It is obvious that heat treatment can change absorption capacity of wood (Kortelainen and Viitaniemi 2006, Kumar and Siddaramaiah 2007, Rousset et al. 2004, Wahl et al 2004). This can be explained by many hypotheses (Hakkou et al. 2006, Rowell et al. 2002): (1) a low affinity to water or increase hydrophobic character, which is unfavorable for fungi growth, (2) generation of toxic compounds acting as fungicides, (3) degradation hemicelluloses, which is main nutritive source for fungi, (4) weight loss due to wood degradation, which reduces concentration of accessible *OH*-groups, causing to reduction in EMC, and (5) increase in the diffusion coefficient of water due to the development of microcracks/voids on the surface and the bulk materials. Wood is normally wetted easily, as shown by contact angle at zero degree ($\theta = 0°$). After heat treatment around 130 to 260°C, the

wettability changes suddenly shown by contact angle at 90 degree (θ = 90°). It was showed that heat treated wood keeps its hydrophobic character (Hakkou et al. 2006).

Heat treatment also can soften the cell wall matrix - mainly the lignin - and increase crystallinity. The hemicelluloses normally are degraded at temperatures above 200°C. Lignin behaves as hydrophilic materials at below its glass-transition and acts as hydrophobic materials at above this temperature. Lignin is plasticized at 160°C at dry condition, which affects the hydrophilic properties of the wood (Hakkou et al. 2005). During the heat treatment, the number of hydrophilic *OH*-groups is decreased by replacing with hydrophobic *O*-acetyl groups (-$COCH_3$) (Hinterstoisser et al. 2003). The use of high levels of heat alone to improve dimensional stability of wood can cause extensive damage to the cellular structures. Steam treatment can be used and it changes several chemistry of wood such as the degradation of the hemicelluloses and part of the cellulose.

2.8.3 Wettability

Wettability is represented by the contact angle. The method to measure contact angle is divided into three methods. The first method is a sessile droplet measurement, which is the direct measurement of a spreading droplet of approximately 20µl. The second method is dynamic contact angle measurement based on the Wilhelmy technique. The third method is based on a Washburn equation by using wood ground to a fine powder in order to control the effects of surface roughness (Meijer et al. 2000). The contact angle of different wood structure may be different. The contact angles on latewood were significantly higher (mean = 82.43) than those on earlywood (mean =

78.20). The cracking within and between cell walls, the relatively smooth surface, and tight surface with fewer lumen openings of latewood may influence on the contact angle (Hse 1972, Ziegler et al. 2006).

2.8.4 Crystallinity

Crystallinity may correlate to moisture sorption, particularly at RH below 75%. Moisture sorption decreases with increasing crystallinity at RH below 75% due to the lower available surface area in high crystallinity regions (Mihranyan et al. 2004). Heat treatment may affect crystallinity due to the reorganization of some molecules in wood and heat treatment under high pressure can increase crystallinity. The deradation of hemicellulose and amorphous regions of cellulose due to heat treatment causes to increase crystallinity (Inoue and Norimoto 1991, Yildiz and Gumuskaya 2007).

2.8.5 Refining process

Chemical, thermal, and mechanical treatments are used in pulping processes. These treatments result in wood chip softening which makes it easy for mechanical chip fibrilization and pulp fiber refining (Leask and Kocurek 1987). Refining is a complicated process, which modifies both the external and internal structure of fibers. A new fiber surface is created. Normally the increase of exterior surface is desirable in order to enhance fiber-to-fiber bonding and mat strength due to new hydrogen bonding sites (Ebeling 1980, Page 1989). The physical changes during refining make chemical components more accessible, especially at the fiber surface as well as within the cell wall (Fardim and Duran 2003). The refining process can remove primary wall and S1 layer of the cell wall while the S2 layer of the cell wall starts swell. After that, the internal

delamination occurs within the S2 layer. The extensive internal delamination and cell wall removal occurs during prolonging refining (Walsh and Banerjee 2007).

2.9 Wood-based composite application

The application of wood-based composites inevitably faces environmental conditions such as thermal/chemical changes, MC changes, internal and external stress, bacteria and fungus degradation, and light exposure. The pressing system is one of the most important and complicated processes for wood-based composites manufacture. Under pressing condition, moisture and heat transfer take place and interaction of dynamic condition occurs, i.e., heat and moisture transfer, gas pressure generation, internal stress relaxation, wood consolidation, resin curing, and bonding formation. The hygroscopicity and EMC of wood composites is typically lower than solid wood. The hygroscopic of wood composites is closely dependent on hygroscopic changes of wood, resin, wax and other additives (Wang 2006).

Adhesive plays a key role for wood composites manufacture. The development of board properties such as dimensional stability and wood decay resistance mainly relies on the added adhesive (Xing et al. 2006). Low molecular weight resins penetrate easily into the cell wall (Furuno et al. 2004). The determination of the optimal resin content of a board requires knowledge of the amount of resin needed to obtain a given set of board properties.

The numerous *OH*-groups of wood, which are strongly polar, result in the hydrophilic character of the material. This characteristic becomes a serious problem when

it is compounded with thermoplastic polymers, which are typically hydrophobic (Follrich et al. 2006). Durability of wood composites can be improved with various strategies: (1) increase resin and/or wax loading level, (2) selection of resin and/or wax types, (3) modification of resin and/or wax formula, (4) addition of biocides, fire retardants, and/or water repellents to the resin and/or wax formulation, (5) improve distribution of resin and wax, (6) broaden resin molecular weight distribution, and (7) reduce liquid surface energy to improve resin penetration and coverage. Adding more resin can improve moisture resistance, biological decay resistance, bonding, and reduce swelling. Wax can also slow water absorption. Although phenolic, melamine, and isocyanate-based resin are moisture-resistant, isocynate-base resins show the best moisture resistance at the same resin loading (Kamke and Miller 2006). Moisture sorption in wood composites can be explained in two ways: (1) at the macroscopic level, water absorption is due to matrix expansion of composites, and (2) at molecular levels, the water molecule diffusion is at the matrix of composits and at the fibre-matrix interface (Kumar and Siddaramaiah 2007).

The use of wood-based composites involves with environmental conditions. All wood polymers contain hydroxyl and other oxygen-containing groups which attract moisture through hydrogen bonding (Rowell 1983). The moisture sorption which changes the structure of wood fiber wall occurs. The breaking bonds and bond formation take place during adsorption and/or desorption process. The hemicellulose, amorphous portion of the cellulose, the surface of the crystalline region of the cellulose, and small portion of lignin is responsible for moisture sortion in wood (Siau 1971). During moisture sorption process, the volume of cell wall increases at the same proportion of the volume of

adsorbed water (Stamm 1964). The dimension change of wood composites and mold growth can cause serious problem of wood composites during services (Levi 1973).

2.10 Summary

This chapter reviews research done in sorption properties of wood and modeling of its sorption behavior. The various properties of wood and water were introduced such as anatomical, chemical, physical, and mechanical properties. Sorption studies mainly concentrate on static, kinetic, and energetic properties. Sorption mechanisms were also introduced such as physi-sorption and chemi-sorption. An introduction of sorption behavior in various wood composites was prepared.

3. WATER VAPOR SORPTION OF SMALL LOBLOLLY PINE SAMPLES

3.1 Introduction

Sorption kinetics and statics are used in many fields of science and engineering, e.g., food science, material science, soil science, pharmaceutical science, and wood science. Sorption behavior and diffusion processes of solid wood are of interest for many reasons, including as a method of evaluating its in-service performance to help understand mold growth on wood, and for evaluating drying kinetics in wood drying (Efremov 2002, Greethamma and Thomas 2005, Pham et al. 1999). Sorption studies can also be used to gather information about composites manufacturing, such as the influence of moisture sorption on resin curing and gluing properties (Kim et al. 2006, Uysal 2006).

Wood is a heterogeneous material and its anatomy and properties vary with position in the tree (Panshin and deZeeuw 1980). Moisture sorption could vary with changes in anatomy and position in the tree because sorption behavior is affected by several parameters such as the size and distribution of cell cavities, intercellular spaces and pit membrane pores, and initial moisture content (MC) of the wood (Choong 1963).

Surface properties may affect water vapor sorption, espeically in the initial sorption period. One of the most important surface properties is wettability, which can be

represented by contact angle. There are inconsistent reports about the relative wettability of earlywood and latewood. Hse (1972) found that the earlywood was wetted more easily than latewood in southern pine, while Shupe et al. (1998) did not observe any effect of earlywood and latewood differences on the wettability of loblolly pine. Maldas and Kamdem (1999) found that latewood wetted more easily than earlywood in loblolly pine because loblolly pine contained lower lignin and extractives content in latewood compared to earlywood.

Wood species and wood grain direction influence water vapor sorption and diffusion coefficients. For Scots pine (*Pinus sylvestris*) in the longitudinal direction, moisture diffusion is six times higher than that for spruce (*Picea abies*) while there is no difference in the radial direction. Moisture movement in the tangential direction of spruce is higher than that of Scots pine (Fakhouri et al. 1993). However, few studies have investigated sorption behavior of different wood tree ring locations within the stem cross-section. The purpose of this study was to investigate the effect of differences among earlywood, latewood, and tree ring location within the stem cross-section of loblolly pine (*Pinus taeda*) on water vapor sorption statics and kinetics under ambient conditions.

3.2 Materials and methods

3.2.1 Wood specimen and basic properties

The wood samples used in this experiment were loblolly pine (*Pinus taeda*) originating from a field in southern Arkansas. Two foot long bolts were cut from three loblolly pine trees every 16 feet along the length of the main stem. These bolts were cut

into longitudinal strips at each compass heading. Specimens containing three growth rings were cut from the wood strips to produce the bending specimens. Although the specimens were too small to be covered by the second method of ASTM standard for smaller clear specimens, they comprised a number of growth rings to reduce the influence of earlywood and latewood differences. These specimens were oven dried at 105ºC and reconditioned at 65% RH and 23±2°C before testing. The small amount of volatile extractives possibly lost during oven drying was neglected. The moduli of elasticity (MOE) and moduli of rupture (MOR) were tested according to the ASTM standard for three-point bending (ASTM 1999). The specific gravity was also calculated from the bending specimens, using a weighted average of the earlywood and latewood. Bending specimens were milled separately for each growth ring and screened until they passed a 20 mesh screen. The earlywood and latewood of each growth ring was milled together due to the small amount of material. The chemical composition was analyzed from the milled specimens using ASTM standard methods for whole biomass analysis (ASTM 1999). National Institute of Standards and Technology (NIST) pine standard reference material #8493 was used as a reference to determine carbohydrate, extractives and lignin content (NIST 1993).

A set of radial strips was cut from the bolts for the sorption studies. These strips were divided into tree ring no. 2, 5, 9, 16, 32 and 50 from the pith to bark. These specimens were visually separated into earlywood and latewood, which were cut from the wood strips into slivers 5 mm (longitudinal) x 5 mm (tangential) x 0.5 mm (radial) for sorption isotherm and sorption kinetics experiments. A diagram of bending sample and sliver preparation from the loblolly pine bolts is shown in Figure 3-1.

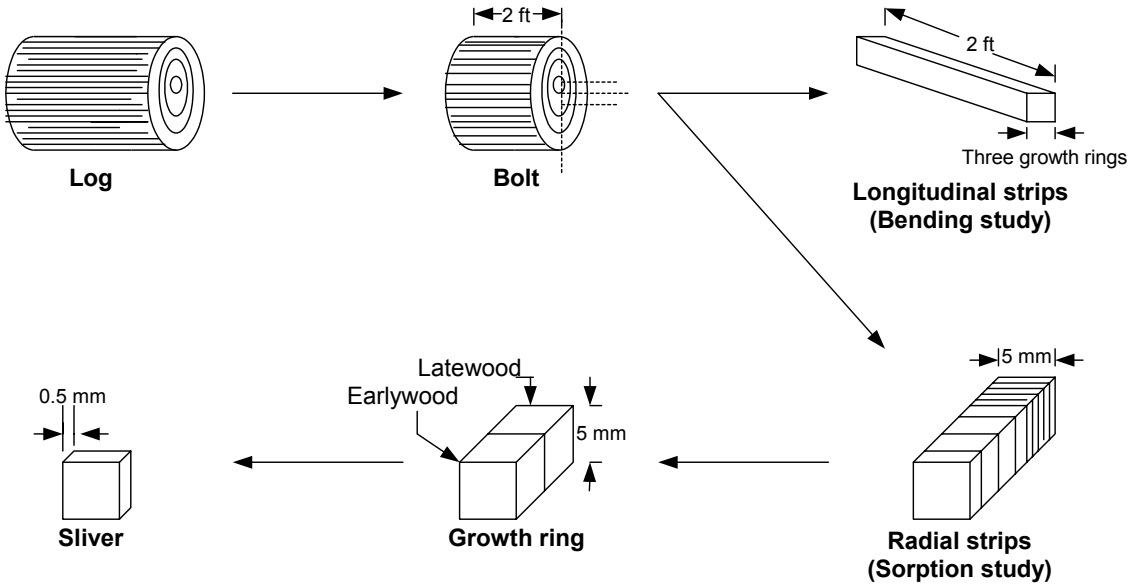


Figure 3-1. Diagram showing sliver preparation from loblolly pine growth increment.

3.2.2 Sorption isotherm

Five replications of earlywood and latewood from different tree rings were conditioned in desiccators above one of the six saturated salt solutions listed in Table 3-1 (Lide 1994). All specimens were weighed to the nearest 0.0001 g once a day until equilibrium was reached (weight change of less than 1% from previous measurement). After the last run, oven-dried weight was measured and MC was calculated based on oven-dried weight. All salt solutions were maintained at a constant laboratory temperature of 23±2ºC.

Table 3-1. Saturated salt solution and resultant relative humidity at 23±2ºC (Lide 1994).

Salt Solution	Formula	RH (%)
Lithium Chloride	LiCl	11.3
Magnesium chloride	$MgCl_26H_2O$	32.8
Potassium carbonate	K_2CO_3	43.2
Sodium bromide	NaBr	57.6
Ammonium chloride	NH_4Cl	78.0
Potassium chloride	KCl	84.3

3.2.3 Sorption kinetics

The measurement of sorption behavior was performed by a vapor sorption method. A second set of specimens, which had the same dimensions as the first set of earlywood and latewood specimens from different tree rings, were prepared from pine trees as described above. The sorption process was performed by changing the relative humidity (RH) from 11% to 89%. The weight change of the specimen during the sorption process was continuously measured and recorded within 4 hours using a Dynamic Contact Angle Analyzer DCA 332 (Thermo Cahn Corp. Madison, Wisconsin USA). The temperature was kept constant at 23±2ºC by a temperature-controlled electric heater and the salt solutions were bubbled in order to keep the RH at the target level at ambient pressure. The air velocity was 0.5 L/min. A data logger kept a record of the climate during the sorption period. The humidity sensor takes only a few seconds to start recording RH changes. Five replications of each condition were used. The experimental

setup of the climate control instrument is shown in Figure 3-2. The specimens were oven-dried after the last weight measurement and MC was calculated based on oven-dried weight.

3.2.4 Evaluation of sorption isotherms

The sorption data obtained in the study at each RH were fitted with an ideal solution equation (Hailwood and Horrobin 1946). From ideal solution behavior, the following equation was obtained:

$$M = M_h + M_d = \frac{1800}{W}\left(\frac{K_1 K_2 h}{100 + K_1 K_2 h}\right) + \frac{1800}{W}\left(\frac{K_2 h}{100 - K_2 h}\right) \quad (3\text{-}1)$$

where:

M = the equilibrium moisture content.

h = the relative humidity.

M_h = the moisture content of the hydrate water (monomolecular sorption).

M_d = the moisture content of the dissolved water (polymolecular sorption).

K_1 = the equilibrium constant of the hydrate formed from dissolved water and dry wood.

K_2 = the equilibrium constant between water vapor and dissolved water.

W = the molecular weight of dry wood per mole of water sorption sites.

For convenience in fitting to the experimental data, the polynomial form was obtained:

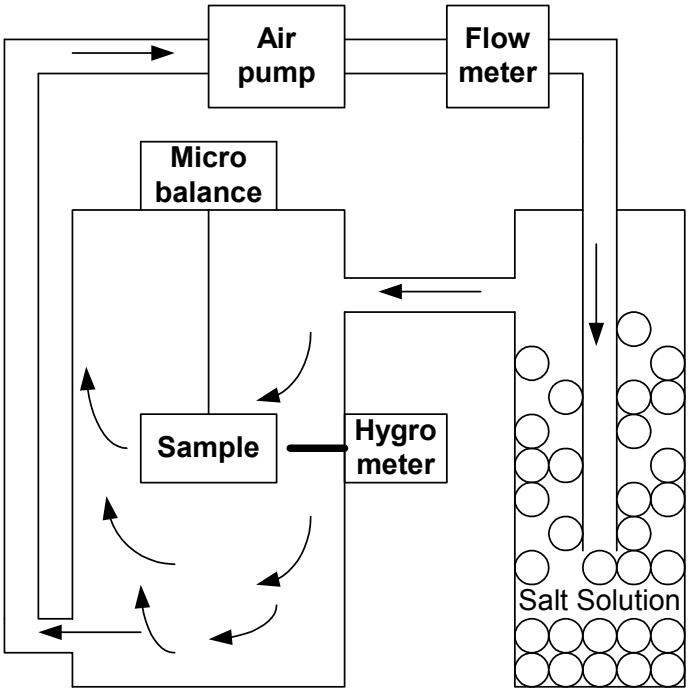


Figure 3-2. Climate control instrument used during the measurement.

$$\frac{h}{M} = A + Bh - Ch^2 \tag{3-2}$$

where:

$$A = \frac{W}{18}\left[\frac{1}{K_2(K_1+1)}\right] \tag{3-3}$$

$$B = \left(\frac{W}{1800}\right)\left[\frac{K_1 - 1}{K_1 + 1}\right] \tag{3-4}$$

$$C = \left(\frac{W}{180000}\right)\left[\frac{K_1 K_2}{K_1 + 1}\right] \tag{3-5}$$

Equation 3-2 shows a parabolic relationship between the ratio of h/M and h. The A, B and C are regression coefficients, which contain the equilibrium constant (K_1, K_2) and W values. The values of K_1, K_2, and W can be calculated as follows:

$$K_1 = 1 + \frac{B^2 + \sqrt{B^2 + 4AC}}{2AC} \tag{3-6}$$

$$K_2 = \frac{200C}{B + \sqrt{B^2 + 4AC}} \tag{3-7}$$

$$W = 1800\left(\frac{4AC + B^2 + B\sqrt{B^2 + 4AC}}{B + \sqrt{B^2 + 4AC}}\right) \tag{3-8}$$

3.2.5 Evaluation of diffusion coefficients

The calculation of diffusion coefficients was based on the solution of a practical problem such as non-perfect RH-step. Therefore, the final part of the sorption curve was used due to the non-perfect RH-step. The accuracy of this calculation was usually best around 60-80% of total sorption (Wadso 1994). The equation to calculate diffusion coefficient is expressed as follows:

$$D = \frac{4l^2}{\pi^2 t}.\ln\left(\frac{8}{\pi^2(1-E)}\right) \tag{3-9}$$

where:

D = the diffusion coefficient (m^2/s).

l = the half of thickness of specimen (m).

t = time (s).

E = the dimensionless sorption.

The calculation of dimensionless sorption is as follows:

$$E = \frac{\Delta M_i}{\Delta M_\infty} \tag{3-10}$$

where:

ΔM_i = the weight change at time $t(s)$.

ΔM_∞ = the weight change at final equilibrium.

This diffusion coefficient is approximated with the following assumptions: the diffusion coefficient is constant, the initial moisture is uniform within the specimen, the instantaneous equilibrium is reached with RH at the cell surface, and there is symmetrical transport of moisture through the cell wall. It was also assumed that the sorption through the edges can be neglected due to a small surface-to-thickness ratio. Therefore, in this experiment diffusion was considered to be unidirectional. The diffusion coefficient calculated based on a graphical analysis of fractional change in MC is shown in Figure 3-3.

3.2.6 Evaluation of surface resistance

Surface resistance is a limited mass transfer coefficient which hinders transport. In wood science, the term "surface emission (σ)", which is the inverse of the surface resistance (S), is used. Liu (1989) proposed a method for the determination of surface emission coefficients. The equation to calculate the surface emission is expressed as follows:

$$\sigma = \left. \frac{0.7010D}{Dt/l - 0.1963l} \right|_{E=0.5} \tag{3-11}$$

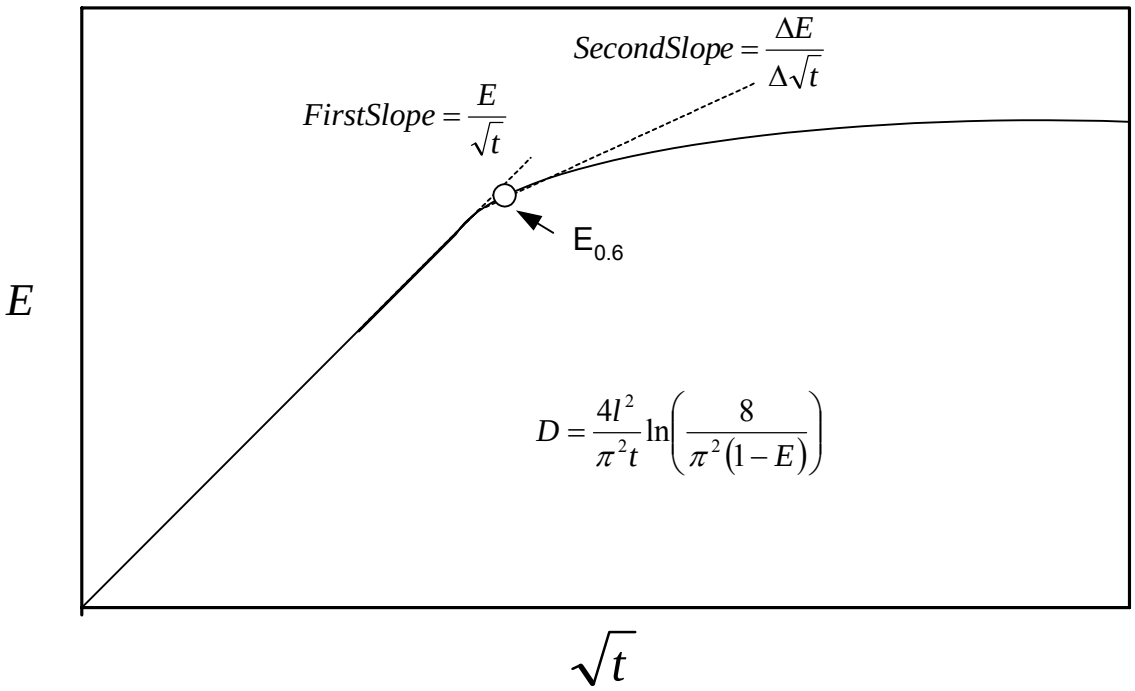


Figure 3-3. The graphical analysis of initial diffusion coefficient.

3.2.7 Evaluation of sorption rate

The sorption rate was determined from the slope of the plot of MC against time (Wang and Liau 1998). The early stage was linearly governed by Fickian sorption, while the second stage was non-linear, due to the slow sorption of the cell wall. The initial sorption rate (K_1) was calculated from the slope within five minutes, while the second slope (K_2) was calculated from the second linear slope within another five minutes.

3.3 Results and discussions

3.3.1 Sorption isotherms

The sorption behavior of wood in the different tree rings was analyzed using the Hailwood-Horrobin (H-H) model. The values of A, B, C, the coefficient of determination (R^2), K_1, K_2 and W of wood at various tree rings are listed in Table 3-2. The equilibrium constants of the EL values were determined by means of a regression analysis with a weighted average from the entire ealywood (EW) and latewood (LW) dataset. The degree of fit was described by the coefficient of determination (R^2) and it ranged from 0.912 to 0.996, indicating a good fit to the experimental results. The H-H model was divided into the moisture sorption of the monomolecular component and the polymolecular component. The constant W describes the molecular weight of the dry wood polymer per mole of water sorption sites. The constant K_1 describes the equilibrium constant where the hydrate is formed from dissolved water and dry wood. The K_1 values varied between 159.18 and 750.64. Most of the K_1 values were higher for earlywood and outer tree rings. Latewood of some tree rings had higher K_1 values. The constant K_2 describes the equilibrium constant between dissolved water and water vapor, or the activity of dissolved water per unit relative vapor pressure. This value should be unity if it has the same activity as liquid water. The K_2 values varied between 0.63 and 0.78, indicating that the dissolved water shows a lower activity than the liquid water. The W value describes the molecular weight of substance absorbed with 1 molecular weight of water in hydrate form at saturation. The higher the W value, the lower is availability of sorption site per unit weight of dry substance (Wangaard and Granados 1967). However, the value of W

Table 3-2. Fitted and physical constants calculated for the Hailwood-Horrobin equation isotherms.

Sample		**A**	**B**	**C**	**K1**	**K2**	**W**	**R^2**
No.2	EW	0.2275	0.2102	0.0014	335.75	0.66	3625.8	0.989
	LW	0.2162	0.2497	0.0018	325.86	0.72	3622.3	0.994
	EL	0.5028	0.1844	0.0012	159.18	0.64	3662.8	0.909
No.5	EW	0.2972	0.1927	0.0013	255.55	0.67	3637.1	0.968
	LW	0.4121	0.1902	0.0013	183.73	0.67	3652.5	0.957
	EL	0.3588	0.1905	0.0013	210.43	0.67	3645.7	0.966
No.9	EW	0.0939	0.2239	0.0016	750.64	0.71	3610.8	0.995
	LW	0.1375	0.2626	0.0020	482.32	0.76	3614.3	0.996
	EL	0.2567	0.1998	0.0014	283.98	0.69	3632.1	0.958
No.16	EW	0.1742	0.2101	0.0015	407.80	0.71	3621.2	0.952
	LW	0.1519	0.2078	0.0015	461.83	0.72	3618.9	0.967
	EL	0.1782	0.2050	0.0015	389.35	0.72	3622.8	0.967
No.32	EW	0.2717	0.1777	0.0014	240.18	0.78	3642.9	0.967
	LW	0.3080	0.1852	0.0014	221.12	0.75	3644.7	0.936
	EL	0.1959	0.1230	0.0014	574.94	0.71	3616.1	0.912
No.50	EW	0.1987	0.1580	0.0012	338.62	0.75	3634.1	0.918
	LW	0.2973	0.1758	0.0012	253.04	0.67	3641.1	0.959
	EL	0.1169	0.1727	0.0011	678.31	0.63	3615.5	0.918

Remark: EW = earlywood, LW = latewood, and EL = average of earlywood and latewood

did not show significant differences among the samples.

3.3.2 Sorption rate

The moisture content (MC) of earlywood and latewood was plotted as a function of the square root of time, as shown in Figure 3-4. Each data point was the average of the 30 samples from all the tree rings. The sorption curve showed the MC changing linearly with the square root of time for the initial period of sorption, although a non-perfect RH-step before 500 seconds was observed. The sorption plot of earlywood and latewood had a similar shape, which is a linear rate at initial sorption, followed by a gradual decrease in sorption rate until MC is constant. The plot of the MC of wood from the various tree rings is shown in Figure 3-5. Each value was the average of ten samples of earlywood and latewood in each tree ring. The highest constant MC values from each plot were considered to be the pseudo-equilibrium values because the true equilibrium cannot be reached in such short time periods. The initial sorption rate and second slope are shown in Table 3-3. The initial sorption rate of ring no. 16, 32 and 50 was higher than the initial sorption rate of ring no. 2, 5 and 9, where ring no. 2 refers to the second tree ring from the center (pith) of the bolt. Tree ring no. 50 had a higher sorption rate than tree ring no. 2. Although differences in the sorption rate of the outer tree rings and inner tree rings were not explicitly studied in this experiment, the sorption rate of outer tree rings was generally higher than that of inner tree rings. The variation of outer tree ring and inner tree rings may have been due to the transition from sapwood to heartwood, although sapwood and heartwood were not identified in these samples. This sapwood-to-heartwood transition is generally accompanied by an increase in extractive content and/or

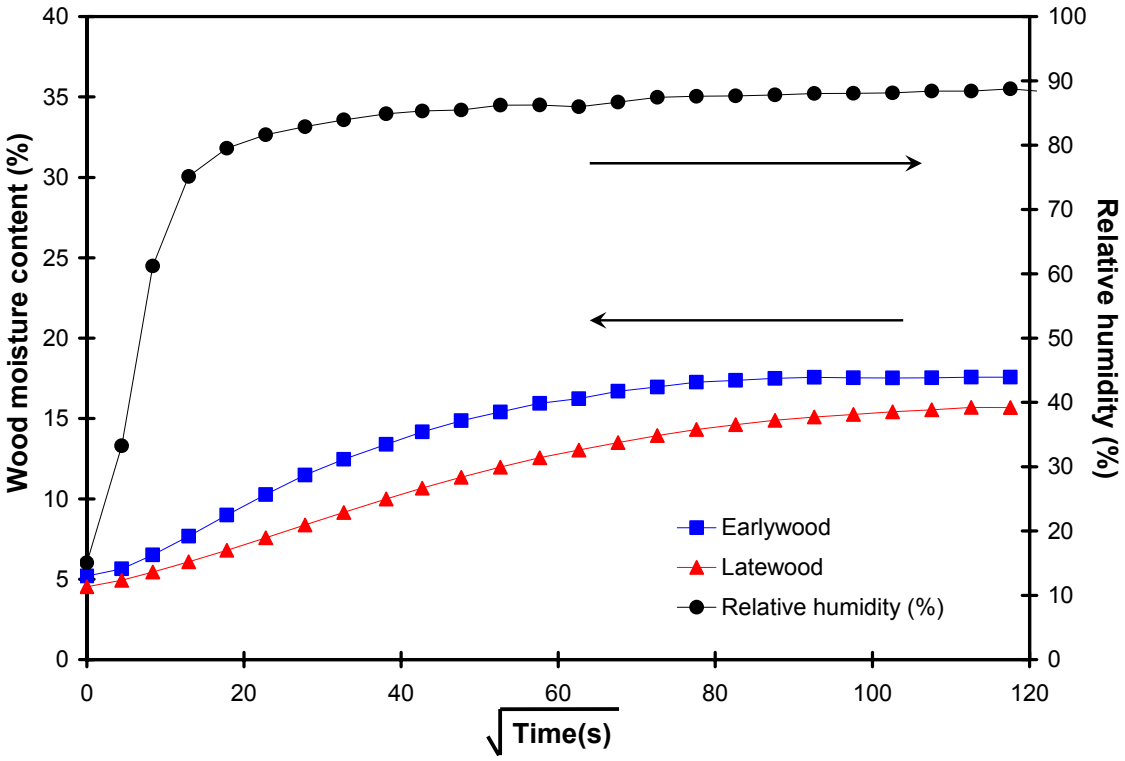


Figure 3-4. Moisture sorption of ealywood and latewood.

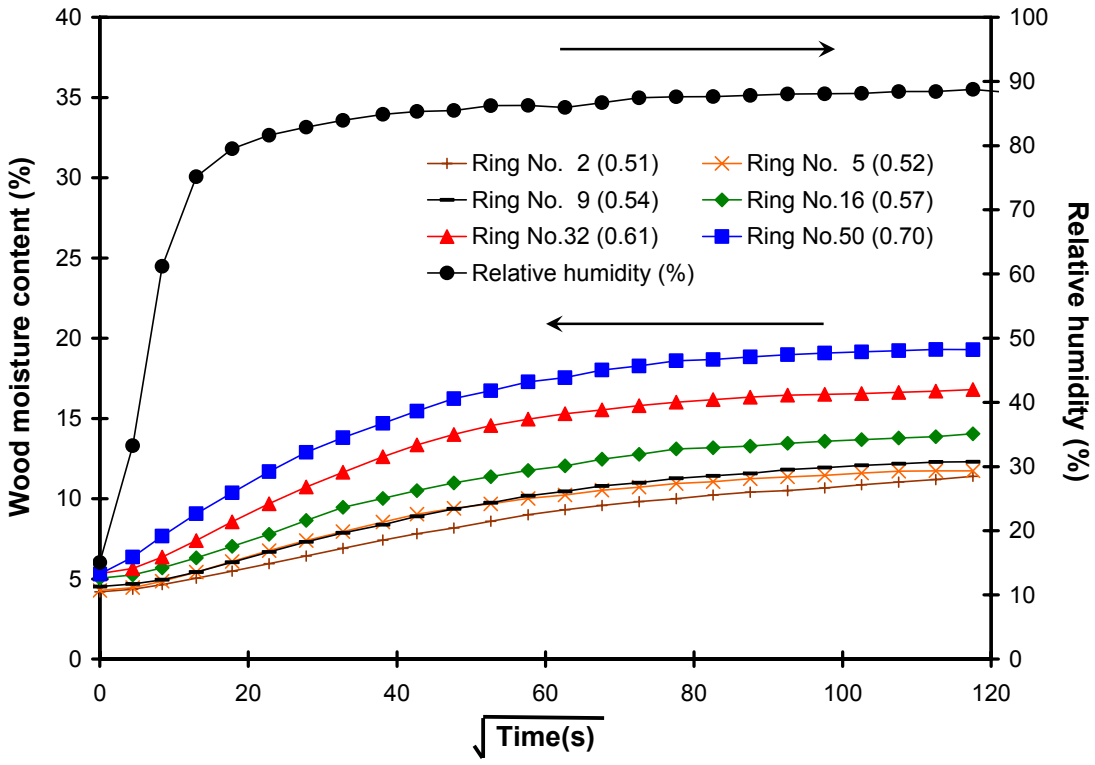


Figure 3-5. The moisture sorption of various tree rings of wood (Number in the bracket is specific gravity).

Table 3-3. Initial sorption rate (K_1), second slope (K_2), diffusion coefficient (D), surface emission coefficient (σ), and surface resistance coefficient (S) of wood.

Ring No.	**Wood**	**K_1 (%/√s) Mean (Std)**	**K_2 (%/√s) Mean (Std)**	**$D_{0.5}$ (10^{-10} m^2/s) Mean (Std)**	**$D_{0.6}$ (10^{-10} m^2/s) Mean (Std)**	**σ (10^{-7}m/s) Mean (Std)**	**S (10^6s/m) Mean (Std)**
No.2	EW	0.027 (0.003)	0.012 (0.002)	3.16 (0.64)	3.13 (0.74)	7.65 (1.48)	1.31 (0.15)
	LW	0.017 (0.005)	0.011 (0.002)	0.45 (0.14)	0.48 (0.35)	1.20 (0.51)	8.34 (0.05)
No.5	EW	0.040 (0.005)	0.015 (0.001)	3.39 (0.66)	3.50 (0.77)	7.19 (1.44)	1.39 (0.14)
	LW	0.037 (0.007)	0.018 (0.009)	1.03 (0.32)	1.12 (0.38)	2.84 (1.35)	3.52 (0.14)
No.9	EW	0.042 (0.009)	0.013 (0.007)	4.27 (0.81)	4.19 (0.61)	10.4 (1.57)	0.97 (0.16)
	LW	0.037 (0.004)	0.017 (0.007)	1.21 (0.44)	1.29 (0.47)	2.81 (1.38)	3.56 (0.14)
No.16	EW	0.057 (0.007)	0.015 (0.009)	5.25 (0.48)	5.32 (0.62)	11.5 (1.66)	0.87 (0.17)
	LW	0.040 (0.006)	0.017 (0.005)	2.67 (0.69)	2.76 (0.78)	5.18 (1.38)	1.93 (0.14)
No.32	EW	0.062 (0.005)	0.017 (0.001)	6.62 (0.48)	8.08 (0.22)	11.8 (2.34)	0.85 (0.23)
	LW	0.059 (0.006)	0.019 (0.004)	2.67 (0.67)	2.87 (0.70)	6.21 (0.64)	1.61 (0.06)
No.50	EW	0.066 (0.010)	0.015 (0.008)	7.63 (0.74)	8.55 (0.72)	13.6 (2.98)	0.74 (0.30)
	LW	0.058 (0.005)	0.026 (0.004)	3.80 (0.17)	3.33 (0.51)	7.47 (4.83)	1.34 (0.48)

Values given are means (STD)
Remark: EW = earlywood, LW = latewood , $D_{0.5}$ = diffusion at 50% of total sorption, and $D_{0.6}$ = diffusion at 60% of total sorption

a change in extractive chemistry. Heartwood extractives can reduce permeability, make heartwood dry slowly, make heartwood hard to impregnate with chemical preservatives, make the wood resistant to fungi or insect attack, increase stability under changing moisture conditions and increase density slightly (USDA Forest Service 1974).

A comparison of the initial sorption rate of earlywood and latewood at different tree rings is shown in Figure 3-6. Multivariate analysis of variance (MANOVA) was used to determined if the differences existed between the two levels of wood section (earlywood and latwood) and six levels of tree ring (No.2, 5, 9, 16, 32, and 50) (Table 3-4). There was a significant effect of tree ring on initial sorption rate. The initial sorption rate of earlywood was always higher than latewood. This may be due to different anatomical structure between earlywood and latewood. Earlywood is characterized by cells with relatively large cavities and thin walls, while latewood has smaller cavities and thicker cell walls (Bodig and Jayne 1993). In general, moisture easily penetrates the empty spaces in wood structures such as the lumen of cells. Pit membranes and the cell wall play an important role in inhibiting moisture flow (Siau 1995), although there are between 100 and 300 pit pairs per tracheid in earlywood and 10 to 15 pit pairs per tracheid in latewood (Time 1998). Therefore, the initial sorption rate is highly dependent on wood structural features such as tracheid length in addition to the temperature, density, microfibril angle and MC of the wood (Comstock 1963).

All plots showed that the sorption behavior was divided into two stages: the first stage is diffusion-controlled and second stage is a slow partial relaxation of the swelling stress, which increases the amount of sorbed water (Downes and Mackay 1958). This phenomenon was described as a surface resistance which hindered the water sorption.

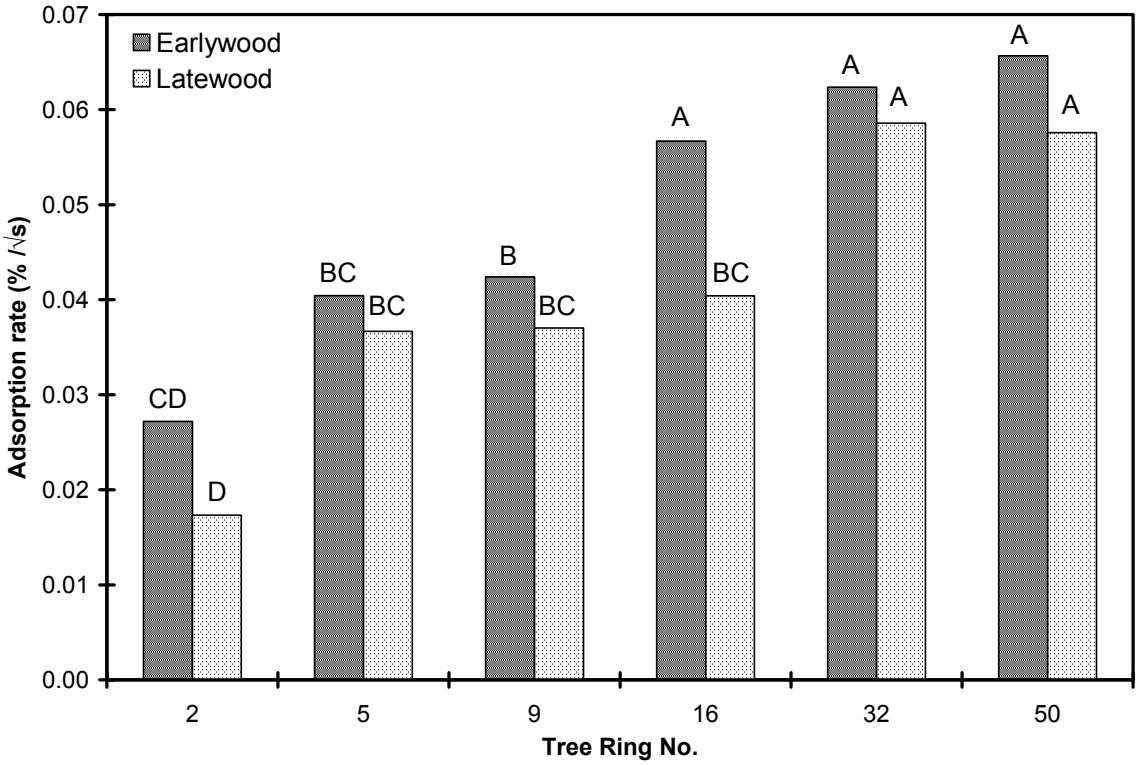


Figure 3-6. The comparison of initial sorption rate of earlywood and latewood at different tree rings (The same letters are not significantly different at α = 5%).

Table 3- 4. MANOVA results and dependent variable ANOVA for intial sorption rate.

MANOVA	**Wilks 'λ p-value**
Interaction	<0.001
Ring	<0.001
Section	0.355

ANOVA for Dependent variables	**Mean 2**	**Mean 5**	**Mean 9**	**Mean 16**	**Mean 32**	**Mean 50**	**p-value**
Initial sorption rate	0.022	0.039	0.040	0.049	0.061	0.062	0.001

The first stage ended at the point after which Fick's law cannot be applied. It is generally about 30% of the total sorption. In the second stage, it is believed to be controlled by sorption in the cell wall. It is about 50% of total sorption (Wadso 1993). The second slope values obtained in this experiment are shown in Table 3-3 and Figure 3-7. There were no significant effects of tree ring and wood section on second slope (Table 3-5). The initial sorption rate was 2-4 times higher than second slope. However, the second slope of earlywood was always lower than latewood, except for tree ring no. 2. The second slope tended to be higher for outer rings than for inner rings.

3.3.3 Sorption diffusion

The diffusion coefficients of earlywood and latewood at different tree rings are shown in Figure 3-8. There was a significant effect of wood section on diffusion coefficient. There was no significant effect of tree ring on diffusion coefficient (Table 3-6). A non-perfect RH-step was noted; however, only the final part of the sorption curve was used to calculate diffusion coefficient. The diffusion coefficients at 50% ($D_{0.5}$) and 60% ($D_{0.6}$) of total sorption, surface emission coefficients (σ), and surface resistance coefficients (S) of earlywood and latewood in different tree rings are shown in Table 3-3. The diffusion coefficient of water vapor at 50% of total sorption was between 0.45×10^{-10} and 7.63×10^{-10} m^2/s, while it was between 0.48×10^{-10} and 8.55×10^{-10} m^2/s at 60% of total sorption. The diffusion coefficient of earlywood was approximately 2-4 times higher than latewood. The diffusion coefficients of outer tree rings were significantly higher than that of inner tree rings. These data suggest that moisture can diffuse more rapidly in earlywood and outer tree rings than in latewood and inner tree rings. In the sorption

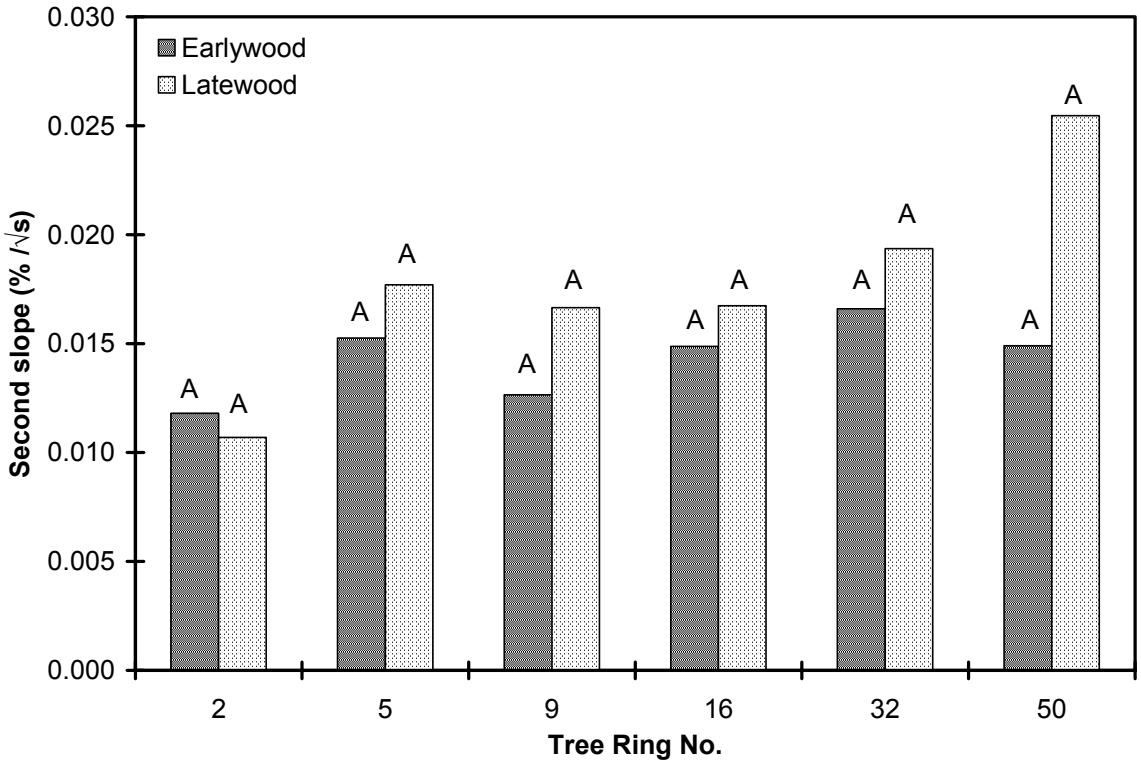


Figure 3-7. The comparison of second slope of earlywood and latewood at different tree rings (The same letters are not significantly different at $\alpha = 5\%$).

Table 3- 5. MANOVA results and dependent variable ANOVA for second slope.

MANOVA	**Wilks' λ p-value**
Interaction	0.402
Ring	0.255
Section	0.763

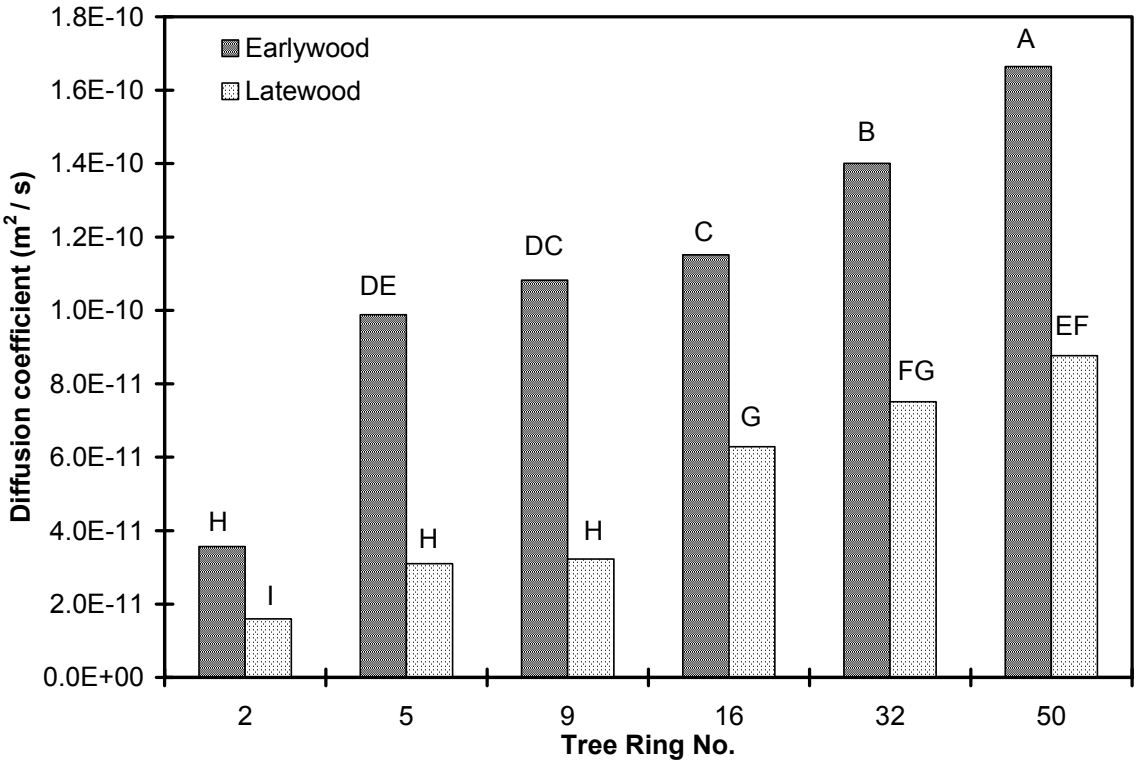


Figure 3-8. Comparison of diffusion coefficient of earlywood and latewood at different tree rings (The same letters are not significantly different at $\alpha = 5\%$).

Table 3- 6. MANOVA results and dependent variable ANOVA for diffusion coefficient.

MANOVA	**Wilks' λ p-value**		
Interaction	0.281		
Ring	0.141		
Section	0.019		
ANOVA for dependent variables	**Mean Earlywod**	**Mean Latewood**	**p-value**
Diffusion coefficient	4.43	2.02	0.012

process, the direct interaction between water vapor and the surface at the monolayer was called chemi-sorption while the interaction of water vapor at the multiple layers was called physi-sorption (Hartley et al. 1992). When MC reaches a constant, it is believed that this point represents equilibrated MC governed by the wood surface. If it is assumed that wood cannot be equilibrated in short time periods, the MC at this point can be called pseudo-equilibrium. The influence of surface emission is closely related to diffusion coefficient as well as to internal surface resistance, which is the inverse of the surface emission. The comparison of surface emission coefficient and surface resistance coefficient of earlywood and latewood at different tree rings was shown in Figures 3-9 and 3-10. There was a significant effect of wood section on surface emission coefficient and surface resistance coefficient. There was no significant effect of tree ring on surface emission coefficient and surface resistance coefficient (Tables 3-7 and 3-8). The higher surface resistance coefficient of latewood and inner tree rings appears to correspond to slower sorption processes (Table 3-3). The calculation of the diffusion coefficient by maximum slope and 80% of total sorption is not appropriate due to the internal surface resistance during the initial sorption process, and non-Fickian effects at the end of the sorption process, respectively. Therefore, the calculation of the diffusion coefficient at 60% of total sorption can be used instead of the traditional method based on a calculation from the maximum slope.

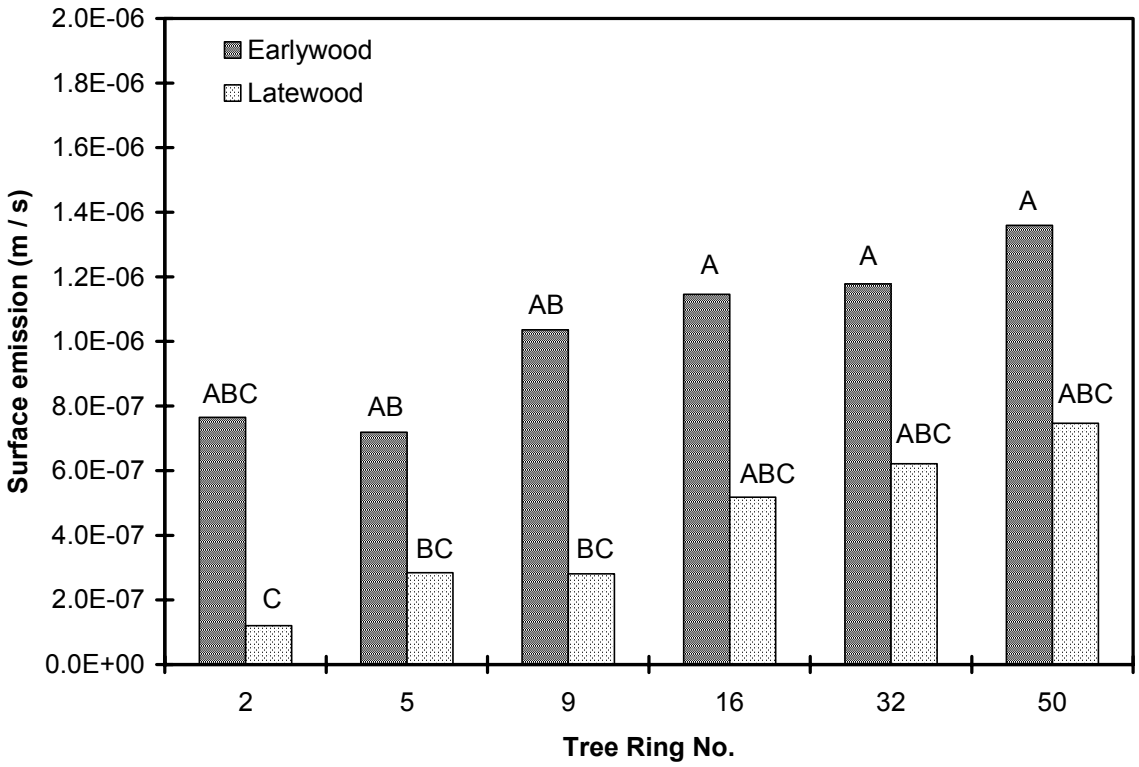


Figure 3-9. Comparison of surface emission coefficient of earlywood and latewood at different tree rings (The same letters are not significantly different at $\alpha = 5\%$).

Table 3- 7. MANOVA results and dependent variable ANOVA for surface emission coefficient.

MANOVA	**Wilks' λ p-value**
Interaction	0.132
Ring	0.075
Section	0.048

ANOVA for dependent variables	**Mean Earlywod**	**Mean Latewood**	**p-value**
Surface emission	10.42	4.53	0.010

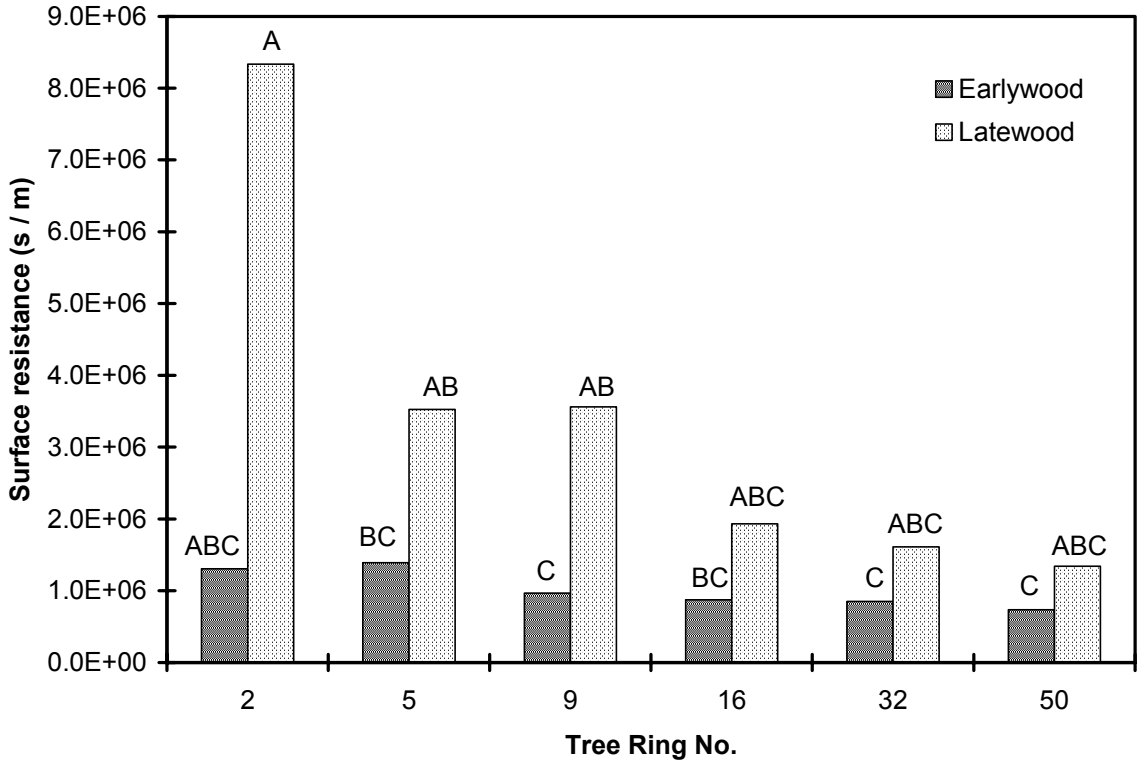


Figure 3-10. Comparison of surface resistance coefficient of earlywood and latewood at different tree rings (The same letters are not significantly different at $\alpha = 5\%$).

Table 3- 8. MANOVA results and dependent variable ANOVA for surface resistance coefficient.

MANOVA	**Wilks' λ p-value**
Interaction	0.112
Ring	0.660
Section	0.011

ANOVA for dependent variables	**Mean Earlywod**	**Mean Latewood**	**p-value**
Surface resistance	1.32	3.78	0.027

3.3.4 Chemical analysis

Table 3-9 shows physical properties, mechanical properties and chemical composition of the loblolly pine samples in different tree rings. Wood near the bark had higher density than wood near the pith. This density difference was probably due to the relative amount of earlywood and latewood changing from pith to bark. The outer tree rings had higher strength and stiffness than inner tree rings, which likely was mostly a function of differences in density. Via et al. (2003) reported that the wood near pith have a higher apparent density due to the higher concentration of resinate extractives than wood near bark. Howerver this higher concentration would not contribute to increased strength or stiffness. These results differ from Via el al.'s finding likely due to the higher latewood percentage of wood near bark. Via et al. (2007) reported the lignin content was found higher in the ring adjacent to the pith in longleaf pine (*Pinus palustris*) but Shupe et al. (1997) reported the higher Klason lignin was found in wood near the bark in loblolly pine (*Pinus taeda*). This different trend was probably due to the effect of various silvicultural treatements on the chemical properties of loblolly pine tree. Erickson and Arima (1974) found that lignin content is higher near the pith in Douglas-fir (*Pseudotsuga menziesii*). However this result showed no statistical difference within the tree rings. The extractives content was found to decrease from pith to bark for loblolly pine (Shupe et al. 1997). The measurement error may occur due to the loss of minor polymeric substances and/or low-molecular-weight substances. Siau (1995) stated that wood density was indirectly related to water vapor sorption. However, the relation of density to water vapor sorption is unclear. Other factor may influence sorption such as tracheid length and microfibril angle. The hemicelluloses usually have higher sorptive

Table 3- 9. The physical properties, mechanical properties, and chemical composition of the loblolly pine (all values are weight percent).

Ring No.	MOR (MPa)	MOE (MPa)	Specific Gravity	Glucose (%)	Hemicellulose (%)	Lignin (%)	Extractives (%)
2	48.1(8.3)	4914.2 (811)	0.51(0.06)	32.2(4.2)	23.1(1.7)	26.4(2.6)	16.4 (8.8)
5	73.1(9.2)	7431.8(1704)	0.52(0.08)	36.7(2.9)	23.0(0.9)	27.5(1.4)	10.2(10.6)
9	87.6(10.6)	9300.2(2255)	0.54(0.05)	41.2(3.0)	23.2(1.4)	27.9(1.0)	7.5 (9.4)
16	98.0(9.4)	10540.7(1234)	0.57(0.07)	43.6(3.8)	22.8(1.8)	28.4(1.3)	5.5(10.5)
32	103.9(11.8)	11436.6(2526)	0.61(0.06)	42.5(3.1)	22.9(2.4)	29.9(2.1)	4.6(12.8)
50	121.3(4.2)	14022.9(2435)	0.70(0.02)	43.3(2.0)	20.9(1.2)	27.9(1.7)	5.7 (8.0)

Values given are means (STD)

capacity than celluloses and lignin (Christensen and Kelsey 1958). The hemicelluloses and lignin content were only slightly different along the tree radius, while cellulose content was lower, and extractive content was higher, in the inner tree rings than in the outer tree rings. Although the lower moisture sorption of inner tree rings seems to be correlated with the lower content of (hydrophilic) cellulose and higher amounts of extractives, the degree to which the chemical differences influenced moisture sorption is uncertain.

3.4 Summary

The differences due to earlywood, latewood, and tree ring location within the stem cross-section on the sorption kinetics and sorption statics of water vapor were observed in loblolly pine (*Pinus taeda*) trees. Earlywood had higher sorption rates and diffusion coefficients than latewood, while outer tree rings had higher sorption rates and diffusion coefficients than inner tree rings. The sorption isotherms of earlywood, latewood, and different tree ring locations with the stem cross-section were fitted very well by a Hailwood-Horrobin model.

4. EFFECTS OF REFINING STEAM PRESSURE ON THE WATER VAPOR SORPTION OF LOBLOLLY PINE FIBERS

4.1 Introduction

Wood fiber is increasingly used in manufacturing due to its availability, biodegradability, renewability, low cost, and high specific strength. It is most commonly used to manufacture medium density fiberboard (MDF) for use in the furniture sector including door skin and cabinets. The efficiency of MDF production depends on how well the solid wood is broken down into wood fibers via refining and on the reassembly of the fibers into a fiberboard. The properties of MDF mostly depend on fiber properties, fiber orientation, fiber-to-fiber stress transfer, board density, density profile, and resin distribution and penetration into individual fibers during blending and pressing (Wang et al. 2001a and b).

Another application of wood fiber is its use in fiber-reinforced polymer composites in the fields of construction, marine environments, infrastructure, and sports. The advantages of wood fiber are better strength, elongation, and impact energy than its wood flour counterpart used in wood-plastic composites (WPC) production (Clemons

2002). The disadvantages of wood fiber are thermal and mechanical degradation, which make it undesirable for certain applications. Several applications of WPC inevitably involve exposure to moisture conditions. This exposure leads to degradation of their mechanical and structural properties, which depends on their stability under varying environmental conditions (Wan et al. 2005). Therefore, the incompatibility between the hydrophilic fiber and the hydrophobic thermoplastic matrix could be compromised. The use of compatibilizers or coupling agents to improve the adhesion between fiber and matrix seems to be necessary (Espert et al. 2004, Sreekala and Thomas 2003). It has long been known that the properties of fiber-based composites are dependent on the properties of the components. Therefore, an inexpensive means to produce superior fiber-based composites is the modification of hydrophilic properties of individual wood fiber to improve the compatibility between fiber and matrix.

The response of wood, as hygroscopic material, to changes in relative humidity (RH) under certain circumstances is complicated. Differences in wood structure and anatomy, such as earlywood, latewood, tree ring location within stem cross-section, influence the sorption behavior of water vapor (Neimsuwan et al. 2007). Wood treated with heat and pressure under hot-pressing influences its physical and chemical structure. This treatment can modify wood structure and its properties. During the past decade, new modification methods were developed with the aim of improving wood properties. Among wood properties, the hygroscopicity, dimensional stability, and durability are notably important (Wikberg and Maunu 2004). Heat treatment is a traditional method used to improve biological durability, dimensional stability, and weather resistance. It is commonly used in a diversity of outdoor and indoor applications (Hakkou et al. 2005,

Kamdem et al. 2002). Under dynamic condition in hot-pressing, flake compression and temperature differs with the panel thickness. This difference may influence moisture uptake, weight loss, and equilibrium moisture content (EMC) of OSB-strands (Paul et al. 2007, Wang and Winistorfer 2001). Heat treatment can also reduce the hygroscopic properties of MDF fiber (Garcia et al. 2006). Therefore, it appears that heat treatment affects wood structure and properties, particularly sorption behavior.

The most common method to break down solid wood into wood fibers is the thermomechanical refining method. Steam pressure plays a key role in determining the quality of wood fiber. This steam pressure might influence individual wood fiber properties, particularly mechanical properties and surface quality. Groom et al. (2000, 2004) observed that there are more fiber bundles at low steam pressure than single fibers, and that fragmented fibers can be observed at high steam pressure. An increase of steam pressure above 4 bar decreases the mechanical properties of fibers, particularly for mature fiber. Groom et al. (2006) also stated that juvenile wood was considered as undesirable for high mechanical fiberboard due to its short fiber. This juvenile fiber contains high percentage of fine particles, which leads to inadequate transfer stress to another fiber and disproportionate absorption of resin.

It is clear that steam pressure has a dramatic effect on the physical and mechanical properties of individual fibers. However, the effect of steam pressure on moisture sorption of refined fiber should be considered. A better understanding of the influence on sorption behavior by steam pressure is useful to engineer wood fiber-based composites.

The long-term goal of this study was to provide sorption information for refined fiber applications both in the composites process and its service performance. The

primary objective of this study was to investigate the water vapor sorption behavior of fibers as affected by steam pressure in thermomechanical refining using small-scale measurements.

4.2 Materials and methods

4.2.1 Specimens

The specimens were prepared from a 54-year-old loblolly pine tree harvested from a plantation in Crossett, Arkansas, USA. The felled loblolly pine logs were separated manually into juvenile and mature wood sections. The juvenile wood was represented by pith to growth rings 8 and mature wood was represented by growth rings 25 to 54. The rest was considered as juvenile–mature transition. The juvenile and mature woods were chipped at Southern Research Station (SRS), Pineville, Louisiana, USA. These wood chips were refined at 2, 8, 10, and 18 bar using a thermomechanical refiner to generate fibers by an Andritz Sprout-Bauer 12 in. pressurized refiner at BioComposites Centre pilot plant, University of Wales, Bangor, UK.

4.2.2 Sorption isotherm

Four replicates of a 50-mg refined fiber were stored in air-sealed container, which had reached equilibrium RH with saturated salt solutions of LiCl, $MgCl_2$, K_2CO_3, NaBr, NH_4Cl, and KCl corresponding to 11, 33, 43, 58, 78, and 84% RH, respectively. The container was controlled at a constant temperature of 25ºC. Refined fibers were weighed daily using an analytical balance with 0.0001 g precision until the weight difference of

two successive measurements was less than 0.0001 g. After the last measurement, the fibers were oven-dried and weighed. The moisture content (MC) was calculated based on oven-dried weight. The sorption isotherm in this study was fitted with a H-H model (Hailwood and Horrobin 1946).

4.2.3 Kinetics of sorption

Refined fibers were first conditioned at 11% RH. Above the equilibration point, a 50-mg fiber sample was taken in an aluminum bucket and placed in a conditioning chamber under changing RH from 11% to 89%. The change in weight was continuously recorded over 60 min using a Dynamic Contact Angle Analyzer DCA 332. Each condition had four replicates. The temperature was kept constant at 25ºC by a temperature-controlled electric heater. The RH was changed by pumping air saturated by a target salt solution. The air velocity was 0.5 L/min. The sorption rate at initial stage can be calculated from the slope of linear portion of the plot between MC and square root of time within 5 minutes. The second slope was calculated from second linear portion of this plot from 5 to 10 minutes. The experimental setup of the climate control instrument is shown in Figure 4-1.

4.2.4 Scanning electron microscopy

Surface morphology of refined fibers was investigated using a Hitachi 4300 SEM scanning electron microscope at 100,000 times magnification. The samples were mounted onto double-sided sticky tape over aluminum stubs and coated with gold under vacuum before scanning.

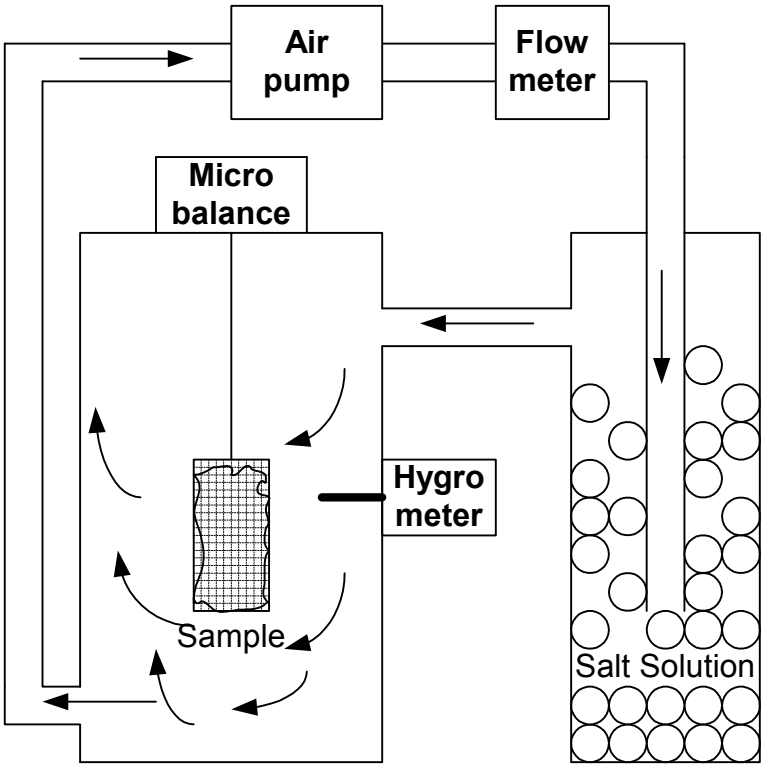


Figure 4-1. Climate control instrument used during the measurement.

4.2.5 X-ray powder diffraction

A wide angle x-ray diffractometer (WAXD) with CuKα_1 radiation (λ = 1.54 °A) was used (Philips XRG3100). The 100-mg refined fibers were packed and placed at a 45º angle to the primary beam. The angle 2θ was set between 5 and 60º, with a step size of 0.02º. The crystallinity (x_{CR}) was calculated using the following equation.

$$x_{CR} = \frac{I_{002} - I_{AM}}{I_{002}} \tag{4-1}$$

where:

I_{002} = the overall intensity of the peak at 2θ of approximately 22.7° (I_{002}, $2\theta = 22.7°$), representing crystalline and amorphous region.

I_{AM} = the intensity of the base line at region 2θ of approximately 18.0° (I_{AM}, $2\theta = 18.0°$), representing only amorphous region (Segal et al. 1959).

4.2.6 Water activity

The 50-mg refined fibers were equilibrated at 65% and 100% RH within an air-sealed container. This container was controlled at a constant temperature of 25ºC. The water activity (a_w) of equilibrated refined fibers was measured with Novasina Aw-Center water activity meter model ms1. The water activity (a_w) value was recorded within 5 minutes and each condition was performed in triplicate.

4.2.7 Contact angle

A column wicking experiment was conducted to measure the contact angle of the refined fiber with water as the probe liquid. Wood fiber was taken in the form of powder to control the effect of surface roughness and capillary penetration. The 200-mg refined fibers were packed in the glass column and hung on the microbalance in Dynamic Contact Angle Analyzer DCA322 over the liquid probe. The glass column was moved with stage speed of 20 μm/s and immersion depth of 1 mm. The wetting force was recorded as a function of time. Each condition was performed in five replicates. The contact angle was calculated with the Washburn equation as follows.

$$h^2 = \left(tR\gamma_L \cos\theta\right)/2\eta \tag{4-2}$$

where:

h = the height of the capillary rise (m).

t = the time (s).

R = the effective capillary radius (m).

γ_L = the surface tension of the liquid (mJ/m^2).

θ = the contact angle (degree).

η = the viscosity of the liquid (Pa s).

Equation 4-2 was re-written as:

$$\cos\theta = \frac{w^2\eta}{t\rho^2\gamma C} \tag{4-3}$$

where:

w = the wetting force (kg).

γ = the surface tension of the liquid (mJ/m^2).

ρ = the liquid density (kg/m^3).

C = the column constant (m^5).

The constant C was determined from the rate of rise of cyclohexane, which wet the column completely and does not cause swelling of the wood.

4.3 Results and discussion

4.3.1 Surface morphology

An image of juvenile and mature fiber refined at 2-bar pressure and 18-bar pressure is shown in Figure 4-2. Fiber refined at 18 bar of pressure contained higher fragment and higher fines percentage than fiber generated at 2 bar of pressure. Low

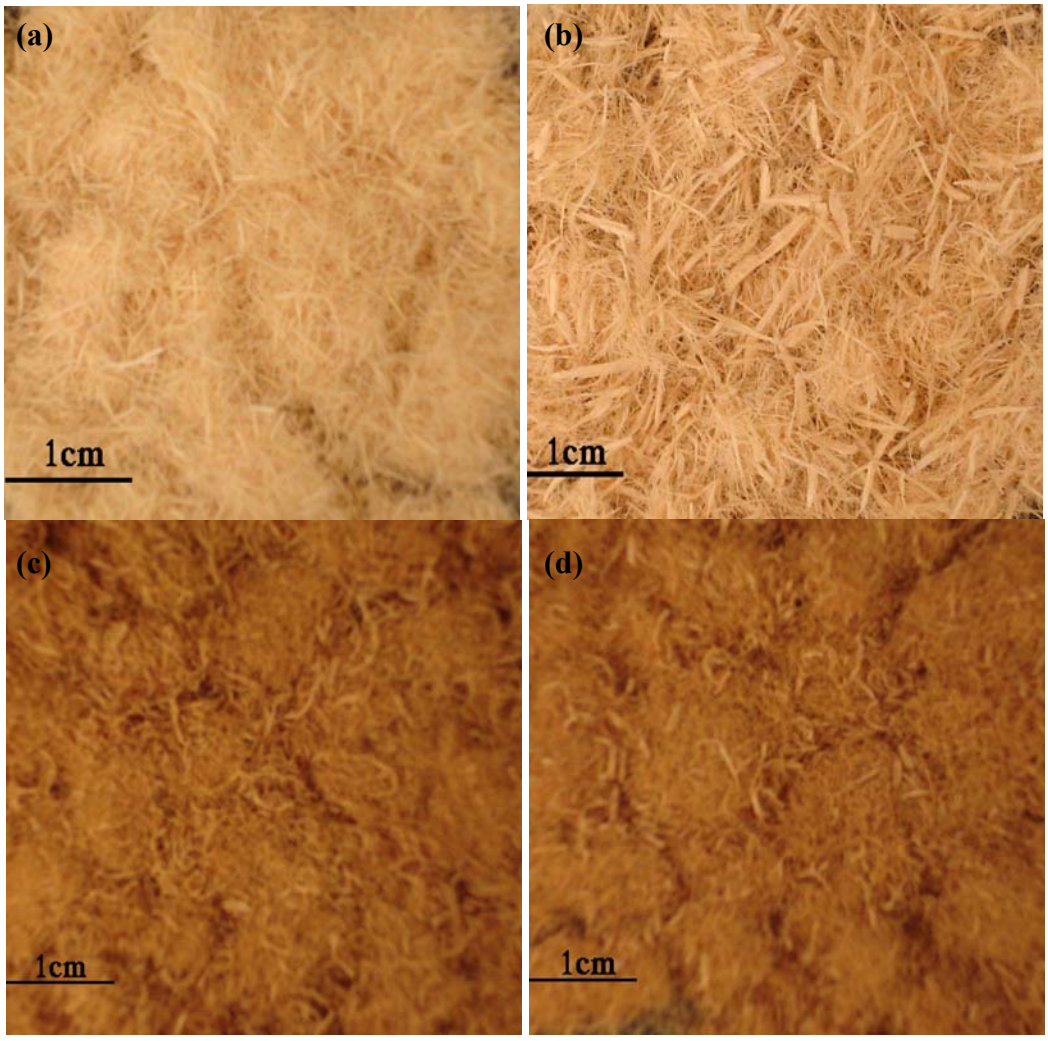


Figure 4-2. The image of wood fiber refined at (a) juvenile wood at 2 bar, b) mature wood at 2 bar, c) juvenile wood at 18 bar, d) mature wood at 18 bar.

steam pressure generated more fiber bundles than high steam pressure. The fiber color continued to darken with increasing steam pressure and agreed with Groom et al. (2006). SEM images (Figure 4-3) showed that fiber refined at 18-bar pressure has extensive damage of both juvenile and mature fibers. Mature fiber had smoother surfaces than juvenile fiber. Surface roughness of juvenile wood may promote more moisture diffusion. Xing et al. (2007a and b) stated that nano cracks occur at the thinner part of the cell wall and the damage occurs inside the lumen and on the surface. The micro cracks occur from inside to outside along cell-wall thickness. This internal damage through cross-section of cell wall at high steam pressure causes increase in surface area that is exposed to environments. However, loss of hemicelluloses due to high heat treatment and loss of capillary pressure due to cell-wall damage under severe conditions probably can lead to decrease in sorption ability (Sreekala and Thomas 2003).

4.3.2 Sorption isotherm

Sorption isotherms of fiber with varying refiner pressure are shown in Figure 4-4. Hailwood-Horrobin (H-H) adsorption model showed a good fit described by coefficient of determination (R^2) between 0.833 and 0.959. The values of A, B, C, R^2, K_1, K_2, and W of fiber with varying refiner pressure are listed in Table 4-1. Fiber refined at 18-bar pressure has the lowest K_1 (0.45) and the highest K_2 (0.94). The constant K_1 describes the equilibrium constant where the hydrate is formed from dissolved water and dry wood, whereas the constant K_2 describes the equilibrium constant between dissolved water and water vapor. Therefore, fiber refined at 18-bar pressure has less hydrate formed from dissolved water and dry wood. The constant W describes the molecular weight of the dry

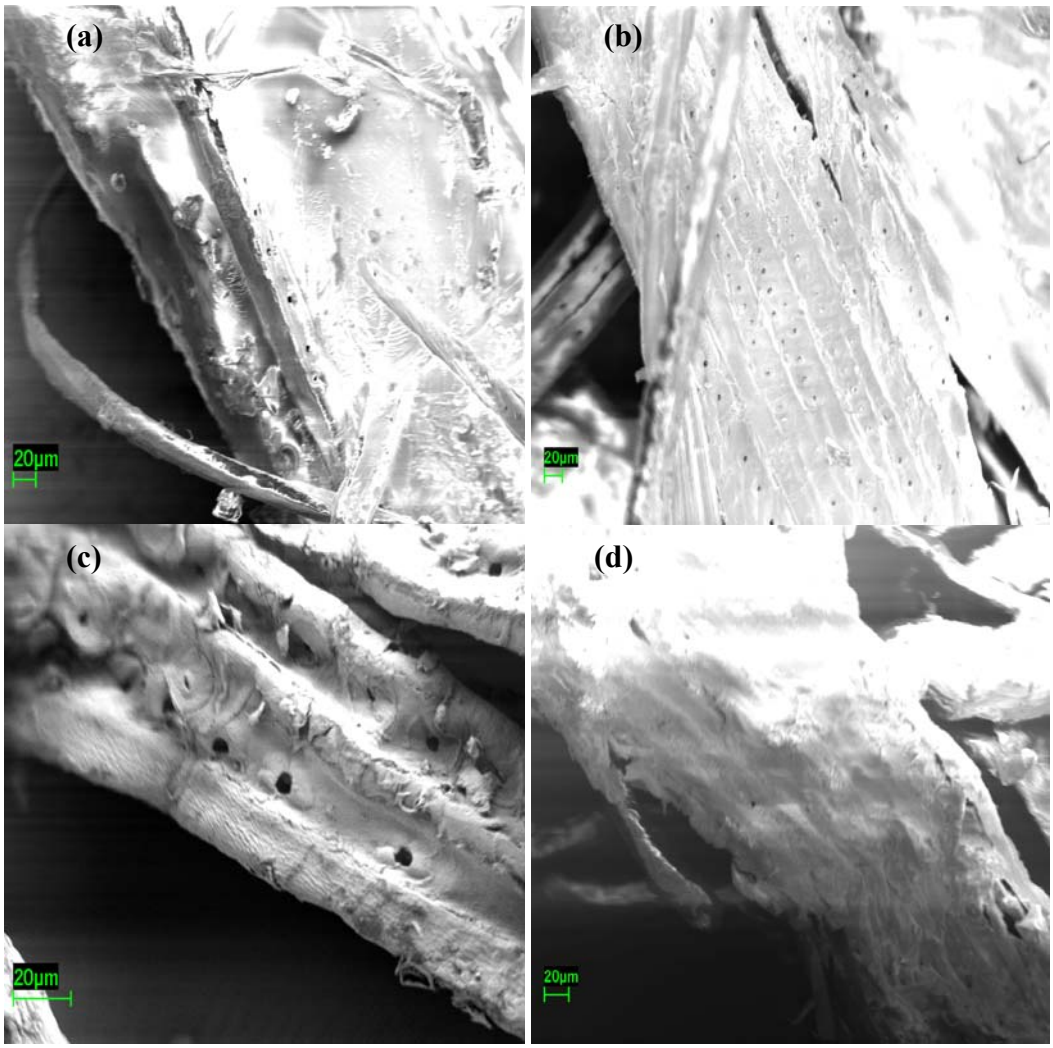


Figure 4-3. The SEM image of wood fiber refined at a) juvenile wood at 2 bar, b) mature wood at 2 bar, c) juvenile wood at 18 bar, d) mature wood at 18 bar.

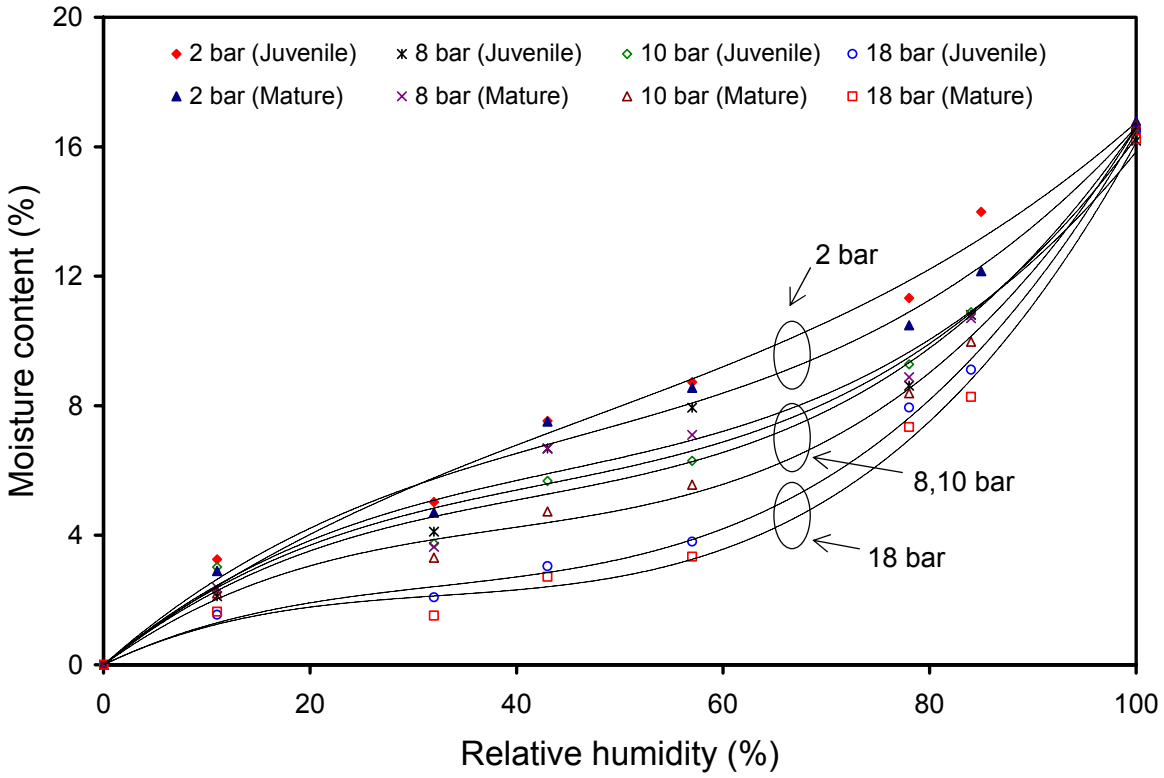


Figure 4-4. Sorption isotherm of lignocellulosic fiber refined under varying pressures.

Table 4-1. Fitted and physical constants calculated for the Hailwood-Horrobin equation.

Sample	Type	A	B	C	K_1	K_2	W	R^2
2 bar	JW	0.7544	0.1867	0.0014	94.62	0.73	3706.0	0.910
	MW	0.8730	0.1965	0.0015	80.99	0.74	3718.2	0.901
	JM	0.8105	0.1915	0.0014	90.49	0.71	3708.1	0.908
8 bar	JW	0.8415	0.2208	0.0016	87.46	0.71	3696.8	0.895
	MW	0.8706	0.2431	0.0019	78.54	0.76	3691.1	0.872
	JM	0.8162	0.2443	0.0019	83.82	0.76	3691.2	0.881
10 bar	JW	0.4569	0.2907	0.0024	137.03	0.82	3646.1	0.959
	MW	0.9380	0.3203	0.0027	67.39	0.82	3686.8	0.948
	JM	0.6544	0.3052	0.0025	97.59	0.81	3662.2	0.957
18 bar	JW	1.2868	0.5278	0.0050	44.15	0.93	3681.3	0.927
	MW	1.2551	0.6355	0.0061	44.45	0.94	3667.0	0.833
	JM	1.2408	0.5763	0.0055	45.26	0.94	3672.5	0.892

JW=Juvenile wood, MW=Mature wood, JM=Average of Juvenile wood and Mature wood.

wood polymer per mole of water sorption sites and this value did not show significant differences. Refining pressure involves refiner temperature, which causes a reduction of the FSP of the cell wall. An average FSP is commonly 28-30% for non-treated wood and 16-18% for heat-treated wood (Tjeerdsma et al. 2005).

4.3.3 Wettability

The fine fiber surface is more hydrophobic than long fiber due to its greater lignin content. Therefore, fiber refined at 18 bar of pressure, which contains higher fine percentage than that refined under other conditions may have lower sorption ability (Deng and Abazeri 1998). However, contact angles shown in Table 4-2 did not show any difference among the steam pressures, likely due to the influence of heat treatment. The contact angle of all refined fibers was approximately 90°. The surface modification of fiber generally affected the change of wetting behavior and penetration. It is known that refining pressure involves refiner temperature (Xing et al. 2007a and 2007b). Refiner pressure changed the physical appearance of the fiber, whereas refiner temperature directly impacted the chemical properties of the fiber, which are closely related to sorption properties. Heat treatment affects the increase of contact angle from 50 to 90º representing a decrease of hydrophilicity. Heat treatment below 120°C showed that wood remains hydrophilic at contact angle at 0º and that after heat treatment above 120ºC, contact angle suddenly increased to 90º (Hakkou et al. 2005, 2006). Therefore, refiner pressure could affect the reduction of hydrophilic properties of refined fibers.

Table 4-2. Contact angle of refined fiber at various refining steam pressure.

Pressure	Type	Contact angle (degree)
2 bar	Juvenile	90.0 (0.5)
	Mature	89.3 (0.2)
8 bar	Juvenile	89.0 (0.4)
	Mature	89.6 (0.2)
10 bar	Juvenile	89.3 (0.4)
	Mature	89.9 (0.7)
18 bar	Juvenile	88.9 (0.4)
	Mature	89.5 (0.4)

Values given are means (STD)

4.3.4 Water activity

The water activity (a_w) of the refined fiber is shown in Table 4-3. The a_w of refined fiber equilibrated at 65% RH ranged from 0.34 to 0.47 (Figure 4-5). The a_w value of fibers refined at 2-bar pressure was significantly higher than that of fibers refined at 18-bar pressure; furthermore, juvenile fiber had a higher a_w value than mature fiber at all levels of steam pressure. Water activity usually is an indicator of water availability for mold growth. It is closely related to physical, chemical, and biological properties. This a_w value, which is closely related to sorption isotherm, is a more reliable indicator to help prolong shelf-life and to resist mold growth than total MC (Guzey et al. 2001). Although mold growth is more related to glass transition temperature (T_g) than water activity (a_w), it is more convenient to predict mold germination using a_w (Slade and Levine 1991, Pham

Table 4-3. Water activity of refined fiber with various refining steam pressure.

Pressure	**Type**	**Water Activity**	
		65%RH	**100%RH**
2 bar	Juvenile	0.47 (0.001)[S]	0.73 (0.032)
	Mature	0.41 (0.001)[S]	0.71 (0.048)
8 bar	Juvenile	0.40 (0.002)[S]	0.74 (0.013)
	Mature	0.38 (0.001)[S]	0.73 (0.018)
10 bar	Juvenile	0.40 (0.001)[S]	0.70 (0.039)
	Mature	0.37 (0.003)[S]	0.71 (0.031)
18 bar	Juvenile	0.37 (0.002)[S]	0.76 (0.016)
	Mature	0.34 (0.003)[S]	0.75 (0.018)

Values given are means (STD)
[S] = statistic significant at $\alpha = 5\%$

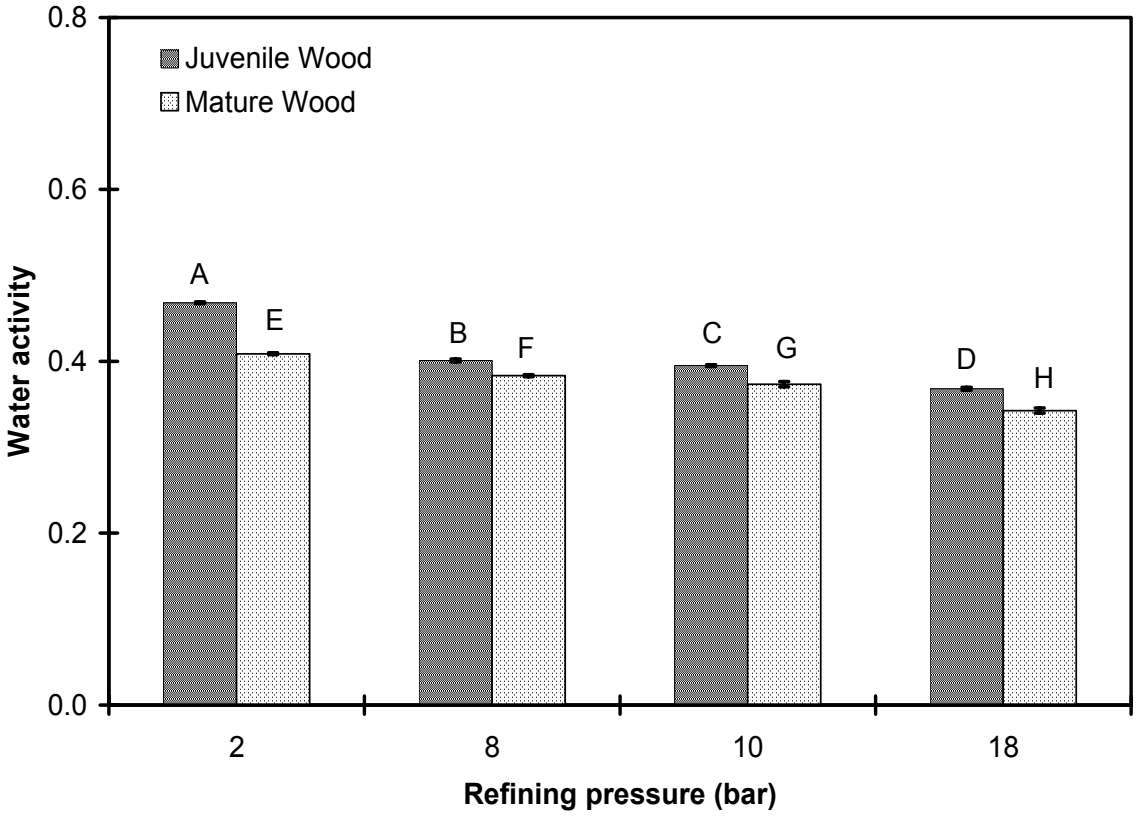


Figure 4-5. Water activity of refined fiber at 65% RH (The same letters are not significantly different at $\alpha = 5\%$).

et al. 1999). At 100% RH, a_w is around 0.70 under all conditions. Usually, no evidence of germination is observed at $a_w \leq 0.89$ (Pham et al. 1999). It has been shown that heat treatment can decrease the susceptibility to fungal decay and decrease the sorption ability of solid wood (Wahl et al. 2004). Therefore, fibers refined at any degree of steam pressure could inhibit sorption ability and mold germination.

4.3.5 Sorption rate

The sorption rate of refined fiber is shown in Table 4-4 and Figure 4-6. The highest initial sorption rate and second slope were 0.0057 and 0.0020 %/√s for juvenile fiber refined at 2-bar pressure. The initial sorption rate and second slope of mature fiber refined at 2-bar pressure were 0.0031 and 0.0008 %/√s. The rest had initial sorption rates and second slopes of approximately 0.0026 and 0.0007 %/√s. The juvenile fiber had approximately 1.8 times the initial sorption rate of mature fiber refined at 2-bar pressure (Figure 4-7). The second slope of juvenile fiber was approximately 2.5 times higher than that of mature fiber refined at 2-bar pressure (Figure 4-8). It is believed that the severe conditions at 18-bar pressure causes high heat treatment, which leads to decrease the hydrophilic properties due to change in its chemical composition. The hydrophilic *OH*-group may be replaced by *O*-acetyl group under severe refining condition. The sorption ability could be decreased by high steam pressure. In general wood polymer (cellulose, hemicelluloses, and lignin) degrades at temperature between 160 and 260°C. The refining pressure at 2-, 8-, 10-, and 18-bar pressure involves the refiner temperature of approximately 120, 170, 180, and 207°C, respectively. The wood polymer may start degrading at 8-bar pressure. Hemicelluloses degrade first at mild heat treatment because

Table 4-4. Sorption rate of refined fibers with various refining steam pressures.

Pressure	**Type**	**Initial sorption rate**	**Second slope**
		%/√s	**%/√s**
2 bar	Juvenile	0.0057 (0.0001)[s]	0.0020 (0.0004)[s]
	Mature	0.0031 (0.0007)	0.0008 (0.0004)
8 bar	Juvenile	0.0027 (0.0002)	0.0007 (0.0003)
	Mature	0.0026 (0.0005)	0.0008 (0.0002)
10 bar	Juvenile	0.0026 (0.0008)	0.0007 (0.0002)
	Mature	0.0025 (0.0003)	0.0007 (0.0002)
18 bar	Juvenile	0.0026 (0.0007)	0.0008 (0.0002)
	Mature	0.0027 (0.0007)	0.0007 (0.0004)

Values given are means (STD)

[S] = statistic significant at $\alpha = 5\%$

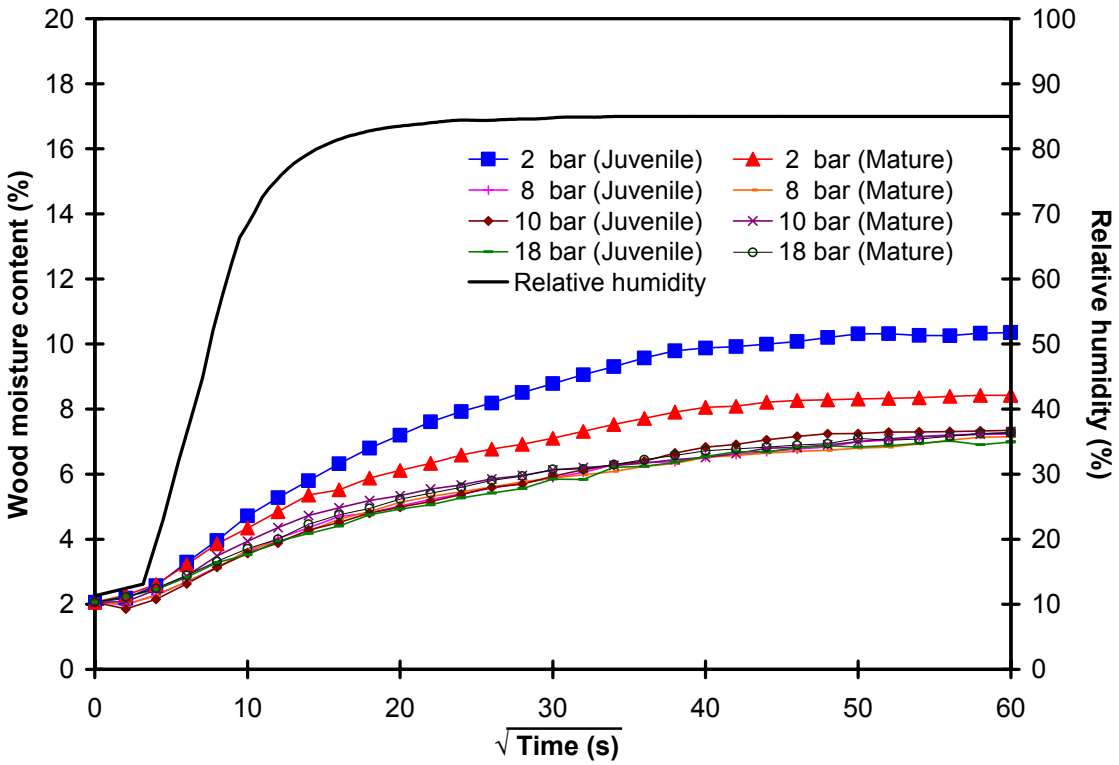


Figure 4-6. Comparison of sorption rate of various refined fibers.

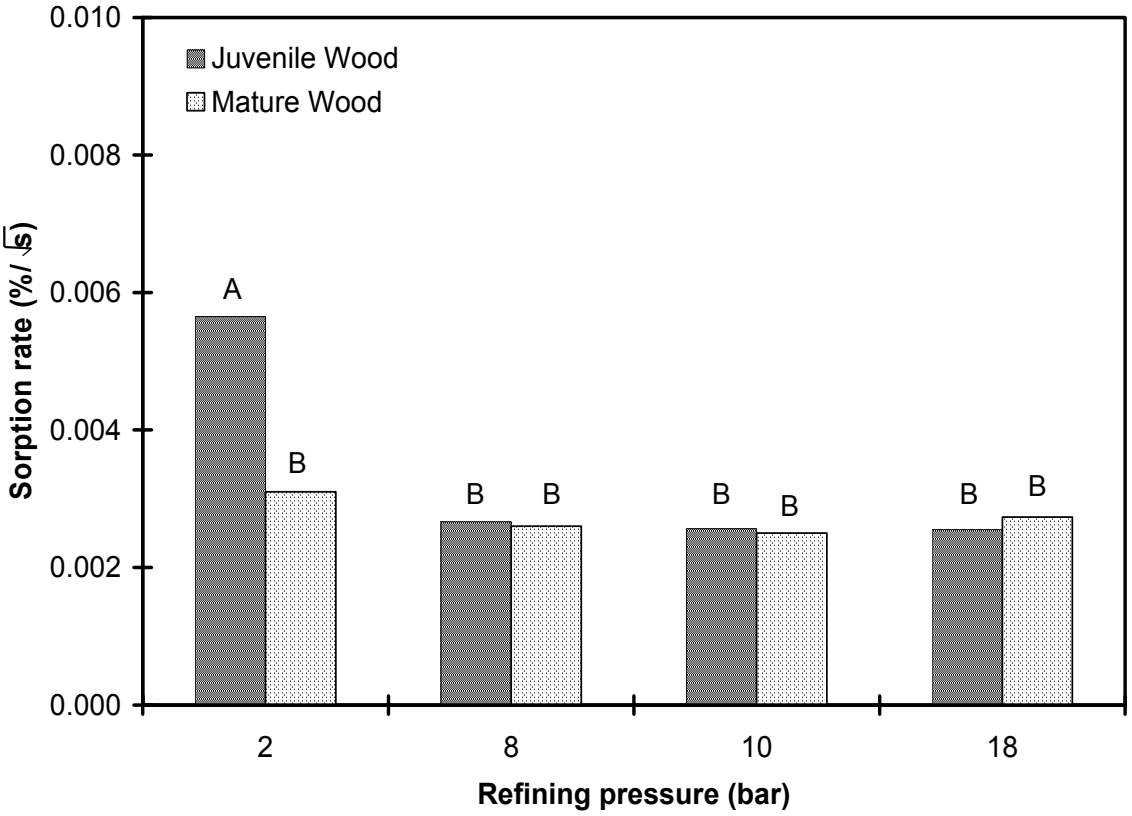


Figure 4-7. Comparison of initial sorption rate of various refined fiber (The same letters are not significantly different at $\alpha = 5\%$).

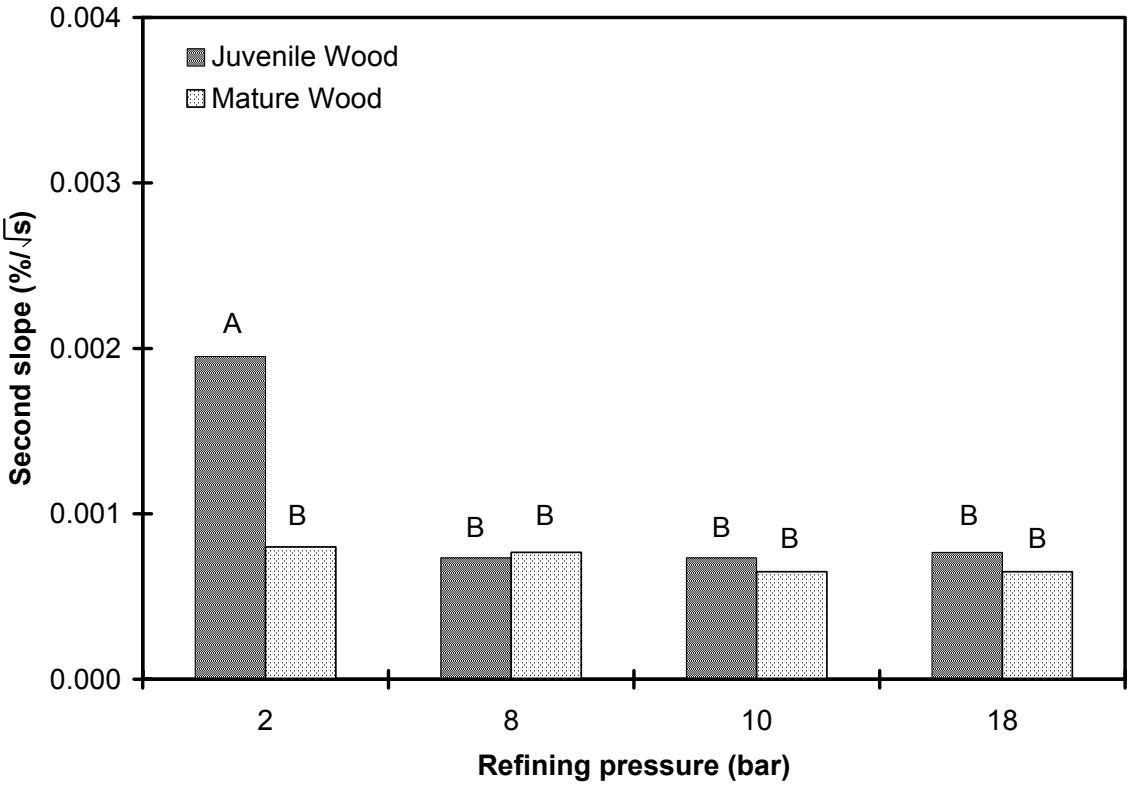


Figure 4-8. Comparison of second slope of various refined fibers (The same letters are not significantly different at $\alpha = 5\%$).

they are more easily hydrolyzed than cellulose. Heat treatment can also break physical bonds between water and hydrophilic groups of wood; moreover, some degradation of some hydrophilic polymers such as hemicelluloses can reduce the sorption ability. Heat treatment can change the chemical structure of hemicelluloses and amorphous cellulose. In addition, the structure of lignin can be modified and the extractives can be evaporated (Kortelainen and Viitaniemi 2006, Poncsak et al. 2006, Rousset et al. 2004, Tjeerdsma and Militz 2005). Therefore, severe refining conditions may cause reductions in the sorption ability including sorption rate of refined fiber.

4.3.6 Crystallinity

Crystallinity is represented by the crystalline index shown in Table 4-5 and Figure 4-9. The highest crystalline index was 0.67 for fiber refined at 18-bar pressure. The crystalline index of fiber refined at 2-bar pressure was significantly lower than that at 18-bar pressure. It is believed that lower crystalline index has more accessible surface available for water molecules, which causes higher moisture sorption, especially below 75% RH (Mihranyan et al. 2004). Wood fiber is mainly composed of linear chains of cellulose and branched-structures of hemicelluloses. Severe refining condition at 207°C can destroy branched structures of hemicelluloses, which degrade at a temperature ranging from160 to 220°C (Bhuiyan and Hirai 2005; Yildiz and Gumuskaya 2007). This phenomenon may affect crystallinity. Generally, crystallinity increases and then gradually decreases during boiling and heating at 120 to 160°C (Poncsak et al. 2006). The decrease of hemicelluloses leads to the increase of crystallinity due to its relatively high cellulose content. Therefore, fiber with higher crystallinity tends to absorb less water

Table 4-5. Crystallinity of refining fiber varying pressures.

Pressure	**Type**	**Crystallinity**
2 bar	Juvenile	0.508
	Mature	0.522
8 bar	Juvenile	0.513
	Mature	0.539
10 bar	Juvenile	0.522
	Mature	0.530
18 bar	Juvenile	0.667
	Mature	0.667

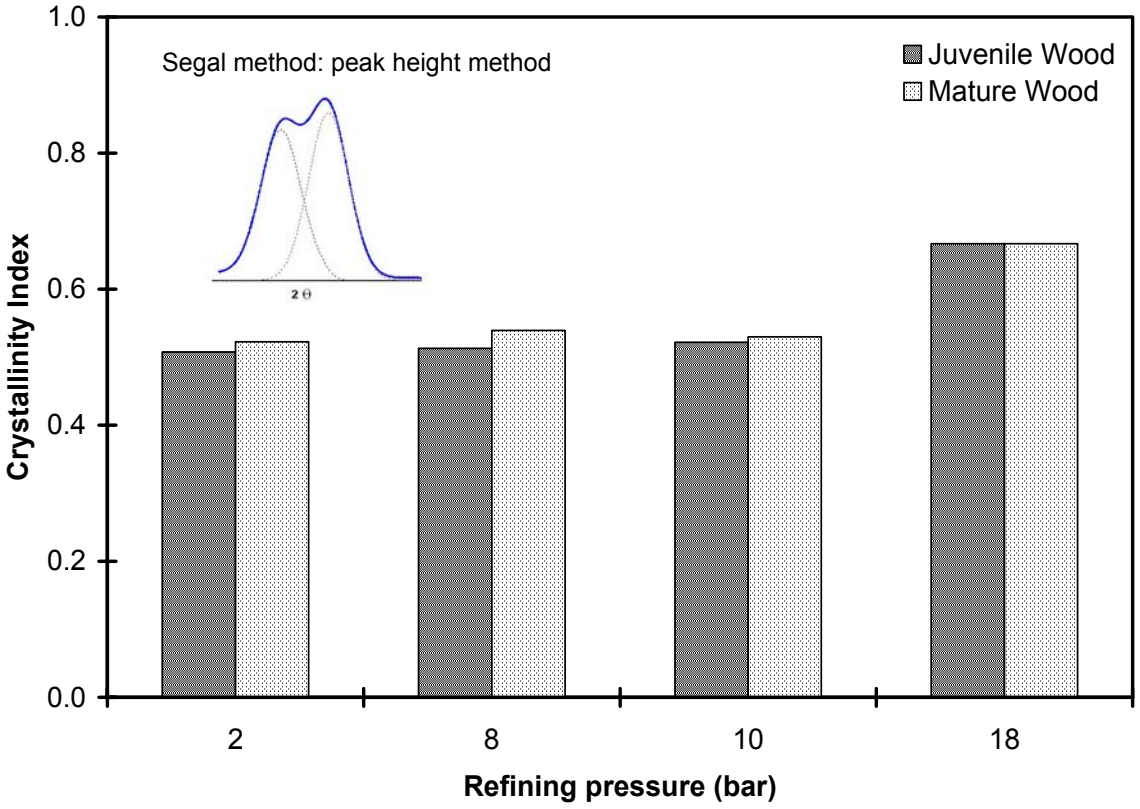


Figure 4-9. Crystallinity of refined fiber from varying refining pressure.

than that with lower crystallinity.

4.4 Summary

The refining steam pressures used in the manufacture of wood fiber-based composites have a dramatic effect on sorption behavior and surface properties of the wood fiber. Wood fiber refined at high steam pressure shows extensive damage as qualitatively determined by SEM. Wood fiber refined at 2-bar steam pressure has significantly higher sorption rate than fiber refined at higher steam pressure. Sorption rate for juvenile fiber is greater than that for the mature fiber counterpart. Water activity decreases with increasing steam pressure, whereas crystallinity was shown to increase with increasing steam pressure. However, the contact angle of refined fiber does not show any significant difference with varying steam pressures. The sorption isotherm of refined fiber was fitted very well by a Hailwood-Horrobin model.

5. EFFECT OF PROCESSING PARAMETERS ON WATER VAPOR SORPTION OF WOOD STRANDS

5.1 Introduction

The volume of oriented strandboard (OSB) produced has significantly increased over the last few decades for applications such as housing. However, outdoor use can be undesirable when exposed to atmospheric vapor or rain. Poor water repellency causes several changes in composites such as dimension changes, strength loss, and color change (Pandey and Pitman 2002, Stark and Matuana 2004). Unlike OSB, medium density fiberboard (MDF) and fiber-reinforced composites can provide a large surface area, which gives a better mechanical interlocking between the fiber and adhesives; therefore, it can reduce water absorption. However, water can easily penetrate into the void and interfacial gaps between fiber and matrix in OSB, causing high water uptake (Jacob et al. 2006). Water content does not only affect the panel in service, but also in manufacturing processes, particularly the hot pressing process.

Hot-pressing is a major and important process for OSB production. A few minutes are used to consolidate a wood mat. The through-mat-thickness sorption of water

vapor takes place simultaneously during the short pressing period, although the mat does not fully experience water vapor because of its short time period. Steam preheating, steam-injection pressing, chemical gas injection pressing, and wax/resin system make the sorption mechanism even more complicated. The diffusion of water into panels is an important parameter for sorption behavior. Diffusion is highly dependent on panel density, particle geometry, surface area, and flake orientation. Diffusion coefficients slightly increase when vapor movement occurs parallel to the machine or suface flake direction. Past research has shown flake orientation to exhibit little influence on diffusion rates, particularly low-density panels (Lehmann 1972). Therefore, factors controlling diffusion rates may come from solid wood characteristics, i.e., lumens, cell walls, and pit openings. Moisture sorption in composites is related to diffusion and permeability, but relative amounts of moisture absorbed are controlled by inherent characteristics (Lehmann 1972). Sorption behavior under this circumstance is useful information for predicting dimensional stability during service.

Several techniques to improve water repellency and thickness swelling of composites, such as increasing resin and wax content, affect sorption behavior of panels. The increase of MDF density may decrease water absorption due to its smaller void and interfacial gaps (Muehl and Krzysik 1997). Phenol-formaldehyde (PF) thermosetting resins are commonly used in the production of molded plastics, wood products, and aerospace components due to its highly hydrophobic properties. Generally, PF resins are used to improve moisture resistance and weatherability for composites (Maloney 1993). Not only PF resin, but the isocyanate adhesive such as methylene diisocaynate (MDI) resin can react with water and form cross-linkages with the wood constitutes, which

reduce the adsorptive nature of wood (Alexander et al. 2000, Harper et al. 2001). A 2% addition of wax can improve water repellency by reducing surface energy, which makes it hydrophobic. Wax properties such as chemical composition, melting point, viscosity, and oil content closely relate to liquid and vapor repellentcy of OSB. These wax properties also influence the spray technology and spray rate (Clad 1985, Hsu et al. 1990).

Several parameters influence the moisture sorption of a panel, such as solid wood properties and wood volume fraction, fiber orientation, temperature, and polarity (Mishra and Verma 2006). However, wood, resin, and wax as the three major raw materials, play the key role in determining properties of the product. How resin and wax affect the water vapor sorption behavior of resinated and waxed strands remains unclear. An understanding of moisture sorption in different resin and other additive systems will contribute to designing a better performing panel. The objective of this study was to investigate the effect of resin and emulsion wax loading on the water vapor sorption behavior of loblolly pine strands, using micro-scale measurements. This study also investigated the influence of pressing parameters, i.e., platen temperature and compression rate on sorption properties of loblolly pine strands.

5.2 Experimental design

Four levels of PF resin loading (0%, 2%, 4%, and 6% based on dry weight) were applied to wood strands for the resin study. Four levels of wax loading (0.0%, 0.5%, 1.0%, and 1.5% based on dry weight) were applied for the wax study. Two compression rates were used (1.05 and 1.65). Three pressing temperatures were used: 120°C, 160°C,

and 200°C. Each parmeter was independently designed. The experiment design is shown in Table 5-1.

5.3 Materials and methods

5.3.1 Materials

Loblolly pine (*Pinus taeda*) strands were provided from a plantation in Crossett, Arkansas, USA. Commercial liquid phenol formaldehyde (PF) resin (solid content at 50.5%) from Dynea USA Inc. and commercial wax emulsion (solid content at 57.04%) from Borden Chemical Co. were used in this study.

5.3.2 Sample preparation

Pure earlywood stands were cut into 5-mm-wide x 1.5-mm-long x 0.5-mm-thick. The grain direction was parallel to the long length of the earlywood strips. These strips were cut from the same area within the wood strand to reduce variability in sorption. The cutting diagram is shown in Figure 5-1. The samples were oven dried at 50°C until the weight was constant and the oven dried weight was recorded. After spraying one-side of the specimen, the sample was oven dried at 50°C for 15 minutes. The resin or wax was sprayed on the other side of the sample and the sample was oven dried at 50°C for 15 minutes. The resin or wax loading was calculated based on oven dried weight. For pressing studies, pairs of samples were pressed together with a hot press system (Carver, Inc.). The pressing parameters are shown in Table 5-1.

Table 5-1. Experimental design for resin study.

Studies	Level (%)	Description	Matric dependent variable
Resin	0.0, 2.0, 4.0, 6.0	No wax	Diffusion, Sorption rate EMC
Wax	0.0, 0.5, 1.0, 1.5	No resin	Diffusion, Sorption rate EMC
Pressing Parameter			
Compression rate	1.05,1.65	4 % resin content No wax 160°C of press temperature 180 second of press time	Diffusion, Sorption rate EMC
Temperature (°C)	120, 160, 200	4 % resin content No wax 1.05 of compression rate 180 second of press time	Diffusion, Sorption rate EMC

Remark: The interaction of resin and wax was not investigated.

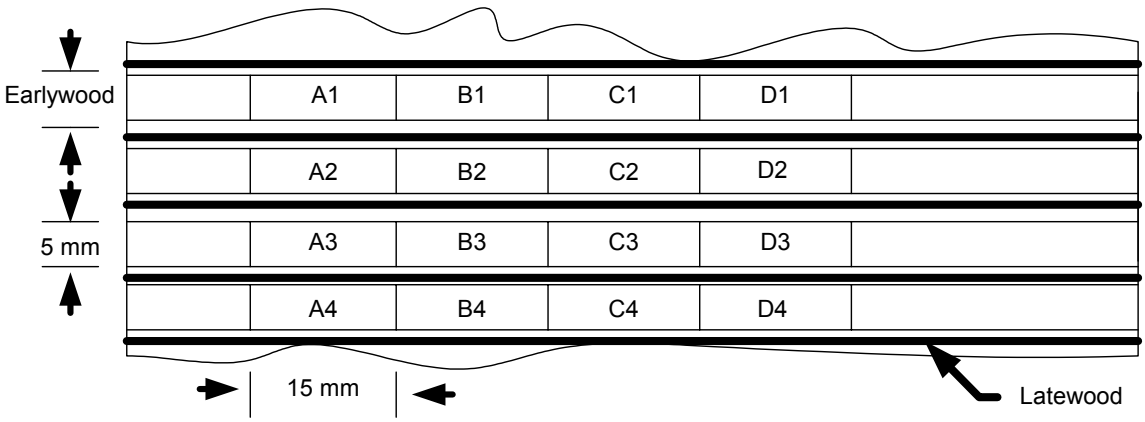


Figure 5-1. The cutting diagram (4 loading level and 4 replications for each study).

5.3.3 Sorption kinetics

All samples were equilibrated at 11% RH over a saturated salt solution. After equilibration, samples were placed in a conditioning chamber under changing RH from 11% to 80%. The weight change was continuingly recorded by Dynamic Contact Angle Analyzer DCA 332. The experimental setup of the climate control instrument was explained in chapter 3. Six replications for each loading level and pressing parameter were used.

5.3.4 Evaluation of sorption kinetics

The sorption rate was determined from the slope of the plot of MC against time. The initial sorption rate (K_1) was calculated from the slope within five minutes, whereas the second slope (K_2) was calculated from the second linear slope within another five minutes. The measurement of equilibrium moisture content (EMC) was also investigated. The calculation of diffusion coefficients (D), surface emission (σ), and surface resistance (S) was described in chapter 3.

5.4 Results and discussion

5.4.1 Resin loading results

Two methods of sorption behavior analysis were used. The first was based on weight gain and the second was based on MC change. The weight gain per volume can be designated as the moisture uptake. The term “water uptake” normally means the uptake of liquid water; however, the term “moisture uptake” used in this study means the amount

of water vapor uptake per sample volume. The moisture uptake behavior of resinated strands loaded with different resin levels is shown in Figure 5-2. The average moisture uptake rate of resinless strands was 8.00 x 10^{-6} (mg/mm^3)/s whereas it was 6.00 x 10^{-6} (mg/mm^3)/s for 6% resin loading (Table 5-2). The moisture uptake rate of resinated strands decreased with an increase in resin loading. It is possibly due to the higher resin coverage resulting in a reduction of available surface area for water vapor sorption. The initial sorption rate of resinless strands was significantly higher than that of resinated strands (p-value = 0.0115). At 2% intervals of resin loading, it may not be possible to detect differences in sorption rate. This could be attributed to the difficulty of uniformly applying a constant resin distribution at the micro-scale. Zhang et al. (2007) stated that the water uptake of resinated strands before pressing was significantly influenced by resin and wax content, grain direction of wood strands, and strand density because the reduction of capillaries diameter or total voids caused a reduction of water uptake. The EMC of resinless strands was 22.7% whereas resinated strands were between 15.1 and 20.4%. The EMC of resinless strands was significantly higher than EMC of resinated strands with 6% of resin loading (p-value = 0.0004). The MC of OSB equilibrated at 100% RH after 30 hours was reported by Ye et al. (2006); it was only between 12.3% and 16.9%. Higher resin loading results in a reduced EMC and sorption rate within the wood strand due to the reduction in voids content (Thomason 1995). The voids were possibly covered by resin, which blocked moisture sorption at high humidities. For PF resin, the sorption properties of phenolic-bonded strands decrease with decreasing its caustic content (Wittmann 1973).

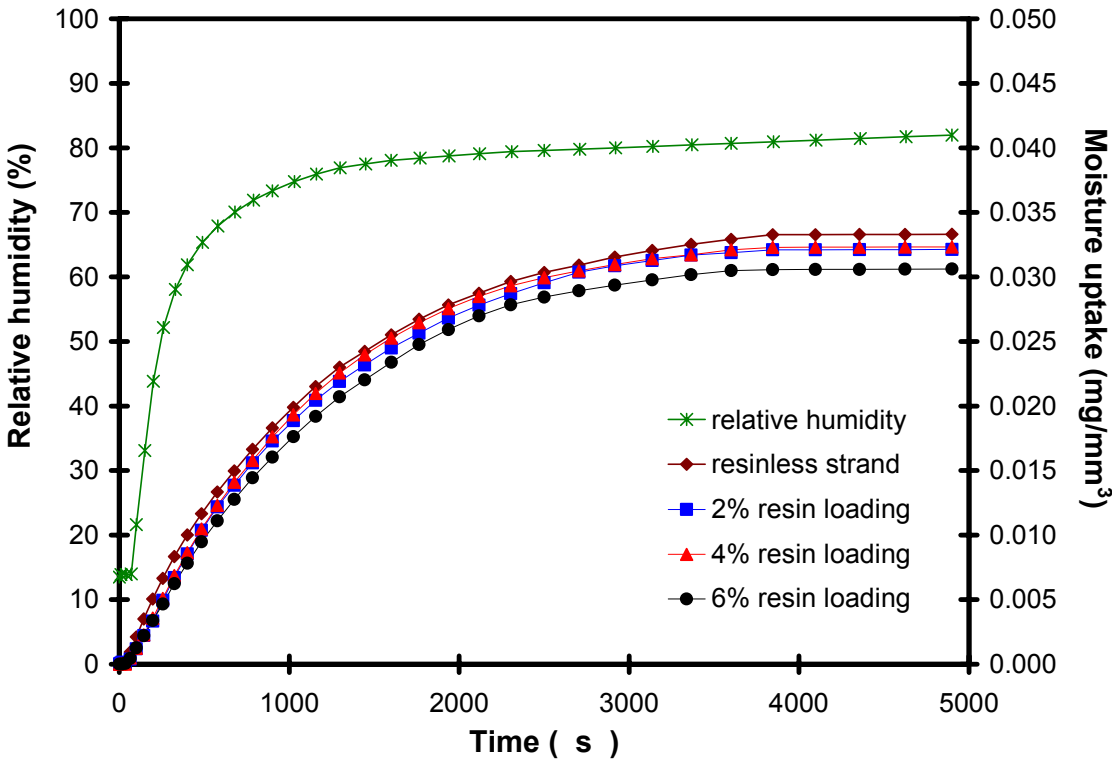


Figure 5-2. Water vapor uptake behavior of strands loaded with different resin levels.

Table 5-2. Water vapor uptake rate and EMC of strands loaded with different resin levels.

Resin loading	**Initial uptake rate**	**EMC**
	x 10^{-6} (mg/mm^3)/s	**(%)**
	(p-value = 0.0115)	**(p-value = 0.0004)**
0%	8.00 (0.82)^{A}	22.7 (0.40)^{A}
2%	6.50 (0.89)^{B}	20.4 (4.29)^{AB}
4%	6.60 (0.84)^{B}	17.0 (1.23)^{BC}
6%	6.00 (0.71)^{B}	15.1 (2.02)^{C}

Values given are means (STD)
The same letters are not significantly different at α = 5%

The cure process of thermosetting resins is influenced by the fraction of space in resin available for water sorption (Enns and Gillharn 1983). During curing, the glass transition temperature of thermosetting resin increases until it reaches cure temperature. At that point, molecular motion and diffusion no longer exist and the uncured resin has a larger unoccupied volume. Therefore, uncured resin had higher propensity to absorb water (Aronhime et al. 1986). During curing, the chemistry of the thermosetting resin is more susceptible to hydrolysis due to its higher degree of chain scission (Karad et al. 2003). The sorption process involves both inherent structure and surface of wood. It can be said that in liquid phase, the sorption process involves both physi- and chemi-sorption whereas in vapor phase the sorption process involves a primary surface or chemi-sorption, which is dependent on the free hydroxyls. These *OH*-groups will interact with themselves instead of with water molecules and, due to the coverage of non-polar moieties, this coverage results in the unavailability of *OH*-groups to form H-bonds with water molecules (Renneckar et al. 2006). Water molecule interacts with strong forces in *OH*-groups, which is greater than the capillary condensation of water vapor (Sheppard and Newsome 1934).

The second analysis method was based on MC change. The MC change can be designated as moisture sorption. The moisture sorption of resinated strands loaded with different resin levels is shown in Figure 5-3. The initial sorption rate and second slope was 0.0022 and 0.0021 %/√s for resinless strand whereas it was 0.0021 and 0.0017 %/√s for 6% resin loading (Table 5-3 and Figure 5-4). These results showed the resin loading affected the moisture sorption rate of resinated strands. The moisture sorption rate of resinated strands decreases with an increase in the resin loading. It was obvious that resin

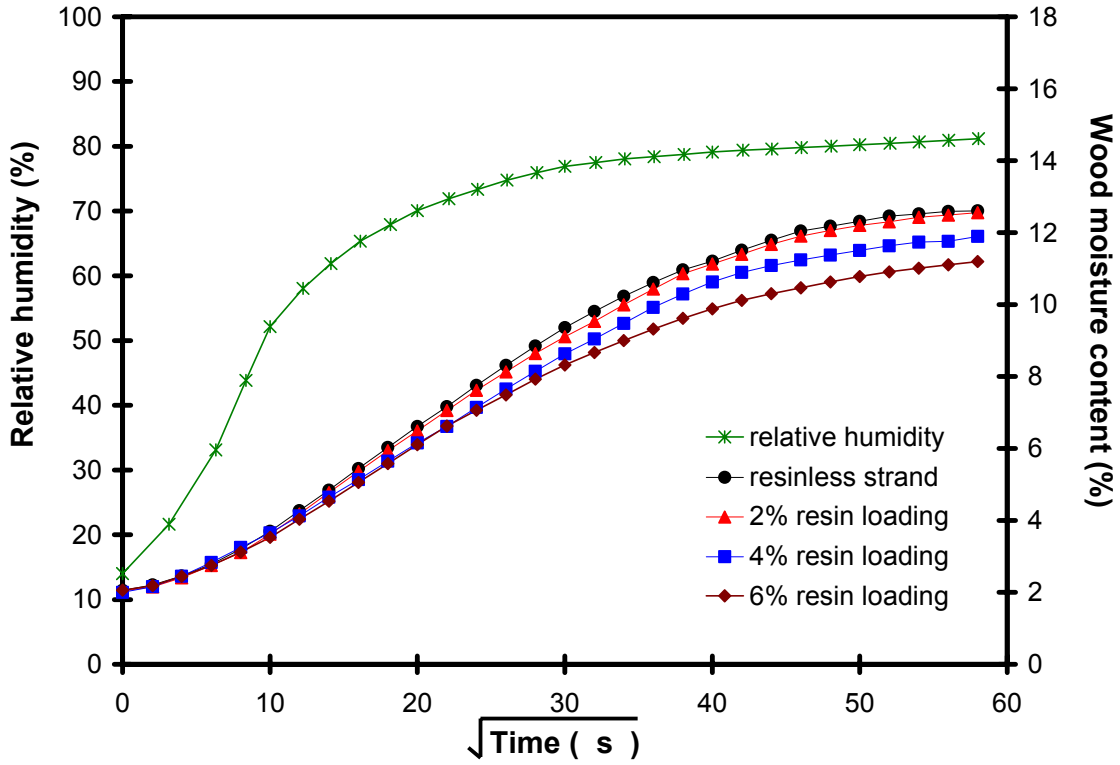


Figure 5-3. The moisture sorption of resinated strand loaded with different resin levels.

Table 5-3. Initial sorption rate (K_1), second slope (K_2), diffusion coefficient (D), surface emission coefficient (σ), and surface resistance coefficient (S) of resinated wood.

Resin loading	**K_1 (%/√s) Mean (Std)**	**K_2 (%/√s) Mean (Std)**	**$D_{0.5}$ (10^{-10} m^2/s) Mean (Std)**	**$D_{0.6}$ (10^{-10} m^2/s) Mean (Std)**	**σ (10^{-7}m/s) Mean (Std)**	**S (10^6s/m) Mean (Std)**
0 %	0.0022 (0.0002)	0.0021 (0.0003)	1.728 (0.056)	1.969 (0.108)	4.851 (0.213)	2.065 (0.094)
2%	0.0022 (0.0003)	0.0021 (0.0002)	1.712 (0.085)	1.946 (0.110)	4.865 (0.279)	2.061 (0.117)
4%	0.0021 (0.0002)	0.0019 (0.0002)	1.647 (0.156)	1.818 (0.112)	4.723 (0.490)	2.135 (0.232)
6%	0.0021 (0.0002)	0.0017 (0.0001)	1.637 (0.111)	1.806 (0.100)	4.776 (0.237)	2.098 (0.108)

Values given are means (STD)
There are no statistically different at α = 5%
Remark: $D_{0.5}$ = diffusion at 50% of total sorption, and $D_{0.6}$ = diffusion at 60% of total sorption

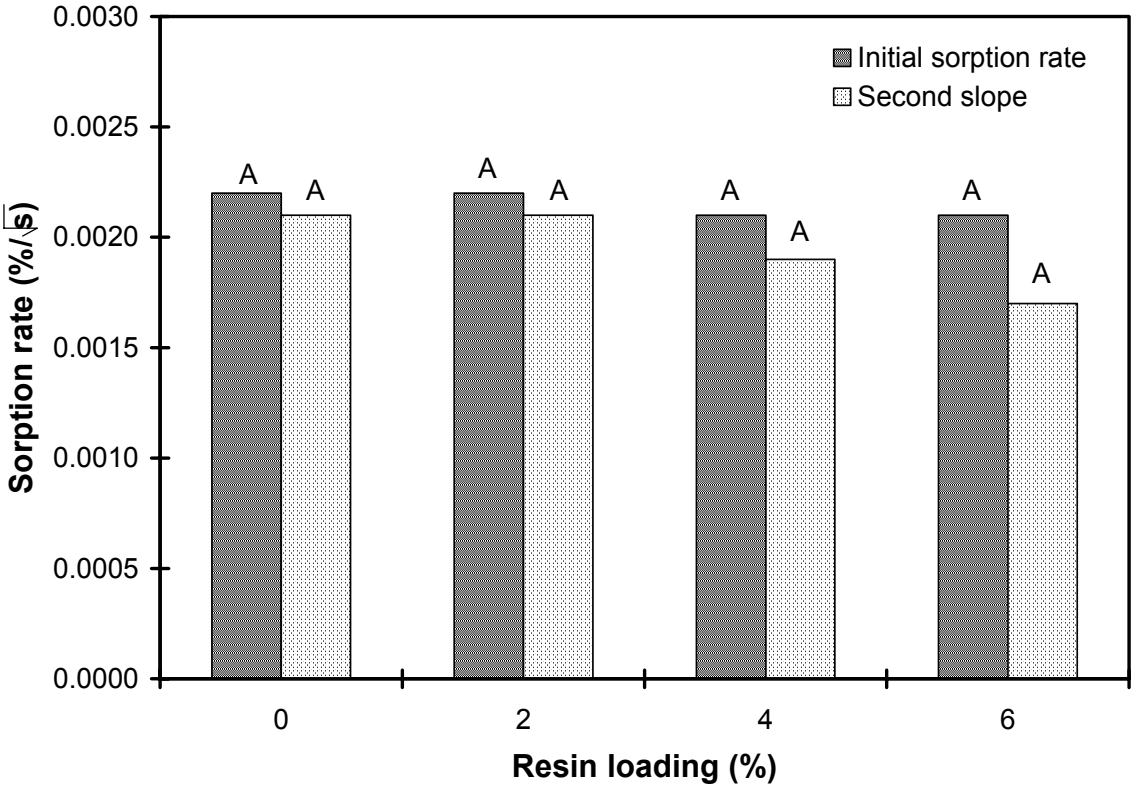


Figure 5-4. Initial sorption rate and second slope of resnated strands (The same letters are not significant at $\alpha = 5\%$).

loading had a more pronounced effect on the second slope of water vapor sorption than initial sorption rate. This is possibly due to the effect of the transition period of RH change at the early stage. The use of the first or the second analysis method depends on the specific information needed. The first method is suitable for short period time whereas the second is more informative.

The diffusion coefficient, surface emission, and surface resistance of resinated strands are shown in Table 5-3 and Figure 5-5. The diffusion coefficient of resinless strand at 60% of total sorption was 1.969×10^{-10} m^2/s whereas it was between 1.949×10^{-10} m^2/s and 1.806×10^{-10} m^2/s for resinated strands. The diffusion coefficient of resinless strands was slightly higher than resinated strands with 2% resin loading. It was approximately 10% higher than resinated strands with 6% resin loading. These data show that moisture can diffuse slightly more in resinless strands. The surface resistance coefficient and surface emission coefficient of resinless strands were 2.065×10^6 s/m and 4.851×10^6 m/s, respectively. There was no big difference of surface coefficients of strands treated with different resin loadings. However surface resistance coefficients were slightly lower than that of resinated strands. The higher surface resistance in resinated strands causes slower sorption processes. Zhang's study reported that resin levels influence the water uptake of strands. A lower resin loading strand had a higher water uptake (Zhang et al. 2007), although the resin loading only slightly affected moisture uptake. It is possibly due to the slower sorption of water vapor than liquid water. Water uptake was dependent on the penetration of resin into wood cell walls and lumens to block capillary action. In contrast, moisture uptake is more dependent to on surface properties (Ye et al. 2006).

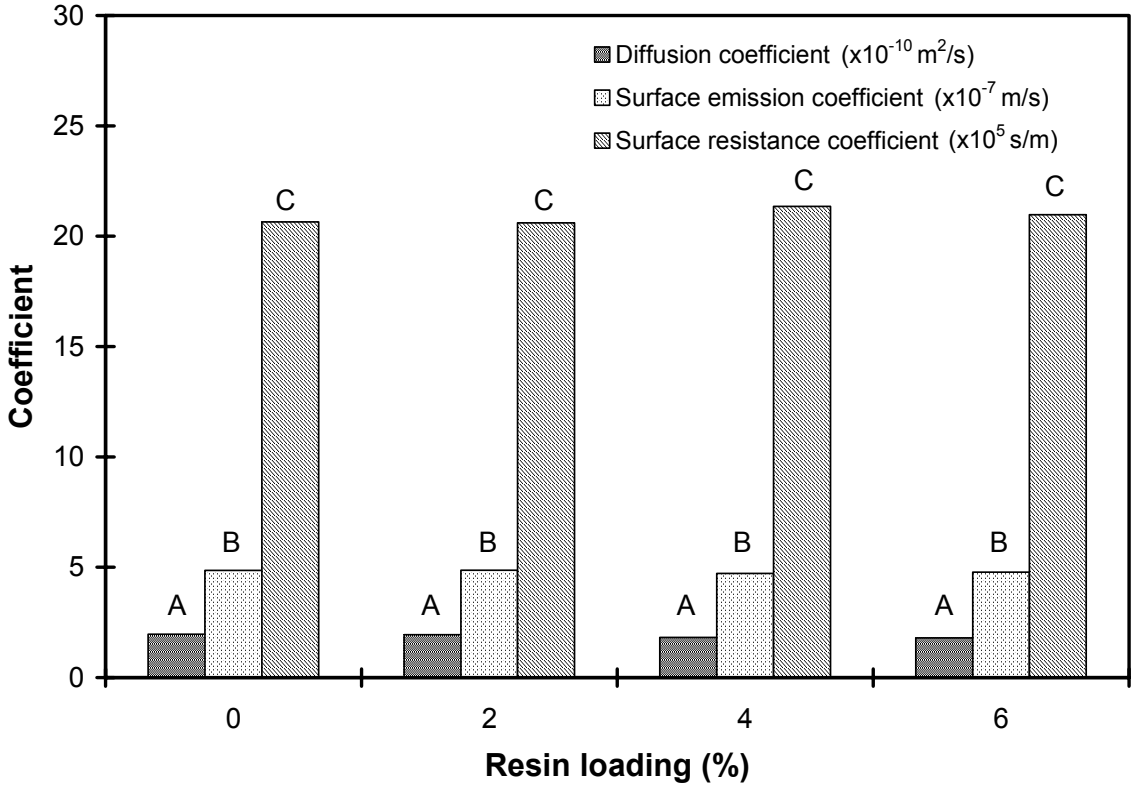


Figure 5-5. Diffusion coefficient, surface emission coefficient, and surface resistance coefficient of resinated strand with various resin loading (The same letters are not significantly different at $\alpha = 5\%$).

Under hot-pressing in composite manufacture, resinated strands experience only a few minutes of environment change during pressing. Resin loading may not significantly influence sorption properties of resinated strands at short time period. However in wood-plastic composites (WPC), several researchers found that moisture uptake of WPC increases with increasing wood content. The different wood forms may affect sorption behavior differently. WPC made from smaller wood particles such as wood flour tend to have lower moisture uptake than WPC made from larger particle such as wood fiber (Bledzki and Faruk 2004). Generally the hemicelluloses on the surface and the amorphous parts of the wood fibrils contain a large amount of accessible hydroxyl groups (Siau 1984). The higher specific surface area can expose more hydroxyl groups in wood flour (Raj et al. 1988). Resin loading may influence the moisture uptake of wood fiber and wood flour differently, depending on its surface coverage and processing method.

5.4.2 Wax loading results

The moisture uptake behavior of waxed strands loaded with different wax levels is shown in Figure 5-6. The moisture uptake rate of wax-free strand was 8.00 x 10^{-6} (mg/mm^3)/s, whereas it was 2.80 x 10^{-6} (mg/mm^3)/s for 1.5% wax loading (Table 5-4). The moisture uptake rate of wax-free strands was approximately 3 times higher than waxed strand loaded with 1.5% wax levels. The results showed that the higher wax loading has significantly reduced moisture uptake rates of waxed strands (p-value < 0.0001). The moisture uptake rate of waxed strands was lower than that of wax-free strands. Garcia et al. (2006) stated that the sorption behavior of wax use is independent of the resin used. The EMC of wax-free strands was 22.5%, whereas waxed strands were

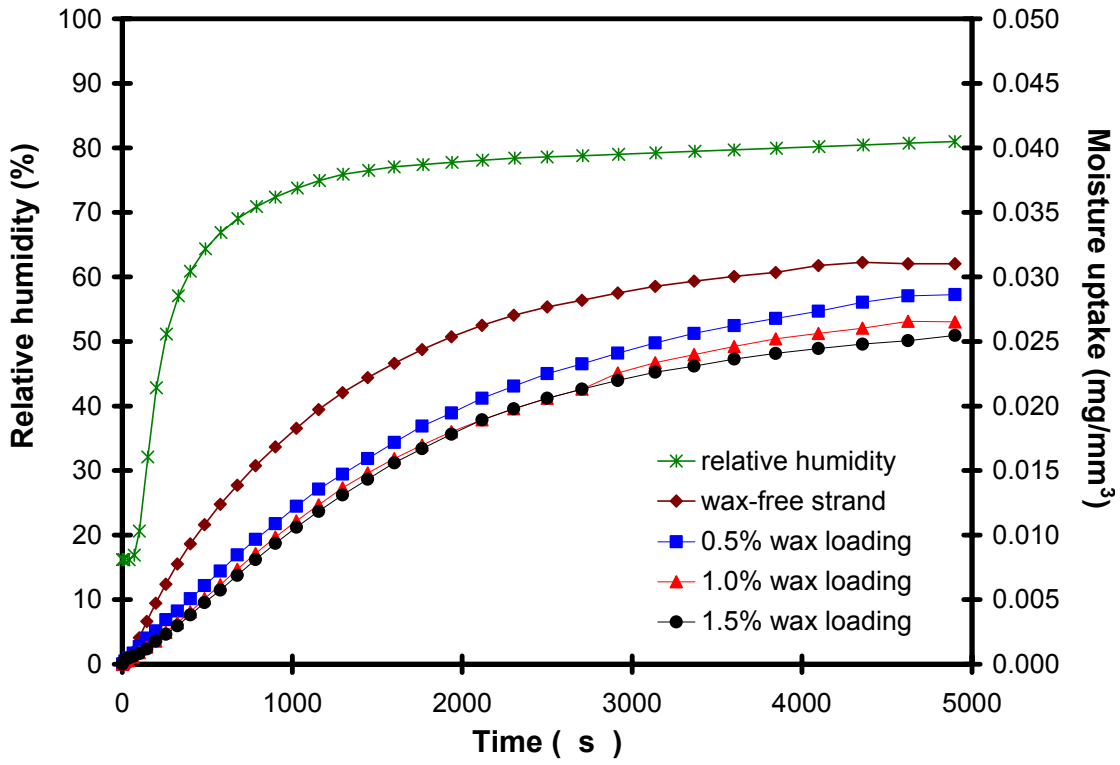


Figure 5-6. Water vapor uptake behavior of wood strands loaded with different wax levels.

Table 5-4. Water vapor uptake rate and EMC of strands loaded with different wax levels.

Resin loading	**Initial uptake rate**	**EMC**
	x 10^{-6} (mg/mm^3)/s	**(%)**
	p-value = 0.0001	**p-value = 0.0087**
0.0%	8.00 (0.82)^{A}	22.5 (0.35)^{A}
0.5%	3.83 (1.17)^{B}	17.4 (1.65)^{B}
1.0%	3.00 (0.38)^{BC}	16.5 (0.73)^{B}
1.5%	2.80 (0.45)^{C}	16.8 (0.97)^{B}

Values given are means (STD)
The same letters are not significantly different at $\alpha = 5\%$

between 16.5 and 17.4%. The EMC of wax-free strands was higher than waxed strands. The waxed strands had a lower sorption amount and moisture uptake rate than wax-free strands. Although the phase use of water is different, this study agrees with Zhang's finding that the high wax content reduces the total sorption amount and decreases the rate of sorption (Zhang et al. 2007).

The moisture sorption of waxed strands loaded with different wax levels is shown in Figure 5-7. The initial sorption rate and second slope of wax-free strands was 0.0023 and 0.0022 %/√s, respectively (Table 5-5 and Figure 5-8). It was 2.5 and 1.5 times higher than waxed strands for initial sorption rate and second slopes, respectively. These results showed the same trend of resin loading. However, the influence of wax loading on water vapor sorption rate and EMC is more obvious than for resin loading. Wax application rate is used commercially to improve water-resistant properties of composites. This application also reduces mechanical properties by decreasing bond quality. In this experiment with individual wood strands, it was clear that wax application may reduce the bond quality of inter-strand attachment.

The diffusion coefficient, surface emission, and surface resistance of waxed strands are shown in Figure 5-9. The diffusion coefficient of wax-free strands at 60% of total sorption was 1.910×10^{-10} m^2/s whereas it was between 1.264×10^{-10} m^2/s and 1.209×10^{-10} m^2/s for waxed strands. The diffusion coefficient of wax-free strands was significantly higher than for waxed strands (p-value = 0.0001). It was approximately 1.5 times higher than waxed strands with 1.5% wax loading. Analysis of the data supported the idea that moisture can diffuse more in a wax-free strand. The surface resistance coefficient of wax-free strands was 2.102×10^{6} s/m. It was higher for wax-free strands

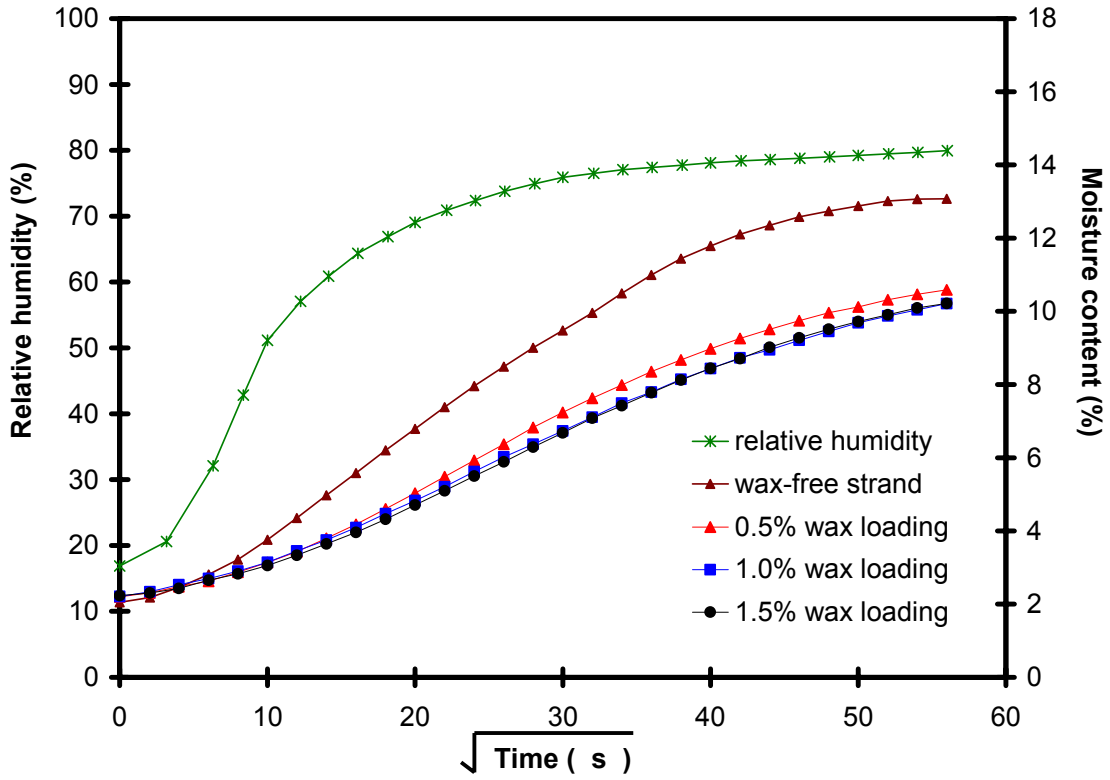


Figure 5-7. Moisture sorption of wood strands loaded with different wax levels.

Table 5-5. Initial sorption rate (K_1), second slope (K_2), diffusion coefficient (D), surface emission coefficient (σ), and surface resistance coefficient (S) of waxed strand.

Resin loading	**K_1 (%/√s) Mean (Std)**	**K_2 (%/√s) Mean (Std)**	**$D_{0.5}$ (10^{-10} m^2/s) Mean (Std)**	**$D_{0.6}$ (10^{-10} m^2/s) Mean (Std)**	**σ (10^{-7}m/s) Mean (Std)**	**S (10^6s/m) Mean (Std)**
0 %	0.0023 (0.0005)^s	0.0022 (0.0003)^s	1.696 (0.069)^s	1.910 (0.065)^s	4.768 (0.249)^s	2.102 (0.113)^s
0.5%	0.0010 (0.0001)	0.0013 (0.0003)	1.128 (0.100)	1.264 (0.106)	3.187 (0.263)	3.154 (0.238)
1.0%	0.0010 (0.0001)	0.0012 (0.0003)	1.122 (0.082)	1.234 (0.176)	3.182 (0.269)	3.160 (0.258)
1.5%	0.0009 (0.0001)	0.0012 (0.0001)	1.028 (0.098)	1.204 (0.135)	2.970 (0.198)	3.378 (0.235)

Values given are means (STD)

^{s} showed statistical difference at α = 5% (p-value = 0.0001)

Remark: $D_{0.5}$ = diffusion at 50% of total sorption, and $D_{0.6}$ = diffusion at 60% of total sorption

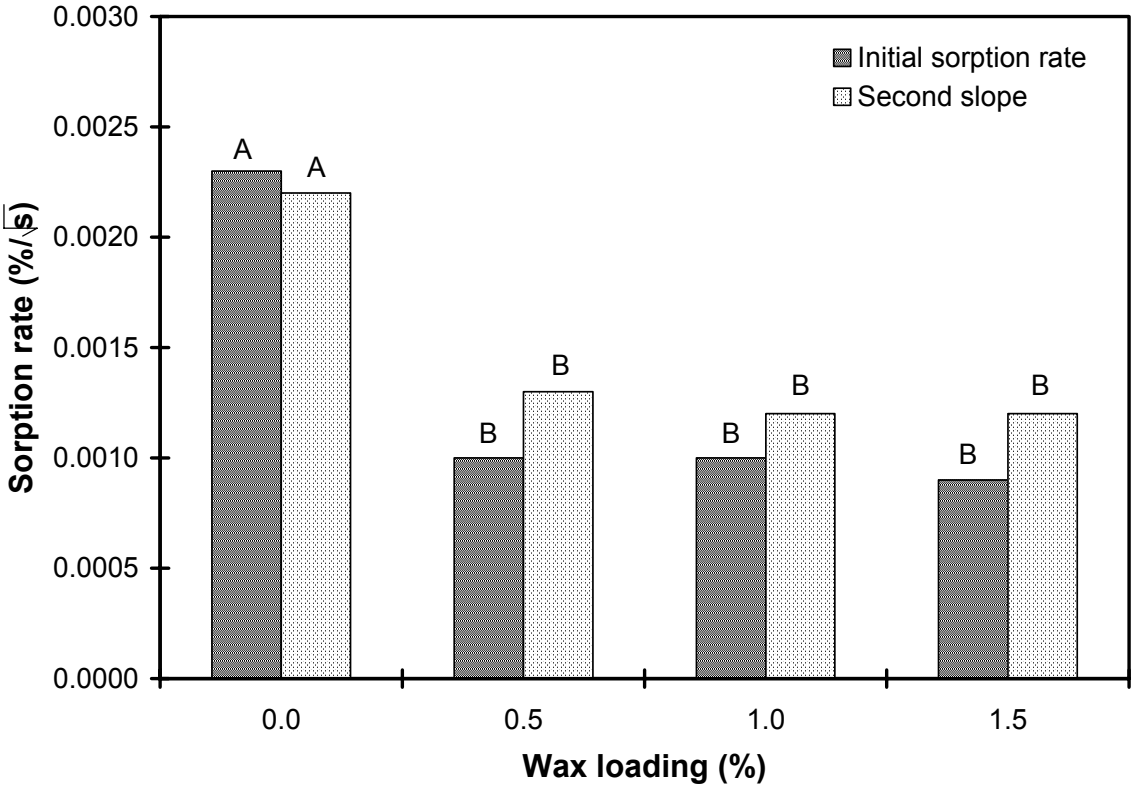


Figure 5-8. Initial sorption rate and second slope of waxed strands (The same letters are not significantly different at $\alpha = 5\%$).

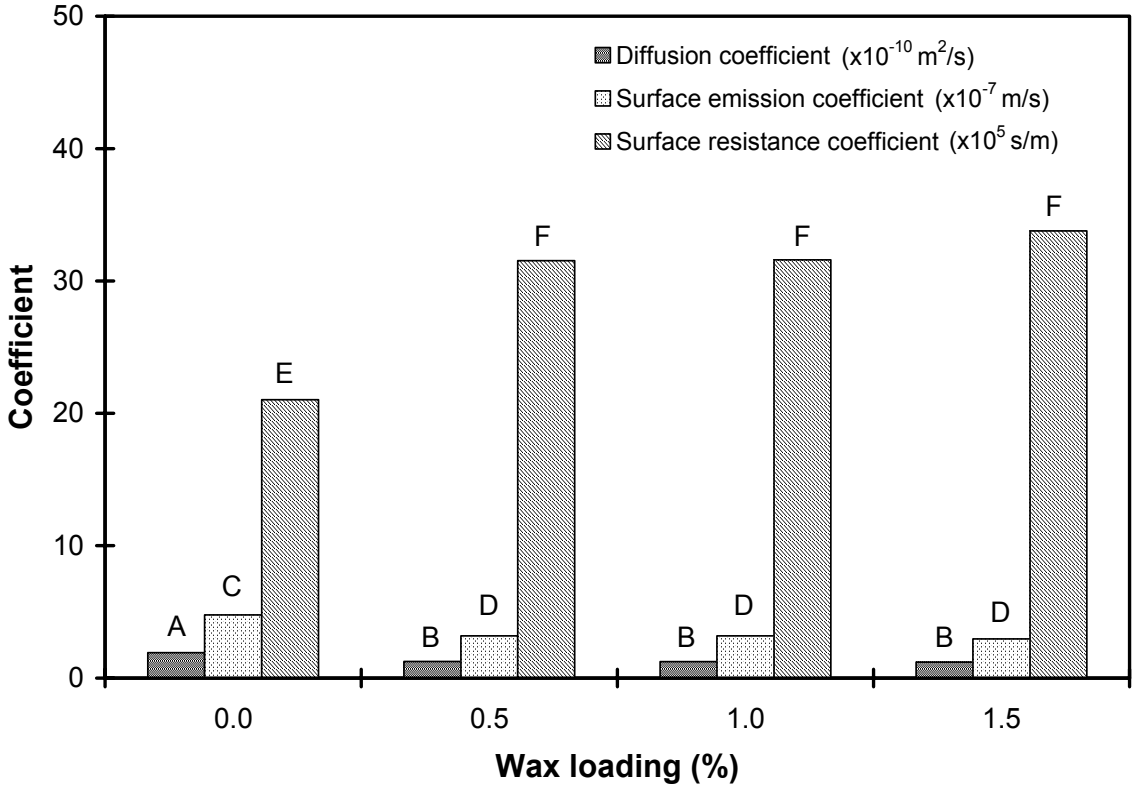


Figure 5-9. Diffusion coefficient, surface emission coefficient, and surface resistance coefficient of waxed strands with various wax loading (The same letters are not significantly different at α= 5%).

than for waxed strands. The diffusion coefficient is characterized as the internal moisture transfer rate in the strand, whereas the surface emission coefficient is characterized as the resistance when the water moves through the strand surface. The higher surface resistance in wax-free strands results in a slower sorption process. In most wood composites, resin application provides bonding of wood elements; while wax resists water absorption (Maloney 1993). From Zhang's study, strands loaded with lower resin and wax level exhibited a higher rate of water uptake during the early stage of sorption (Zhang et al. 2007). Results from this study supported the idea that higher resin and wax loading can resist water vapor sorption but it may have a small effect in relation to overall board sorpton. Wax loading has more influence on water vapor sorption rate and EMC than resin loading, although the wax penetration into wood was not investigated. Under hot-pressing, the influence of wax on water vapor properties in the short time period was more pronound than the influence of PF resin. This information provides a more clear view of wood behavior at early stage under hot-pressing.

5.4.3 Pressing parameters

Hot-pressing parameters that may affect sorption properties were investigated. Figures 5-10 and 5-11 show the sorption uptake behavior of resinated strands pressing with various compression rates and platen temperatures. The initial uptake rate is 7.50 x 10^{-6} (mg/mm^3)/s for 1.05 of compression rate and 7.00 x 10^{-6} (mg/mm^3)/s for 1.65 of compression rate (Table 5-6). An increase in compression rate resulted in a slight decrease in initial sorption rate. The water vapor sorption of compressed strands firstly involved chemi-sorption at surface. However, in liquid phase, the water penetration

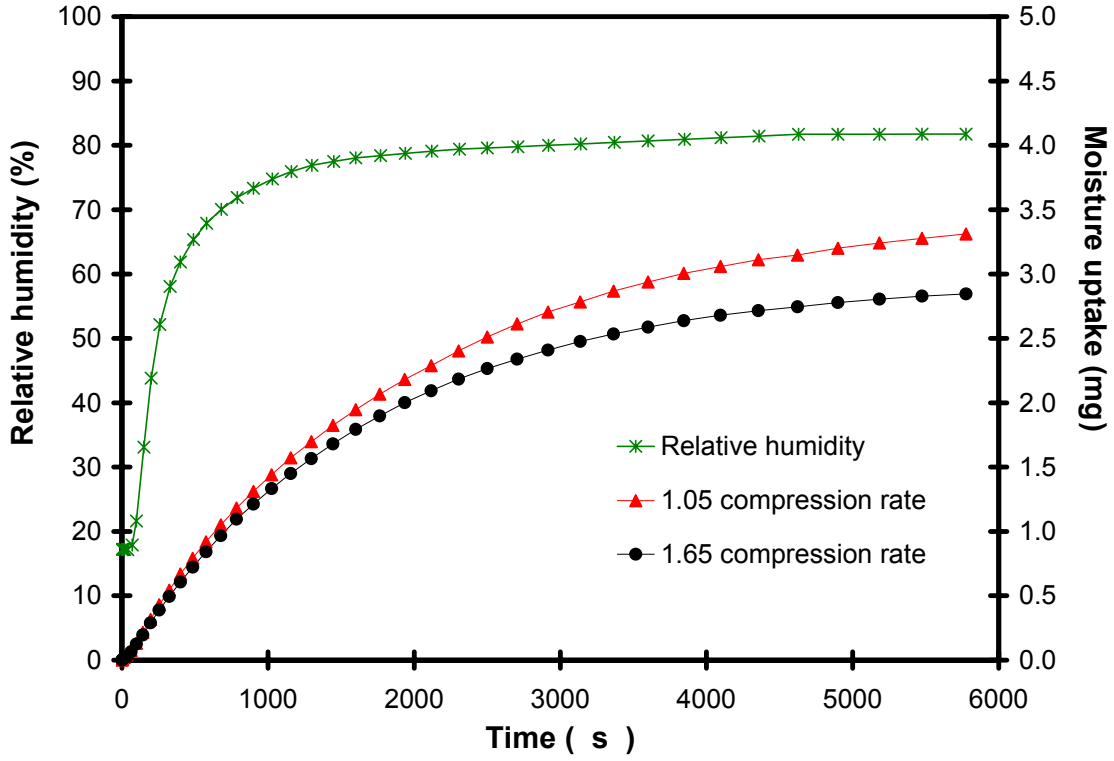


Figure 5-10. Water vapor uptake behavior of resinated strands pressing with different compression rates.

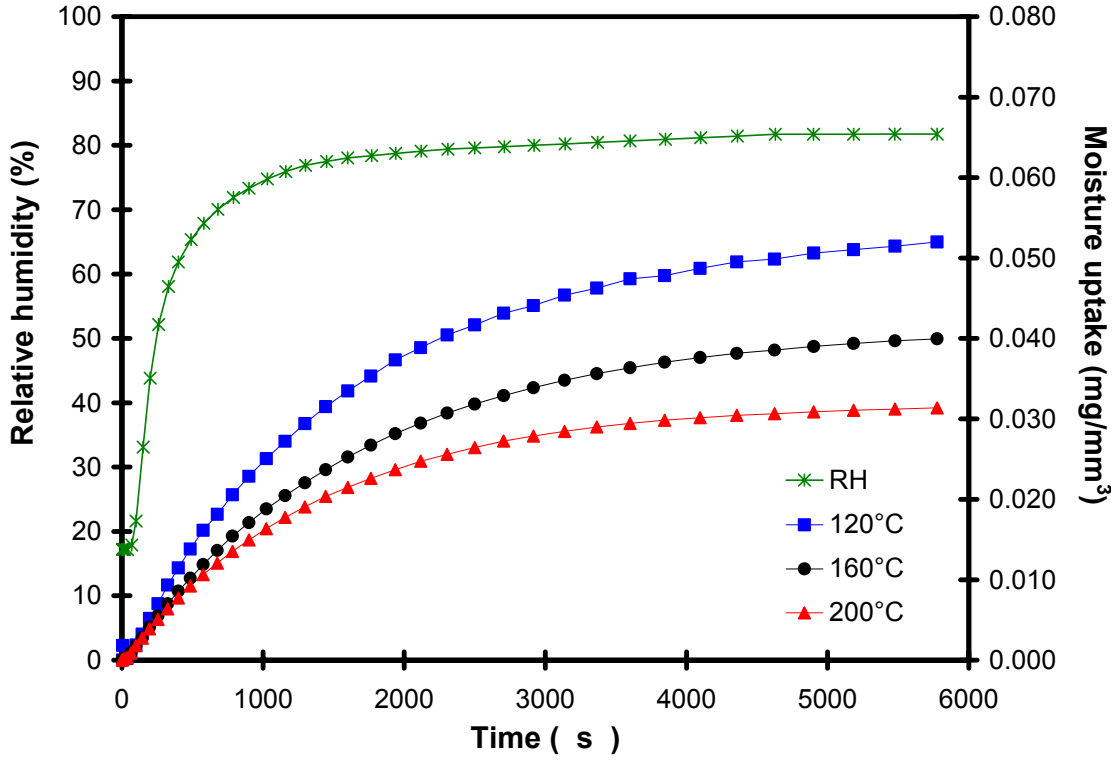


Figure 5-11. Water vapor uptake behavior of resinated strands pressing with different platen temperatures.

Table 5-6. Initial uptake rate and EMC of strands pressing with different platen temperatures and compression rates.

Parameter	**Initial uptake rate**	**EMC**
	x 10^{-6} (mg/mm^3)/s	**(%)**
Compression rate		
1.05	7.50 (0.71)	18.4 (1.24)
1.65	7.00 (1.41)	18.1 (0.67)
Platen temperature		
120 °C	8.50 (1.53)	18.5 (0.58)
160 °C	7.50 (0.71)	18.4 (1.24)
200 °C	6.00 (1.41)	16.9 (0.56)

Values given are means (STD)
There are no statistically different at $\alpha = 5\%$

behavior into the strands with higher density is difficult because of variation in void content (Zhang et al. 2007). In solid wood, pits openings contribute above 70% of the flow resistance to water vapor (Bolton and Petty 1978). The permeability decrease is due to increases in the thickness of bordered pit membranes (Bank and Levy 1980). The compression rate may have more affect on pore size than pit aspiration, which mainly occurs in the longitudinal direction of fibers. The pit thickness and cavity diameter may not significantly change under compression. The influence of pore size or voids on water vapor flow may overcome the influence of pit aspiration.

The moisture uptake rate was 8.50×10^{-6}, 7.50×10^{-6}, and 6.00×10^{-6} $(mg/mm^3)/s$ for 120, 160, and 200°C, respectively (Table 5-6). Results demonstrated platen temperature exhibited a strong influence on the moisture uptake rate of a resinated strand. An increase in platen temperature resulted in a decrease in moisture uptake rate. Resinated strands pressed at 120°C exhibited a moisture uptake 1.5 times higher than a resinated strands pressed at 200°C. This phenomenon was possibly due to the heat treatment leading to a decrease in hygrophilic properties. The *OH*-groups of wood strands may be replaced with *O*-acetyl groups during heat treatment (Hinterstoisser et al. 2003). The EMC of resinated strands pressed with different compression rates and platen temperatures is slightly different. Tabarsa and Chui (1997) reported that compression rate had a slight effect on EMC. A higher compression rate of composites boards leads to a slight decrease in EMC. Resinated strands pressed with 200°C of platen temperature exhibited 9% lower EMC than other pressing parameters.

Figures 5-12 and 5-13 show the moisture sorption of resinated strands pressed with different compression rates and platen temperatures. The initial sorption rate and

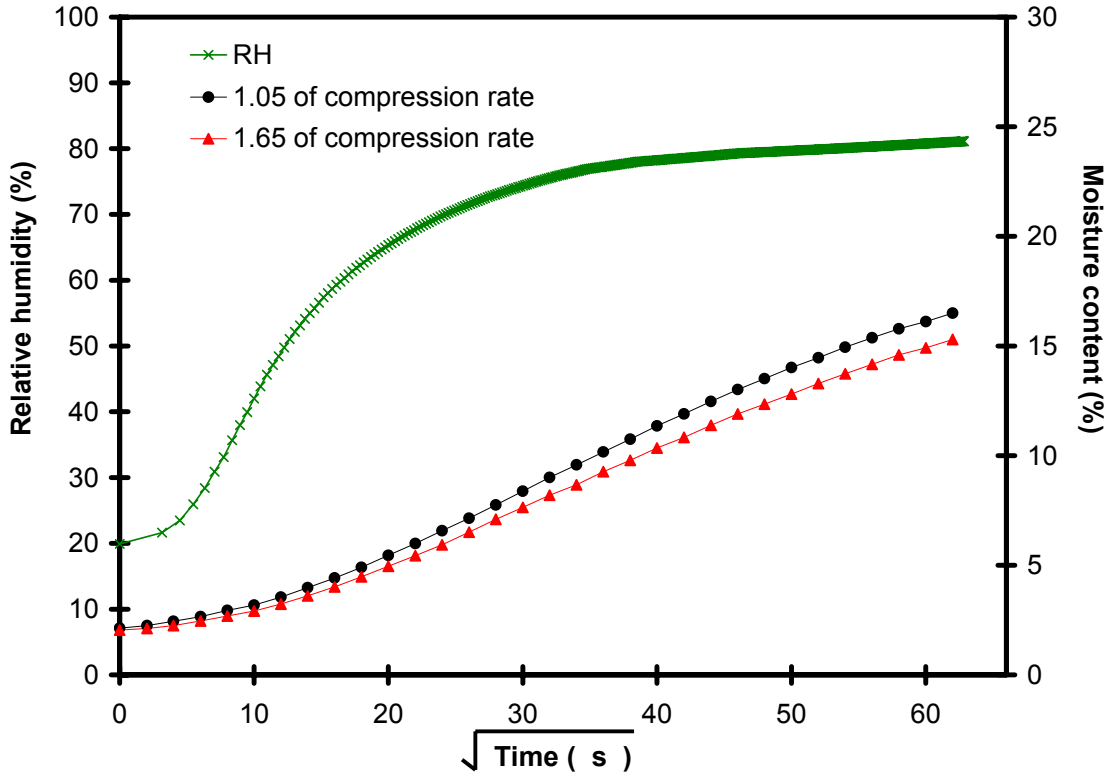


Figure 5-12. The moisture sorption of resinated strand pressed with different compression rates.

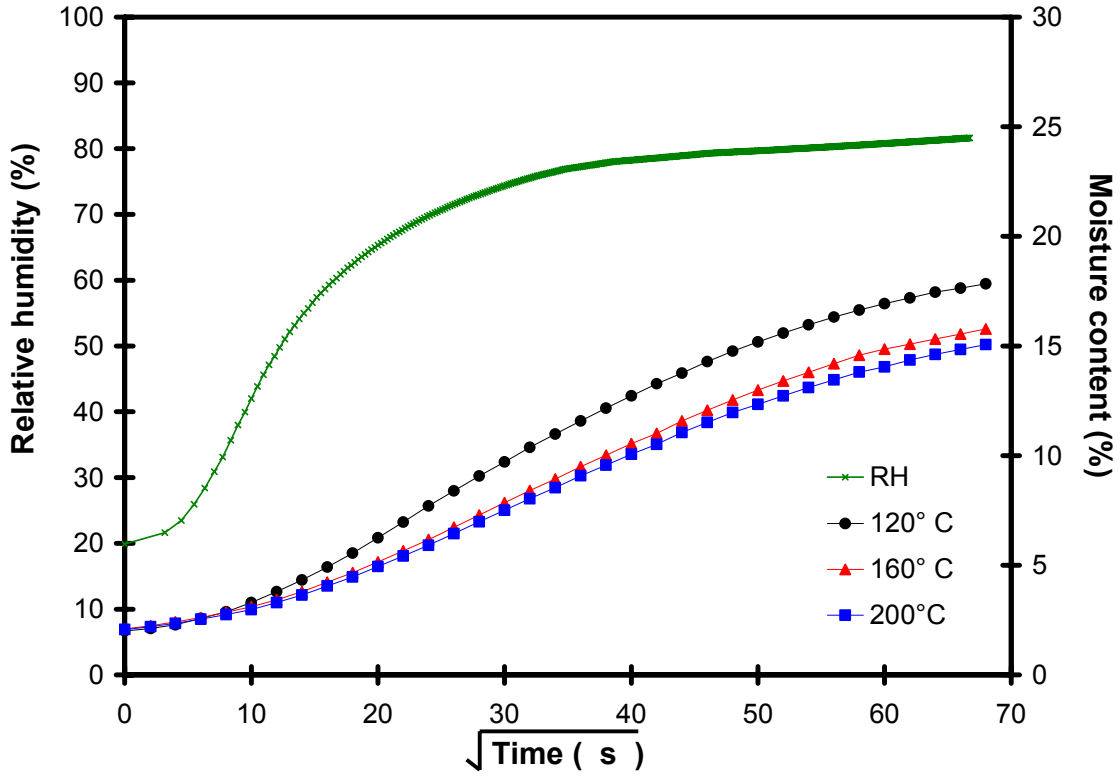


Figure 5-13. The moisture sorption of resinated strand pressed with different platen temperatures.

second slope of strands pressed with 1.05 compression rate was 0.0013 and 0.0015 %/√s, respectively. The initial sorption rate and second slope of strands pressed with 1.65 compression rate was 0.0012 and 0.0014 %/√s, respectively (Table 5-7 and Figure 5-14). The influence of strand density on liquid water penetration was reported by Zhang et al. (2007). The water penetration was low for high density strand. However, in my test, there were no differences in sorption rates between strands pressed with 1.05 and 1.65 of compression rate (p-value > 0.05). The initial sorption rate and second slope of strands pressed at 120°C platen temperature was 0.0017 and 0.0021 %/√s, respectively. It was approximately 1.5 times higher than for strands pressed at 200°C of platen temperature for both initial sorption rate and second slope. The platen temperature has more influence on sorption properties of resinated strands than compression rate. Since these effects were investigated one factor at a time, the interaction between platen temperature and compression rate was not investigated. The interaction of compression rate with platen temperature may supercede the effect of temperature or compression rate alone.

The diffusion coefficient, surface emission, and surface resistance of pressed strands are shown in Figure 5-15. The diffusion coefficient at 60% of total sorption was 3.377×10^{-10} m^2/s and 2.728×10^{-10} m^2/s for resinated strands pressed with 1.05 and 1.65 compression rate, respectively. The diffusion coefficient of resinated strands pressed with 1.05 and 1.65 of compression rate was slightly different (p-value = 0.0254). The surface resistance was 2.125×10^6 s/m and 2.530×10^6 s/m for 1.05 and 1.65 compression rates, respectively.

The diffusion coefficient at 60% of total sorption was 4.356×10^{-10} m^2/s, 3.777×10^{-10} m^2/s, and 3.166×10^{-10} m^2/s for resinated strands pressed with 120, 160, and 200°C

Table 5-7. Initial sorption rate ($K_{1)}$, second slope (K_2), diffusion coefficient (D), surface emission coefficient (σ), and surface resistance coefficient (S) of resinated strand pressed with different compression rates and temperature.

Pressing Parameter	**K_1 (%/√s) Mean (Std)**	**K_2 (%/√s) Mean (Std)**	**$D_{0.5}$ (10^{-10} m^2/s) Mean (Std)**	**$D_{0.6}$ (10^{-10} m^2/s) Mean (Std)**	**σ (10^{-7}m/s) Mean (Std)**	**S (10^6s/m) Mean (Std)**
Compression rate						
1.05	0.0013 (0.0003)	0.0015 (0.0002)	2.987 (0.164)^s	3.377 (0.284)^s	4.716 (0.266)^s	2.125 (0.124)^s
1.65	0.0012 (0.0002)	0.0014 (0.0003)	2.291 (0.112)	2.728 (0.154)	3.961 (0.219)	2.530 (0.144)
Platen temperature (°C)						
120	0.0017 (0.0002)	0.0021 (0.0003)	3.733 (0.221)^s	4.356 (0.304)^s	5.606 (0.205)^s	1.785 (0.064)^s
160	0.0013 (0.0003)	0.0015 (0.0002)	2.987 (0.164)	3.377 (0.284)	4.716 (0.266)	2.125 (0.124)
200	0.0012 (0.0003)	0.0014 (0.0003)	2.945 (0.110)	3.166 (0.177)	4.639 (0.087)	2.156 (0.040)

Values given are means (STD)

^{s} showed statistical difference at α = 5% (p-value = < 0.05)

Remark: $D_{0.5}$ = diffusion at 50% of total sorption, and $D_{0.6}$ = diffusion at 60% of total sorption

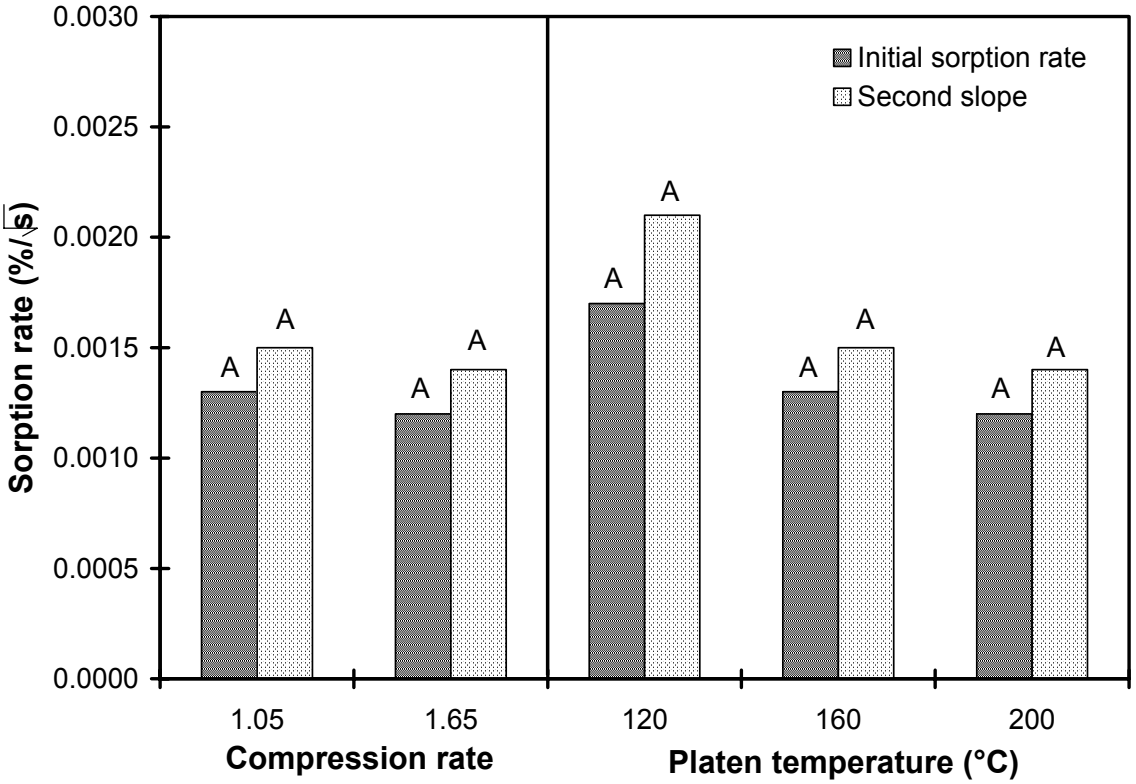


Figure 5-14. Initial sorption rate and second slope of pressed strands (The same letters are not significantly different at $\alpha = 5\%$).

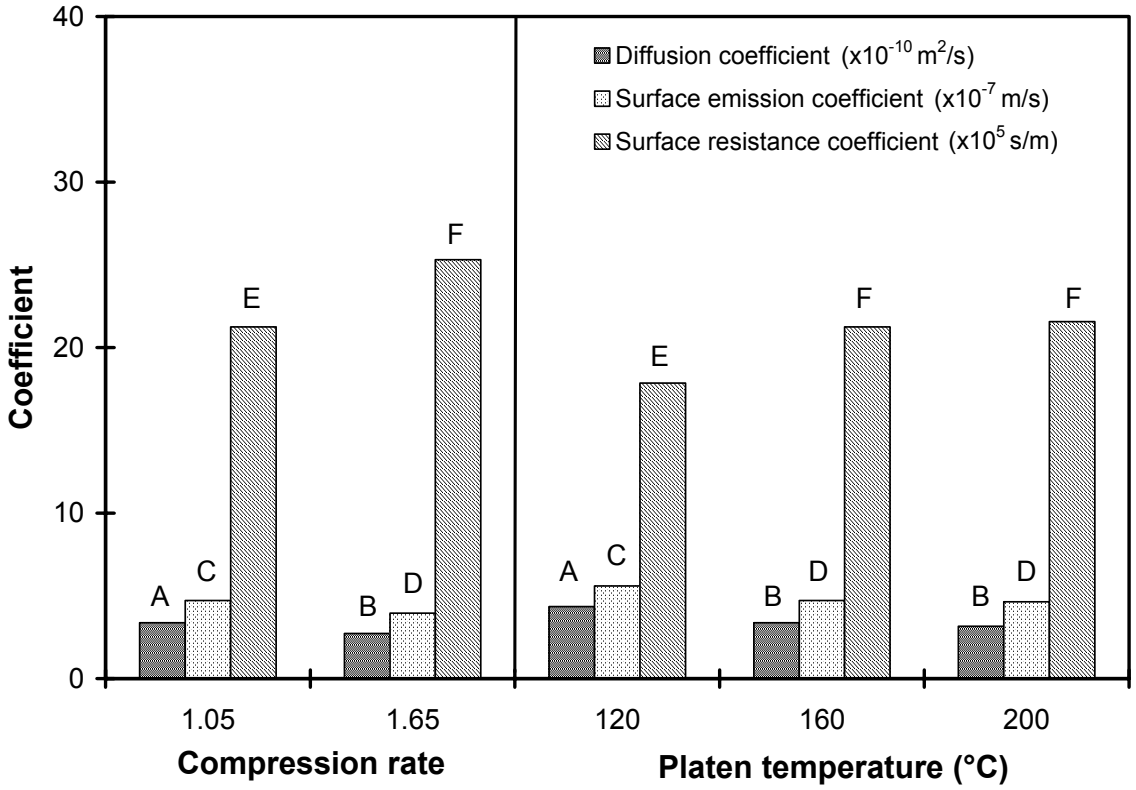


Figure 5-15. Diffusion coefficient, surface emission coefficient, and surface resistance coefficient of pressed strands (The same letters are not significantly different at $\alpha = 5\%$).

of platen temperature. The diffusion coefficient at 120°C was 1.4 times higher than that at 200°C. The surface resistance coefficient was 1.785 x 10^6 s/m, 2.125 x 10^6 s/m, and 2.156 x 10^6 s/m for 120, 160, and 200°C of platen temperature. At 200°C, the pressed strands exhibited resistance to water sorption. Assuming no interaction, these data support the idea that moisture can diffuse more at 1.05 compression rate with 200°C of platen temperature. These results suggest that platen temperature influences water vapor sorption rates and EMC more than compression rate. This may be because the compression rate involves only the sample thickness, whereas the platen temperature affects wood throughout the mat. Tabarsa and Chui (1997) found EMC decreased with platen temperature with a considerable reduction in EMC between 100°C and 150°C. They stated that the reduction in EMC was due to hemicellulose degradation, whereby the number of available hydrogen bond sites was decreased. However, the influence of the interaction between compression and temperature on EMC was not discussed. Under hot-pressing, the influence of platen temperature may dominate water vapor properties.

In composition boards, diffusion is controlled by board density, fiber orientation, and the degree of interfiber capillaries. The diffusion coefficient increases with decreasing board density because the water vapor in low-density board easily passes through the interfiber capillaries. Fiber orientation slightly influences diffusion in composition board. The factor controlling diffusion may be dependent on solid wood, i.e., lumens, cell walls, and pit opening, the degree of interfiber voids and capillaries. However, the permeability in composition boards was controlled by the extent of interparticle capillaries rather than anatomical features of the woods (Lehmann 1972).

5.5 Summary

This evaluation of water vapor sorption of resinated and waxed commercial strands provides fundamental knowledge to improve OSB manufacture and application. The water vapor sorption of loblolly pine strand changed with resin/wax loading levels, pressing temperatures, and compression rates. Higher resin/wax loading reduced water vapor sorption over short time periods. Wax loading had more influence on water vapor sorption than resin loading. Higher platen temperatures and higher compression rates caused reduced water vapor sorption. Platen temperatures had more influence on water vapor sorption than compression rate. The processing factors dominating water vapor sorption over short time periods were wax loading and platen temperature. In summary, platen temperature, wax loading, compression rate, and resin loading were influential, in decreasing order, on sorption behaviour.

6. CONCLUSIONS AND RECOMMENDATIONS

6.1 Conclusions

This dissertation is a study of the influence of selected wood characteristics and composites production parameters on the sorption behavior of wood materials. This work was divided into three experiments.

The results of the first experiment provide a better understanding of the sorption behavior of different wood structures, which could be useful in protecting wood against wood deterioration and fungal attack. Under relative humidity (RH) changes from 11% to 89%, earlywood had higher sorption rates and diffusion coefficients than latewood, whereas outer tree rings had higher sorption rates and diffusion coefficients than inner tree rings of loblolly pine (*Pinus taeda*).

The results of the second experiment provide an understanding of the sorption behavior of fiber refined under varying refiner steam pressure. Refiner pressure has a dramatic effect on sorption behavior and surface properties of refined fiber. Extensive damage appeared in fibers refined at high steam pressures. Under RH changes from 11% to 89%, a higher rate of sorption was found in juvenile fibers refined under low steam

pressures. Higher water activity and lower cystallinity was found at low steam pressure refined fibers as well.

The last experiment evaluated water vapor sorption of processing parameters in order to provide fundamental knowledge to improve OSB manufacture and application. Higher resin and wax loading levels resulted in reduced water vapor sorption in early sorption periods. Higher press platen temperatures and compression rates also decreased the sorption properties of resinated loblolly pine strands. Wax loading had more influence on sorption properties than resin loading. Press platen temperatures had more influence on sorption behavior than compression rate.

6.2 Recommendations for future work

The experimental work involving exposing wood to humidity changes was tedious and time-consuming. Reaching the equilibrated point for each specimen took a very long time, although it was relatively fast to use small specimens. The sorption isotherm should be conducted carefully. Due to the small scale of the measurements, the variability among wood samples is high, and it is important to control the homogeneity of every replication.

Under hot-pressing, it is not only moisture vapor affecting sorption behavior of the mat, but also the steam that was generated during pressing. Temperature has an influence on the pressed strand, in particular steam-treatment and heat-treatment effects. To fulfill this understanding, future works investigate the thermal moisture diffusion coefficient and the effect of steam on pressed wood under hot-pressing conditions.

Further understanding of moisture sorption in wood due to a thermal gradients also should be investigated.

Sorption behavior at the microscale involves inherent characteristics and surface properties of wood. Ultra-structural change and/or nano-scale changes may influence and/or contribute to sorption behavior. The *in-situ* sorption behavior of wood under hot-pressing environments should be investigated.

6.3 List of publications

This doctorial dissertation is based on the following papers and abstracts:

I. **Neimsuwan, T.**, S. Wang, A.M. Taylor, and T.G. Rials.
"Statics and kinetics of water vapor sorption of small loblolly pine samples"
Wood Science and Technology (in print).

II. **Neimsuwan, T**., S. Wang, and X.P. Ye.
"Effects of refining stream pressure on the water vapor sorption of loblolly pine fibers"
Submitted to Holzforschung.

III. Wang, S. and **T. Neimsuwan**. 2006. The relationship of surface characteristics and water uptake of wood and composition. Abstract IN: Biographies and Abstracts. Forest Products Society 60th International Convention, Newport Beach, California, June 25-28. pp. 21.

IV. **Neimsuwan, T.** and S. Wang. 2006. Prediction of furnish and OSB properties by NIR spectroscopy. Abstract IN: Biographies and Abstracts. Forest Products

Society 60th International Convention, Newport Beach, California, June 25-28. pp. 48.

V. **Neimsuwan, T.** and S. Wang. 2007. Effect of resin and wax on sorption behavior of wood strands. Abstract IN: Biographies and Abstracts. Forest Products Society 61st International Convention, Knoxville, Tennessee, June 10-13. pp. 14.

VI. **Neimsuwan, T.** and S. Wang. 2007. Sorption behavior by refining fiber of varying pressure. Abstract IN: Biographies and Abstracts. Forest Products Society 61st International Convention, Knoxville, Tennessee, June 10-13. pp. 30.

REFERENCES

Chapter 2

Adler, E. 1977. Lignin chemistry-past, present and future. Wood Sci.Tehcnol. 11:169-218.

Avramidis, S. and J.F. Siau. 1987. An investigation of the external and internal resistance to moisture diffusion in wood. Wood Sci. Technol. 21:249-256.

Banks, W.B. and J.F. Levy. 1980. The effect of cell wall swelling on the permeability of Grand Fir wood. Wood Sci. Technol. 14:49-62.

Bergstrom, M. and A. Blom. 2006a. Differences in properties between Norway spruce (*Picea abies*) heartwood and sapwood. Part 1. Accelerated durability testing. Wood Protection. Omni Royal Orleans Hotel, New Orleans, Louisiana, USA, March 21-23, 2006. pp. 339-345.

Bergstrom, M. and A. Blom. 2006b. Differences in properties between Norway spruce (*Picea abies*) heartwood and sapwood. Part 2. Vapor and liquid permeability. Wood Protection. Omni Royal Orleans Hotel, New Orleans, Louisiana, USA, March 21-23, 2006. pp. 347-352.

Bertaud, F. and B. Holmblom. 2004. Chemical composition of earlywood and latewood in Norway spruce heartwood, sapwood and transition zone wood. Wood Sci. Technol. 38:245-256.

Berthold, J., J. Desbrieres, M. Rinaudo, and L. Salmen. 1994. Types of adsorbed water in relation to the ionic groups and their counter-ions for some cellulose derivatives. Polymer 35(26):5729-5736.

Bessadok, A., S. Marais, F. Gouanva, L. Colasse, I. Zommerlin, S. Roudesli, and M. Metayer. 2007. Effect of chemical treatments of Alfa (*Stipa tenacissima*) fibres on water-sorption properties. Composite Sci. Tech. 67: 685-697.

Bodig, J. and B.A. Jayne. 1982. Mechanics of wood and wood composites. Van Nostrand Reinhold Company, New York, USA. 710 pp.

Brunauer, S., P.H. Emmett, and E. Teller. 1938. Adsorption of gases in multimolecular layers. J. Am. Chem. Soc. 60:309-319.

Cao, J. and D.P. Kamdem. 2004. Moisture adsorption thermodynamics of wood from fractal-geometry approach. Holzforschung 58:274-279.

Chin, J.W., T. Nguyen, and K. Aouadi. 1999. Sorption and diffusion of water, salt water, and concrete pore solution in composite matrices. J. Appl. Polymer Sci. 71:483-492.

Choong, E.T. and C. Skaar. 1969. Separating internal and external resistance to moisture removal in wood drying. Wood Sci. 1:200-202.

Choong, E.T. and C. Skarr. 1975. Diffusivity and surface emissivity in wood drying. Wood Fiber. 4:80-86.

Christensen, G.N. and K.E. Kelsey. 1958. The sorption of water vapour by the constituents of wood: Determination of sorption isotherms. Austr. J. Appl. Sci. 9:265-282.

Dent, R.W. 1977. A multilayer theory for gas sorption. I. Sorption of a single gas. Text. Res. J. 47:145-152.

Droin, A., J.L. Taverdet, and J.M. Vergnaud. 1988. Modelling the absorption and desorption of moisture by wood in an atmosphere of constant and programmed relative humidity. Wood Sci. Technol. 22:299-310.

Ebeling, K.A. 1980. Critical review of current theories for the refining of chemical pulps. *In*: Int'l Symp. on Fund. Concepts of Refining., Appleton, Wisconsin, USA, September 16-18, 1980. pp. 1.

Ekman, R. 1979. Analysis of the nonvolatile extractives in Norway spruce sapwood and heartwood. Acta Acad. Abo., Ser. B. 39:4.

Fardim, P. and N. Duran. 2003. Modification of fibre surfaces during pulping and refining as analysed by SEM, XPS and ToF-SIMS. Colloids Surf. 223(1-3):263-276.

Fengel, D. and G. Wegener. 1984. Wood: Chemistry, ultrastructure, reactions. Walter de Gruyter, Berlin, New York. 613 pp.

Follrich, J., U. Muller, and W. Gindl. 2006. Effects of thermal modification on the adhesion between spruce wood (*Picea abies* Karst.) and a thermoplastic polymer. Holz Roh-Werkst. 64:373-376.

Furuno, T., Y. Imamura, and H. Kajita. 2004. The modification of wood by treatment with low molecular weight phenol-formaldehyde resin: a properties enhancement

with neutralized phenolic-resin and resin penetration into wood cell walls. Wood Sci. Technol. 37: 349-361.

Hailwood, A.J. and S. Horrobin. 1946. Absorption of water by polymer: Analysis in terms of a simple model. Trans. Faraday Soc. 42B:84-92. (General Discussions 42B:93-102).

Hakkou, M., M. Petrissans, P. Gerardin, and A. Zoulalian. 2006. Investigations of the reasons for fungal durability of heat-treated beech wood. Polym. Degrad. Stabil. 91:393-397.

Hakkou, M., M. Petrissans, A. Zoulalian, and P. Gerardin. 2005. Investigation of wood wettability changes during heat treatment on the basis of chemical analysis. Polym. Degrad. Stabil. 89:1-5.

Hartley, I.D. and S. Avramidis. 1993. Analysis of the wood sorption isotherm using clustering theory. Holzforchung 47(2):93-102.

Hartley, I.D. and S. Avramidis. 1994. Water clustering phenomenon in two softwoods during adsorption and desorption processes. J. Inst. Wood Sci. 13(4): 467-474.

Hartley, I.D., F.A. Kamke, and H. Peemoeller. 1992. Cluster theory for water sorption in wood. Wood Sci. Technol. 26(2):83-99.

Hatakeyama, T., K. Nakamura, and H. Hatakeyama. 2000. Vaporization of bound water associated with cellulose fibres. Thermochimica Acta 352-353:233-239.

Haygreen, J.G. and J.L. Bowyer. 1996. Forest products and wood science: An introduction. Iowa State University Press, Ames, Iowa, USA. 484 pp.

Hinterstoisser, B., M. Schwanninger, B. Stefke, R. Stingl, and M. Patzelt. 2003. Surface analyses of chemically and thermally modified wood by FT-NIR. *In*: van Acker J., C. Hill (eds). Proc. of the 1st European Conference on Wood Modification, The First International Conference of the European Society for Wood Mechanics, Ghent, Belgium. April 2-4, 2003. pp. 65-70.

Hse, C.Y. 1972. Wettability of southern pine veneer by phenol-formaldehyde wood adhesives. Forest Prod. J. 22(1):51-56.

Inoue, M. and M. Norimoto. 1991. Heat treatment and steam treatment of wood. Wood industry 49: 588-592.

Kamke, F.A. and T.R. Miller. 2006. Enhancing composites durability: Using resins and waxes. Wood Protection. Omni Royal Orleans Hotel, New Orleans, Louisiana, USA, March 21-23, 2006. pp. 187-194.

Kollmann, F.F.P. and W.A. Côte. 1968. Principles of wood science and technology. I. Solid wood. Springer-Verlag, New York, USA. 591 pp.

Kortelainen, S.M., T. Antikainen, and P. Viitaniemi. 2006. The water absorption of sapwood and heartwood of Scots pine and Norway spruce heat-treated at 170°C, 190°C, 210°C and 230°C. Holz Roh-Werkst. 64:192-197.

Kortelainen, S.M. and P. Viitaniemi. 2006. Thermally modified timber as durable wood for exterior applications: background and properties. Wood Protection. Omni Royal Orleans Hotel, New Orleans, Louisiana, USA, March 21-23, 2006. pp. 131-135.

Kumar, M.N.S. and Siddaramaiah. 2007. Sorption and diffusion of water into melamine formaldehyde-incorporated poly(vinyl acetate)-polyester nonwoven fabric composites. Polymer Int. 56:409-414.

Labuza, T.P. 1984. Moisture sorption: Practical aspects of isotherm measurements and use. American Association of Cereal Chemists, St. Paul, Minnesota, USA pp. 2-8.

Leask, R.A. and M.J. Kocurek. 1987. Pulp and paper manufacturing. Mechanical Pulping. Edit. Tappi Textbook Committee. 2:1-187.

Lehmann, W.F. 1972. Moisture-stability relationships in wood-base composition boards. Forest Prod. J. 22(7):53-59.

Lenth, C.A. and A.N. Haslett. 2003. Moisture uptake patterns in pressure steaming of Radiata Pine. Holz Roh-Werkst. 61: 444-448.

Levi, M.P. 1973. Control methods. *In:* Nicholas, D.D. (editor). Wood deterioration and its prevention by preservation treatment. Vol. I. Degradation and protection of wood. Syracuse University Press, Syracuse, New York, USA. 380 pp.

Li, W., L. Yan, and J. Yang. 2006. AFM study of crystalline cellulose in the cell walls of straw. Polymer Int. 55(1):87-92.

Ma, Q. and V. Rudolph. 2006. Prediction of vapor-moisture equilibrium for a wood moisture system using a modified UNIQUAC model. Chem. Eng. Sci. 61:6077-6084.

Maloney, T.C. and H. Poulapuro. 1999. The formation of pores in the cell wall. J. Pulp Paper Sci. 25:430-436.

Maloney, T.C., H. Poulapuro, and P. Stenius. 1998. Hydration and swelling of pulp fibers measured with differential scanning calorimetry. Nordic Pulp and Paper Res. J. 13(1):31-36.

Meijer, M., S. Haemers, W. Cobben, and H. Militz. 2000. Surface energy determinations of wood: Comparison of methods and wood species. Langmuir 16:9352-9359.

Mihranyan, A., A.P. Llagostera, R. Karmhag, M. Stromme, and R. Ek. 2004. Moisture sorption by cellulose powders of varying crystallinity. Int. J. Pharm. 269:433-442.

Muhtaseb, A.H., W.A.M. McMinn, and T.R.A. Magee. 2004. Water sorption isotherms of starch powders. Part 2. Thermodynamic characteristics. J. Food Eng. 62:135-142.

Olek, W., P. Perre, and J. Weres. 2005. Inverse analysis of the transient bound water diffusion in wood. Holzforschung 59:38-45.

Page, D.H. 1989. The beating of chemical pulps-the action and the effects. *In*: Transactions of Ninth Fundamental Research Symposium, Fundamentals of papermaking, MEP, London, UK. pp. 1.

Panshin AJ, and C. deZeeuw. 1980. Textbook of wood technology, structure, identification, properties, and uses of the commercial woods of the United States and Canada, 4th edn. McGraw-Hill, New York, USA. 736 pp.

Papadopoulos, A.N. and C.A.S. Hill. 2003. The sorption of water vapour by anhydride modified softwood. Wood Sci. Technol. 37:221-231.

Pham, X, E. Vittadini, R.E. Levin, and P. Chinachoni. 1999. Role of water mobility on mold spore germination. J Agric. Food Chem. 47:4976-4983.

Rousset, P., P. Perre, and P. Girard. 2004. Modification of mass transfer properties in poplar wood (*P.robusta*) by a thermal treatment at high temperature. Holz Roh-Werkst. 62:113-119.

Rowell, R.M. 1983. Chemical modification of wood. For. Prod. Abstr. 6:363-382.

Rowell, R., S. Lange, J McSweeny, and M. Davis. 2002. Modification of wood fiber using steam. Proc. 6th Pacific Rim Bio-Based Composites Symp.. Portland, Oregon, USA. November 10-13, 2002. pp. 606-615.

Scott, W.J. 1953. Water relations of *Staphylococcus aureus* at 30°C. Aust. J. Bacteriol. Sci. 6:549-564.

Sheppard, S.E. and P.T. Newsome. 1934. The sorption of water by cellulose. Indust. Eng. Chem. 26(3):285-290.

Siau, J.F. 1971. Flow in wood. Syracuse University Press, New York, USA. 131 pp.

Siau, J.F. 1984. Transport processes in wood. Springer-Verlag, Berlin, Heidelberg, New York, Tokyo. 245 pp.

Siau, J.F. 1995. Wood: Influence of moisture on physical properties. Department of Wood Science and Forest Products, Virginia Tech., Virginia, USA. 227 pp.

Skarr, C. 1984. Wood-water relations. *In*: Rowell, R.M. (Ed.): The chemistry of solid wood. Am. Chem. Soc., Washington, DC, USA. pp. 127-172.

Skarr, C. 1988. Wood-water relations. Springer, Berlin, Heidelberg, New York. 283 pp.

Sreekala, M.S. and S. Thomas. 2003. Effect of fibre surface modification on water-sorption characteristics of oil palm fibres. Composites Sci. and Technol. 63: 861-869.

Stamm, A.J. 1964. Wood and cellulose science. The Ronald Press Co. New York, USA. 549 pp.

Stamm, A.J. and W.E. Smith. 1969. Laminar sorption and swelling theory for wood and cellulose. Wood Sci. Technol. 3:301-323.

Time, B. 1998. Hygroscopic moisture transport in wood. Ph.D. Dissertation. Dep. Building and Construction Engineering, Norwegian Univ. Sci. Tech, Tribdgeun, Norway. 217 pp.

Wahl, P., S.P. Simonaho, T. Pakarinen, and R. Silvennoinen. 2004. Effect of heat-treatment on scattering of laser light from wood grains. Holz Roh-Workst. 62:343-345.

Walsh, F.L. and S. Banerjee. 2007. Characterization of thin water layers in pulp by tritium exchange. Part 2. Effect of refining on water absorption. Holzforschung 61:120-123.

Wang, S. 2006. Enhancing composite durability via pressing technology. Wood Protection. Omni Royal Orleans Hotel, New Orleans, Louisiana, USA, March 21-23, 2006. pp. 181-185.

Wangaard, F.F. and L.A. Granados. 1967. The effect of extractives on water-vapor sorption by wood. Wood Sci. Technol.1:253-277.

Xing, C, B. Riedl, A. Cloutier, J. Deng, and S.Y. Zhang. 2006. UF resin efficiency of MDF as affected by resin content loss, coverage level and pre-cure. Holz Roh-Workst. 64:221-226.

Yasuda, R., K. Minato, and M. Norimoto. 1995. Moisture adsorption thermodynamics of chemically modified wood. Holzforschung 49:548-554.

Ye, X., S. Wang, R. Ruan, J. Qi, A.R. Womac, and C.J. Doona. 2006. Water mobility and mold susceptibility of engineered wood products. Transactions of the ASABE. 49(4):1159-1165.

Yildiz, S. and E. Gumuskaya. 2007. The effects of thermal modification on crystalline structure of cellulose in soft and hardwood. Build. Environ. 42:62-67.

Ziegler, I.M., Z. Horvolgyi, A. Toth, W. Forsling, and A. Holmgren. 2006. Wettability and spectroscopic characterization of silylated wood samples. J. Polymers for Advanced Technol. 17:932-939.

Zografi, G. 1988. States of water associated with solids. Drug Dev. Ind. Pharm. 14:1905-1919.

Chapter 3

American Society for Testing Materials (ASTM). 1999. Standard test methods for evaluating properties of wood-base fiber and particle panel materials. ASTM D 1037-99. ASTM, Philadelphia, USA.

Bodig, J. and A.J. Jayne. 1993. Mechanics of wood and wood composites. Van Nostrand Reinhold, New York, USA. 736 pp.

Choong, E.T. 1963. Movement of moisture through a softwood in the hygroscopic range. Forest Prod. J. 13(11):489-498.

Christensen, G.N. and K.E. Kelsey. 1958. The sorption of water vapour by the constituents of wood: determination of sorption isotherms. Austr. J. Appl. Sci. 9: 265-282.

Comstock, L.G. 1963. Moisture diffusion coefficients in wood as calculated from adsorption, desorption, and steady state data. Forest Prod. J. 13(3):97-103.

Downes, J.G. and B.H. Mackay. 1958. Sorption kinetics of water vapor in wool fibers. J. Polymer Sci. 28:45-67.

Efremov, G.I. 2002. Drying kinetics derived from diffusion equation with flux-type boundary condition. Drying Technol. 20(1):55-66.

Erickson, H.D. and T. Arima. 1974. Douglas-fir wood quality studies. Part II. Effects of age and stimulated growth on fibril angle and chemical constituents. Wood Sci. Technol. 8:255-265.

Fakhouri, B., M. Mounji, and J.M. Vergnaud. 1993. Comparison of the adsorption and desorption of water between Scots pine and spruce after submersion in water. Holzforschung 47:271-277.

Greethamma, V.G. and S. Thomas. 2005. Diffusion of water and artificial seawater through coir fiber reinforced natural rubber composites. Polym. Comp. 26:136-143.

Hailwood, A.J. and S. Horrobin. 1946. Absorption of water by polymers: analysis in terms of simple model. Trans. Faraday Soc. 42B:84-102.

Hartley, I.D., F.A. Kamke, and H. Peemoeller. 1992. Cluster theory for water sorption in wood. Wood Sci. Technol. 26:83-99.

Hse, C.Y. 1972. Wettability of southern pine veneer by phenol formaldehyde wood adhesives. Forest Prod. J. 22(1):51-56.

Kim, J.W., K. Carlborn, L.M. Matuana, and P.A. Heiden. 2006. Thermoplastic modification of urea-formaldehyde wood adhesives to improve moisture resistance. J. Appl. Polym. Sci. 101:4222-4229.

Lide, D.R. 1994. CRC handbook of chemistry and physics, 75th edn. CRC Press, Boca Raton, Florida, USA. 2608 pp.

Liu, J.Y. 1989. A new method for separating diffusion coefficient and surface emission coefficient. Wood Fiber Sci. 21:133-141.

Maldas, D.C. and D.P. Kamdem. 1999. Wettability of extracted southern pine. Forest Prod. J. 49(11/12):91-93.

National Institute of Standards and Technology (NIST). 1993. Pine standard reference material-8493. NIST, Gaithersburg, Maryland, USA.

Panshin A.J. and C. deZeeuw. 1980. Textbook of wood technology. 4th Ed. McGraw-Hill, New York, USA. 722 pp.

Pham, X., E. Vittadini, R.E. Levin, and P. Chinachoni. 1999. Role of water mobility on mold spore germination. J. Agric. Food Chem. 47:4976-4983.

Shupe, T.F., C.Y. Hse, E.T. Choong, and L.H. Groom. 1997. Differences in some chemical properties of innerwood and outerwood from five silviculturally different loblolly pine strands. Wood Fiber Sci. 29(1):91-97.

Shupe, T.E., C.Y. Hse, E.T. Choong, and L.H. Groom. 1998. Effect of wood grain and veneer side of loblolly pine veneer wettability. Forest Prod. J. 46(6):95-97.

Siau, J.F. 1995. Wood: Influence of moisture on physical properties. Dept. of Wood Sci. and For. Prod., Virginia Tech.,Virginia, USA. 227 pp.

Time, B. 1998. Hygroscopic moisture transport in wood. Ph.D disseration. Department of Building and Construction Engineering. Norwegian Univ. Sci. Tech. Norway. 216 pp.

U.S. Department of Agriculture, Forest Service (USDA Forest Service). 1974. Wood handbook: Wood as an engineering material. Forest Products Laboratory, Washington, DC, USA. 433 pp.

Uysal, B. 2006. Effects of the steam test on bonding strength of laminated veneer lumbers manufactured by using different adhesives. J. Appl. Polym. Sci. 99:2973-2977.

Via, B.K., T.F. Shupe, L.H. Groom, M. Stine, and C.L. So. 2003. Multivariate modeling of density, strength and stiffness from near infrared spectra for mature, juvenile

and pith wood of longleaf pine (*Pinus palustris*). J. Near Infrared Spectrosc. 11:365-378.

Via, B.K., C.L. So, L.H. Groom, T.F. Shupe, M. Stine, and J. Wikaira. 2007. Within tree variation of lignin, extractives, and microfibril angle coupled with the theoretical and near infrared modeling of microfibril angle. IAWA Journal. 28(2):189-209.

Wadso, L. 1993. Measurements of water vapour sorption in wood. Part 2. Results. Wood Sci. Technol. 28:59-65.

Wadso, L. 1994. A test of different methods to evaluate the diffusivity from unsteady-state sorption measurement. Drying Technol. 12(8):1863-1876.

Wang, S.Y. and C.F. Liau. 1998. Assessment of hygroscopic conditioning performance of interior decorative materials. IV. Sorption characteristics of wood under high relative humidity condition. J. Wood Sci. 44:260-266.

Wangaard, F.F. and L.A. Granados. 1967. The effect of extractives on water-vapor sorption by wood. Wood Sci. Technol.1:253-277.

Chapter 4

Bhuiyan, M.T.R. and N. Hirai. 2005. Study of crystalline behavior of heat-treated wood cellulose during treatments in water. J. Wood Sci. 51:42-47.

Clemons, C. 2002. Wood-plastics composites in the United States. Forest Prod. J. 52(6):10-18.

Deng, Y. and M. Abazeri. 1998. Contact angle measurement of wood fibers in surfactant and polymer solutions. Wood Fiber Sci. 30(2):155-164.

Espert, A., F. Vilaplana, and S. Karlsson. 2004. Comparison of water absorption in natural cellulosic fibres from wood and one-year crops in polypropylene composites and its influence on their mechanical properties. Composites A 35:1267-1276.

Garcia, R.A., A. Cloutier, and B. Riedl. 2006. Dimensional stability of MDF panels produced from heat-treated fibers. Holzforschung 60:278-284.

Groom, L., T. Rials, and R. Snell. 2000. Effect of refiner pressure on the mechanical properties of loblolly pine fibres. *In*: Proc. 4th European Panel Products Symp. Llandudno, Wales, UK. October 11-13, 2000. pp. 81-94.

Groom, L., C.L. So, T. Elder, T. Pesacreta, and T. Rials. 2004. Effect of refining pressure and resin viscosity on resin flow, distribution, and penetration of MDF fibers. The 7th Pacific Rim Bio-Based Composites Symp., Nanjing, China. October 31-November 2, 2004. pp. 227-239.

Groom, L., C.L. So, T. Elder, T. Pesacreta, and T. Rials. 2006. Effect of refiner pressure on the properties of individual wood fiber. *In*: Characterization of the cellulosic cell wall. Iowa State University Press, Iowa, USA. pp. 227-240.

Guzey, D., M. Ozdemir, F.G. Seyhan, H. Dogan, and Y.O. Devres. 2001. Adsorption isotherms of raw and roasted hazelnuts. Drying technol. 19(3&4): 691-699.

Hailwood, A.J. and S. Horrobin. 1946. Absorption of water by polymers: Analysis in terms of simple model. Trans. Faraday Soc. 42B:84-102.

Hakkou, M., M. Petrissans, P. Gerardin, and A. Zoulalian. 2006. Investigations of the reasons for fungal durability of heat-treated beech wood. Polym. Degrad. Stabil. 91:393-397.

Hakkou, M., M. Petrissans, A. Zoulalian, and P. Gerardin. 2005. Investigation of wood wettability changes during heat treatment on the basis of chemical analysis. Polym. Degrad. Stabil. 89:1-5.

Kamdem, D.P., A. Pizzi, and A. Jermannaud. 2002. Durability of heat-treated wood. Holz Roh-Workst. 60:1-6.

Kortelainen, S.M. and P. Viitaniemi. 2006. Thermally modified timber as durable wood for exterior applications: background and properties. Wood Protection. Omni Royal Orleans Hotel, New Orleans, Louisiana, USA, March 21-23, 2006. pp. 131-135.

Mihranyan, A., A.P. Llagostera, R. Karmhag, M. Stromme, and R. Ek. 2004. Moisture sorption by cellulose powders of varying crystallinity. Int. J. Pharm. 269:433-442.

Neimsuwan, T., S. Wang, A.M. Taylor, and T.G. Rials. 2007. Statics and kinetics of water vapor sorption of small loblolly pine samples. Wood Sci. Technol. (in press)

Paul, W., M. Ohlmeyer, and H. Leithoff. 2007. Thermal modification of OSB-strands by a one-step heat pre-treatment: Influcence of temperature on weight loss, hygroscopicity and improved fungal resistance. Holz Roh-Workst. 65:57-63.

Pham, X., E. Vittadini, R.E. Levin, and P. Chinachoti. 1999. Role of water mobility on mold spore germination. J. Agric. Food Chem. 47:4976-4983.

Poncsak, S., D. Kocaefe, M. Bouazara, and A. Pichette. 2006. Effect of high temperature treatment on the mechanical properties of birch (*Betula papyrifera*). Wood Sci. Technol. 40:647-663.

Rousset, P., P. Perre, and P. Girard. 2004. Modification of mass transfer properties in poplar wood (*P.robusta*) by a thermal treatment at high temperature. Holz Roh-Werkst. 62:113-119.

Segal, L., J.J. Creely, Jr. A.E. Martin, and C.M. Conrad. 1959. An empirical method for estimating the degree of crystallinity of native cellulose using the X-ray diffractometer. Textile Res. J. 29:786-794.

Slade, L. and H. Levine. 1991. Beyond water activity; recent advances based on alternative approach to the assessment of food quality and safety. Crit. Rev. Food Sci. Nutr. 30:115-360.

Sreekala, M.S. and S. Thomas. 2003. Effect of fibre surface modification on water sorption characteristics of oil palm fibres. Composites Sci. Technol. 63:861-869.

Tjeerdsma, B.F. and H. Militz. 2005. Chemical changes in hydrothermal treated wood: FTIR analysis of combined hydrothermal and dry heat-treated wood. Holz Roh-Werkst. 63:102-111.

Wahl, P., S.P. Simonaho, T. Pakarinen, and R. Silvennoinen. 2004. Effect of heat-treatment on scattering of laser light from wood grains. Holz Roh-Workst. 62:343-345.

Wan, Y.Z., K.Y. Han, Y.L. Wang, and Y. Huang. 2005. Moisture sorption of a three-dimensional braided carbon fiber-epoxy composite under different media. J. Appl. Polymer Sci. 97:507-512.

Wang, S. and P.M. Winistorfer. 2001. Flake compression behavior in a resinless mat as related to dimensional stability. Wood Sci. Technol. 35:379-393.

Wang, S., P.M. Winistorfer, T.M. Young, and C. Helton. 2001a. Step-closing pressing of medium density fiberboard. Part 1. Influence on the vertical density profile. Holz Roh–Werkst. 59(1/2):19-26.

Wang, S. P.M. Winistorfer, T.M. Young, and C. Helton. 2001b. Step-closing pressing of medium density fiberboard. Part 2. Influences on the panel performance and layer characteristics. Holz Roh-Werkst. 59(5):311-318.

Wikberg, H. and S.L. Maunu. 2004. Characterization of thermally modified hard- and softwoods by 13C CPMAS NMR. Carbohydrate Polym. 58:461-466.

Xing, C., S. Wang, and G. Pharr. 2007a. Comparison of the effects of thermomechanical refining pressure on the properties of refined fiber of juvenile and mature wood. Cellulose (in print).

Xing, C., S. Wang, G. Pharr, and L.H. Groom. 2007b. The use of nanoindentation to determine the effect of thermomechanical refining pressure on the properties of wood fibers. Holzforchung (in print).

Yildiz, S. and E. Gumuskaya. 2007. The effects of thermal modification on crystalline structure of cellulose in soft and hardwood. Build. Environ. 42:62-67.

Chapter 5

Alexander, J., S. Shaler, and W. Wright. 2000. Effect of resin type on OSB durability. *In*: Proc. 4th European Panel Products Symp., Llandudno, Wales, UK. October 11-13, 2000. pp. 34-44.

Aronhime, M.T., X. Peng, J.K. Gillham, and R.D. Small. 1986. Effect of time-temperature path of cure on the water absorption of high Tg epoxy resins. J. Appl. Polymer Sci. 32:3589-3626.

Bank, W.B. and J.F. Levy. 1980. The effect of cell wall swelling on the permeability of Grand Fir wood. Wood Sci. Technol. 14:49-62.

Bledzki, A.K. and O. Faruk. 2004. Creep and impact properties of wood fibre-polypropylene composites: Influence of temperature and moisture content. Compos. Sci. Technol. 64:693-700.

Bolton, A.J. and J.A. Petty. 1978. A model describing axial flow of liquids through conifer wood. Wood Sci. Technol. 12:37-48.

Chad, D.W. 1985. Trail manufacture of lightweight particleboard with improved swelling properties. Holz-Zentralblatt 111(32):514.

Enns, J.B. and J.K. Gillham. 1983. Effect of the extent of cure on the modulus, glass transition, water absorption, and density of amine-cured epoxy. J. Appl. Polymer Sci. 28:2831-2846.

Garcia, R.A., A. Cloutier, and B. Riedl. 2006. Chemical modification and wetting of medium density fiberboard panels produced from fibers treated with maleated polypropylene wax. Wood Sci. Technol. 40:402-416.

Harper, D.P., M.P. Wolcott, and T.G. Rials. 2001. Evaluating cure of a pMDI-wood bondline using spectroscopic, calorimetric and mechanical methods. J. Adhesion. 76(1):55-74.

Hinterstoisser, B., M. Schwanninger, B. Stefke, R. Stingl, and M. Patzelt. 2003. Surface analyses of chemically and thermally modified wood by FT-NIR. *In*: van Acker J., C. Hill (eds). Proc. of the 1st European Conference on Wood Modification, The First International Conference of the European Society for Wood Mechanics, Ghent, Belgium. April 2-4, 2003. pp. 65-70.

Hsu, W.E., R.J. Melanson, and P.J. Kozak. 1990. The effect of wax type and content on waferboard properties. *In*: Proc. of the 24th International Particleboard/Composite Materials Symp., T. Maloney, Ed., Washington State U., Pullman, WA. USA. April 5, 1990. pp. 85-93.

Jacob, M., K.T. Varughese, and S. Thomas. 2006. A study on the moisture sorption characteristics in woven sisal fabric reinforced natural rubber biocomposites. J. Appl. Polymer Sci. 102:416-423.

Karad, S.K., D. Attwood, and F.R. Jones. 2003. Moisture absorption by cyanate ester modified epoxy resin matrices. Part IV. Effect of curing schedules. Polymer Comp. 24(4):567-576.

Lehmann, W.F. 1972. Moisture-stability relationships in wood-base composition boards. Forest Prod. J. 22(7):53-59.

Maloney, T.M. 1993. Modern particleboard and dry-process fiberboard manufacturing. Miller Freeman Inc. San Francisco. 681 pp.

Mishra, S. and J. Verma. 2006. Effect of compatibilizers on water absorption kinetics of polypropylene/wood flour foamed composites. J. Appl. Polym. Sci. 101:2530-2537.

Muehl, J.H. and A.M. Krzysik. 1997. Effect of resin and wax on mechanical and physical properties of hardboard from air-laid mats. Drvna industrija 48(1):3-9.

Pandey, K.K. and A.J. Pitman. 2002. Weathering characteristics of modified rubberwood (*Hevea brasiliensis*). J. Appl. Polym. Sci. 85:622-631.

Raj, R.G., B.V. Kokta, F. Dembele, and C. Sanschagrain. 1988. Compounding of cellulose fibers with polypropylene: Effect of fiber treatment on dispersion in the polymer matrix. J. Appl. Polym. Sci. 38:1987-1996.

Renneckar, S., A.Z. Sharp, and W.G. Glasser. 2006. Fiber surface modification by steam-exposion: sorption studies with co-refined wood and polyolefins. Wood Fiber Sci. 38(3):427-438.

Sheppard, S.E. and P.T. Newsome. 1934. The sorption of water by cellulose. Indust. Eng. Chem. 26(3):285-290.

Siau, J.F. 1984. Transport processes in wood. Springer-Verlag, Berlin, Heidelberg, New York, Tokyo. 245 pp.

Stark, N.M. and L.M. Matuana. 2004. Surface chemistry and mechanical property changes of wood-flour/high-density-polyethylene composites after accelerated weathering. J. Appl. Polym. Sci. 94:2263-2273.

Tabarsa, T. and Y.H. Chui. 1997. Effects of hot-pressing on properties of white spruce. Forest Prod. J. 47(5):71-76.

Thomason, J.L. 1995. The interface region in glass fibre-reinforced epoxy resin composites. 2. Water absorption, voids and the interface. Composites 26:477-485.

Wittmann, O. 1973. Alkali in phenolic resin bonded particleboard. Holz Roh-Werkst. 31(11):419-425.

Ye, X., S. Wang, R. Ruan, J. Qi, A.R. Womac, and C.J. Doona. 2006. Water mobility and mold susceptibility of engineered wood products. Transactions of the ASABE 49(4):1159-1165.

Zhang, Y., J. Jin, and S.Wang. 2007. Effects of resin and wax on the water uptake behavior of wood strands. Wood Fiber Sci. 39(2):271-278.

VITA

Trairat Neimsuwan was born in Phetchabun, Thailand and he received the B.S. in forestry from Kasetsart University, Bangkok, Thailand, in 1999. After graduation, he joined Kasetsart University as Lecturer in the Department of Forest Products, Faculty of Forestry. He received an M.S in forestry from the University of Tennessee, Knoxville in 2004. In January, 2005, he entered the Ph.D. program in Natural Resources at the University of Tennessee, Knoxville. While pursuing his Ph.D., Neimsuwan worked as a graduate research assistant for Dr. Siqun Wang in the department of Forestry, Wildlifes and Fisheries.